



Calhoun: The NPS Institutional Archive
DSpace Repository

Theses and Dissertations

1. Thesis and Dissertation Collection, all items

2015-06

Maneuverability estimation of high-speed craft

Aslan, Nazmi

Monterey, California: Naval Postgraduate School

<http://hdl.handle.net/10945/45808>

Downloaded from NPS Archive: Calhoun



Calhoun is a project of the Dudley Knox Library at NPS, furthering the precepts and goals of open government and government transparency. All information contained herein has been approved for release by the NPS Public Affairs Officer.

Dudley Knox Library / Naval Postgraduate School
411 Dyer Road / 1 University Circle
Monterey, California USA 93943

<http://www.nps.edu/library>



**NAVAL
POSTGRADUATE
SCHOOL**

MONTEREY, CALIFORNIA

THESIS

**MANEUVERABILITY ESTIMATION OF HIGH-SPEED
CRAFT**

by

Nazmi Aslan

June 2015

Thesis Advisor:

Morris Driels

Co-Advisor:

Fotis A. Papoulias

Approved for public release; distribution is unlimited

THIS PAGE INTENTIONALLY LEFT BLANK

REPORT DOCUMENTATION PAGE			<i>Form Approved OMB No. 0704-0188</i>	
Public reporting burden for this collection of information is estimated to average 1 hour per response, including the time for reviewing instruction, searching existing data sources, gathering and maintaining the data needed, and completing and reviewing the collection of information. Send comments regarding this burden estimate or any other aspect of this collection of information, including suggestions for reducing this burden, to Washington headquarters Services, Directorate for Information Operations and Reports, 1215 Jefferson Davis Highway, Suite 1204, Arlington, VA 22202-4302, and to the Office of Management and Budget, Paperwork Reduction Project (0704-0188) Washington DC 20503.				
1. AGENCY USE ONLY (Leave blank)		2. REPORT DATE June 2015	3. REPORT TYPE AND DATES COVERED Master's Thesis	
4. TITLE AND SUBTITLE MANEUVERABILITY ESTIMATION OF HIGH-SPEED CRAFT			5. FUNDING NUMBERS	
6. AUTHOR(S) Nazmi Aslan				
7. PERFORMING ORGANIZATION NAME(S) AND ADDRESS(ES) Naval Postgraduate School Monterey, CA 93943-5000			8. PERFORMING ORGANIZATION REPORT NUMBER	
9. SPONSORING /MONITORING AGENCY NAME(S) AND ADDRESS(ES) N/A			10. SPONSORING/MONITORING AGENCY REPORT NUMBER	
11. SUPPLEMENTARY NOTES The views expressed in this thesis are those of the author and do not reflect the official policy or position of the Department of Defense or the U.S. Government. IRB Protocol number ____N/A____.				
12a. DISTRIBUTION / AVAILABILITY STATEMENT Approved for public release; distribution is unlimited			12b. DISTRIBUTION CODE	
13. ABSTRACT (maximum 200 words) This thesis focuses on the problem of predicting the maneuvering characteristic of high-speed craft. A mathematical model is derived based on equations by Lewandowski and Denny-Hubble in order to find the fundamental maneuvering characteristics. The model is developed in the MATLAB Simulink in-time domain with the help of Nomoto's first-order model, which encapsulates the fundamental dynamics of turning on the horizontal plane. After the development of the model, Predator and Prey interactions are analyzed in order to estimate helmsman reaction when the vessel is attacked by a missile. Three different attacking situations are analyzed in missile-vessel interactions for the safety of the vessel, and the optimum distance has been found to start the escape maneuver. According to these escape situations, the missile should maintain a certain g-force to make an adequate turn and hit the vessel. These critical g-forces are calculated for each situation.				
14. SUBJECT TERMS High-Speed Craft, Maneuverability Estimation, Control Law, Attack and Avoidance, Missile-Vessel Interactions.			15. NUMBER OF PAGES 121	
			16. PRICE CODE	
17. SECURITY CLASSIFICATION OF REPORT Unclassified	18. SECURITY CLASSIFICATION OF THIS PAGE Unclassified	19. SECURITY CLASSIFICATION OF ABSTRACT Unclassified	20. LIMITATION OF ABSTRACT UU	

THIS PAGE INTENTIONALLY LEFT BLANK

Approved for public release; distribution is unlimited

MANEUVERABILITY ESTIMATION OF HIGH-SPEED CRAFT

Nazmi Aslan
Lieutenant Junior Grade, Turkish Navy
B.S., Turkish Naval Academy, 2009

Submitted in partial fulfillment of the
requirements for the degree of

MASTER OF SCIENCE IN MECHANICAL ENGINEERING

from the

**NAVAL POSTGRADUATE SCHOOL
June 2015**

Author: Nazmi Aslan

Approved by: Morris Driels
Thesis Advisor

Fotis A. Papoulias
Co-Advisor

Garth V. Hobson
Chair, Department of Mechanical and Aerospace Engineering

THIS PAGE INTENTIONALLY LEFT BLANK

ABSTRACT

This thesis focuses on the problem of predicting the maneuvering characteristic of high-speed craft. A mathematical model is derived based on equations by Lewandowski and Denny-Hubble in order to find the fundamental maneuvering characteristics. The model is developed in the MATLAB Simulink in-time domain with the help of Nomoto's first-order model, which encapsulates the fundamental dynamics of turning on the horizontal plane. After the development of the model, Predator and Prey interactions are analyzed in order to estimate helmsman reaction when the vessel is attacked by a missile. Three different attacking situations are analyzed in missile-vessel interactions for the safety of the vessel, and the optimum distance has been found to start the escape maneuver. According to these escape situations, the missile should maintain a certain g-force to make an adequate turn and hit the vessel. These critical g-forces are calculated for each situation.

THIS PAGE INTENTIONALLY LEFT BLANK

TABLE OF CONTENTS

I.	INTRODUCTION.....	1
A.	MOTIVATION	1
B.	BACKGROUND AND THESIS OVERVIEW	2
1.	Background	2
2.	Thesis Overview	4
II.	LITERATURE REVIEW	7
A.	SHIP MOTIONS AND MANEUVERABILITY	7
B.	EQUATIONS OF MOTION.....	11
1.	Coordinate Systems	11
2.	Hydrodynamic Forces	13
C.	MANEUVERING CHARACTERISTICS.....	16
III.	ANALYZING EXISTING MANEUVERING MODELS	17
A.	INTRODUCTION.....	17
B.	MANEUVERING PREDICTION PROGRAM (UNIVERSITY OF MICHIGAN)	17
1.	Program Information	17
2.	Results and Discussions	23
C.	MATLAB SIMULATIONS BY FOSSEN	26
1.	Program Information	26
2.	Results and Discussions	28
IV.	MODEL DEVELOPMENT & SIMULATION MODEL	33
A.	INTRODUCTION.....	33
B.	EQUATIONS BY LEWANDOWSKI.....	33
C.	EQUATIONS BY DENNY AND HUBBLE	43
D.	NOMOTO EQUATIONS (STABILITY AND CONTROL).....	45
E.	MODEL IN MATLAB SIMULINK.....	47
F.	RESULTS AND DISCUSSION	50
V.	ATTACK AND AVOIDANCE	57
A.	INTRODUCTION.....	57
B.	PREY AND PREDATOR INTERACTIONS IN NATURE	57
C.	CATCH/ESCAPE CONDITIONS AND GENERALIZED CIRCLE INTERSECTION POINTS	58
1.	Generalized Circle Intersection.....	59
2.	Escape/Catch Analysis for Different Situations in Missiles-Ships Interactions.....	63
a.	<i>Escape/Catch Analysis in Pursuit Attack Situation</i>	<i>63</i>
b.	<i>Escape/Catch Analysis in Beam Attack Situation</i>	<i>67</i>
c.	<i>Escape/Catch Analysis in Head-to-Head Attack Situation ...</i>	<i>69</i>
D.	ANALYZING SPECIFIC MISSILE-VESSEL INTERACTIONS	71
E.	THE CRITICAL G-FORCE FOR THE MISSILE	75

VI.	CONCLUSION AND RECOMMENDATIONS	81
A.	CONCLUSION	81
B.	RECOMMENDATIONS.....	81
	APPENDIX A. IMO REQUIREMENTS.....	83
	APPENDIX B. MODEL BLOCKS	85
	APPENDIX C. MATLAB CODES FOR OPTIMUM X0 DISTANCE IN PURSUIT ATTACK, BEAM ATTACK, AND HEAD-TO-HEAD ATTACK SITUATIONS.....	87
	APPENDIX D. MATLAB CODES FOR CRITICAL G-FORCE IN PURSUIT ATTACK, BEAM ATTACK, AND HEAD-TO-HEAD ATTACK SITUATIONS.....	93
	APPENDIX E. CLOSEST APPROACH FUNCTIONS IN THE MATLAB CODES ..	99
	LIST OF REFERENCES	103
	INITIAL DISTRIBUTION LIST	105

LIST OF FIGURES

Figure 1.	Bradstone Challenger with Missiles, from [3].....	1
Figure 2.	High-Speed Craft in Turning, from [7].....	3
Figure 3.	Six Degrees of Freedom with Positive Angles and Moments, from [4].....	4
Figure 4.	Ship Translation Motions, from [9]	7
Figure 5.	Ship Rotation Motion, from [9]	8
Figure 6.	Straight Line Stability, from [5].....	9
Figure 7.	Course-Keeping Ability, from [5].....	9
Figure 8.	Turning Ability, from [5].....	10
Figure 9.	The Earth-Fixed Coordinate System and The Body-Fixed Coordinate System, from [11]	11
Figure 10.	Free Body Diagram in a Steady Turn, from [4].....	15
Figure 11.	Advance, Transfer, and Tactical Diameter, from [5].....	16
Figure 12.	Vessel Characteristics at Input Page	18
Figure 13.	Length on Waterline of a Vessel, from [13]	18
Figure 14.	Steering Characteristics of the Vessel.....	19
Figure 15.	Typical Hull of the High-Speed Craft, from [15]	20
Figure 16.	Operating Conditions	20
Figure 17.	Water Properties.....	21
Figure 18.	The Analysis Page.....	21
Figure 19.	Turning Speed Ratio vs. Normalized Turning Diameter	25
Figure 20.	The Vehicles in MATLAB Program.....	27
Figure 21.	Turning Motion of Multirole Naval Ship with 15.43 m/s [30 knots]	29
Figure 22.	Turning Motion of Multirole Naval Ship with 20.57 m/s [40 knots]	29
Figure 23.	Turning Motion of Multirole Naval Ship with 25.72 m/s [50 knots]	30
Figure 24.	Turning Motion of Multirole Naval Ship with 30.86 m/s [60 knots]	30
Figure 25.	Steady Speed Change in Time for 30.86 m/s [60 knots]	31
Figure 26.	L_k and L_c of the Vessel, from [6]	34
Figure 27.	L_k/L vs. Volumetric Froude Number	37
Figure 28.	L_c/L vs. Volumetric Froude Number.....	38
Figure 29.	The Correlation Between Length and Displacement.....	39
Figure 30.	Standard Turning Diameter vs. Length.....	40
Figure 31.	Normalized Turning Diameter vs. Length.....	40
Figure 32.	TD/LOA Comparison Between Full Scale Data and Prediction By Lewandowski, from [4].....	41
Figure 33.	Normalized Turning Diameter vs. Rudder Angle for MRTP 16 Fast Intervention Craft.....	42
Figure 34.	Normalized Turning Diameter vs. Speed for MRTP 16 Fast Intervention Craft	42
Figure 35.	The Plots of Turning Radius for Different U_c/U_a Values, from [16].....	44
Figure 36.	Comparison of Turning Diameter of Shaldag Class Vessel	45
Figure 37.	Speed Reduction with Given Rudder Angle.....	45
Figure 38.	The Basic Diagram of the Mathematical Model.....	48

Figure 39.	The Block Diagram of the Mathematical Model	49
Figure 40.	Vessel Movement with 40 Knots and 0 Rudder Angle.....	50
Figure 41.	Turning Radius of a Vessel with 40 Knots and 30 Rudder Angle.....	51
Figure 42.	Turning Radius of a Vessel with 50 Knots and 30 Rudder Angle.....	51
Figure 43.	Turning Radius of a Vessel with 60 Knots and 30 Rudder Angle.....	52
Figure 44.	Standard Turning Radius from Lewandowski Equation.....	53
Figure 45.	Turning Radius in Nomoto's Equation.....	53
Figure 46.	The Motion of the Vessel on the Horizontal Plane with Time	54
Figure 47.	Speed Change vs. Time.....	54
Figure 48.	Rudder Angle Change vs. Time.....	55
Figure 49.	The Prey-Predator Interactions in a Pursuit Situation, from [23]	58
Figure 50.	Chord Lengths of the Predator and Prey	62
Figure 51.	Vessel-Missile Interactions in Pursuit Attack Situation	63
Figure 52.	Catch/Escape Conditions vs. x_0 Distance in Pursuit Attack	64
Figure 53.	Miss Distance Illustration in Pursuit Attack	64
Figure 54.	Miss Distances vs. x_0 Distances in Pursuit Attack.....	65
Figure 55.	Closest Approach Illustration in Pursuit Attack	66
Figure 56.	Miss Distance vs. Time in Pursuit Attack.....	66
Figure 57.	Closest Approach Distances vs. x_0 Distances in Pursuit Attack.....	67
Figure 58.	Vessel-Missile Interactions in Beam Attack Situation	67
Figure 59.	Catch/Escape Conditions for x_0 Distances in Beam Attack.....	68
Figure 60.	Miss Distances vs. x_0 Distance in Beam Attack	68
Figure 61.	Closest Approach vs. x_0 Distance in Beam Attack	69
Figure 62.	The Vessel-Missile Interactions in Head-to-Head Situation	69
Figure 63.	Catch/Escape Conditions for x_0 Distances in Head-to-Head Attack	70
Figure 64.	Miss Distances vs. x_0 Distance in Head-to-Head Attack.....	71
Figure 65.	Closest Approach vs. x_0 Distance in Head-to-Head Attack.....	71
Figure 66.	Catch/Escape Conditions for x_0 Distances in Pursuit Attack.....	73
Figure 67.	Catch/Escape Conditions for x_0 Distances in Head-to-Head Attack	73
Figure 68.	Catch/Escape Conditions for x_0 Distances in Beam Attack.....	74
Figure 69.	Miss Distances vs. x_0 Distances in Beam Attack.....	74
Figure 70.	Closest Approach Distance vs. x_0 Distances in Beam Attack	75
Figure 71.	Catch/Escape Conditions vs. g-force in Pursuit Attack	76
Figure 72.	Catch/Escape Conditions vs. g-force in Beam Attack	76
Figure 73.	Catch/Escape Conditions vs. g-force in Head-to-Head Attack	77
Figure 74.	Miss Distances vs. g-force in Pursuit Situation	77
Figure 75.	Closest Approach Distances vs. g-force in Pursuit Situation	78
Figure 76.	Miss Distances vs. g-force in Beam Situation	78
Figure 77.	Closest Approach Distances vs. g-force in Beam Situation	79
Figure 78.	Miss Distances vs. g-force in Head-to-Head Situation.....	79
Figure 79.	Closest Approach Distances vs. g-force in Head-to-Head Situation	80

LIST OF TABLES

Table 1.	Vessel Characteristics with Units	18
Table 2.	Basic Characteristics of the High-speed Crafts	22
Table 3.	Block Coefficients of the High-Speed Crafts	23
Table 4.	Results of the MPP.....	24
Table 5.	The Vessel Characteristics of Mariner Class Ship.....	28
Table 6.	The Vessel Characteristics of High-speed Container	28
Table 7.	The Vessel Characteristics of Multirole Naval Ship.....	28
Table 8.	Variables in the Lewandowski Equations.....	34
Table 9.	Volume Coefficients and Volumetric Froude Number of The Vessels	36
Table 10.	Length and Displacement Data of the Vessels	39
Table 11.	Sample High-Speed Boat Characteristics	72

THIS PAGE INTENTIONALLY LEFT BLANK

ACKNOWLEDGMENTS

First, I wish to thank my advisors, Professor Morris Driels and Professor Fotis A. Papoulias, for their support and guidance throughout this project. Their innovative and sophisticated approaches have been both very helpful and enlightening while conducting my thesis research.

I would like to thank to my instructors and professors who provided a worthwhile learning experience with their proven knowledge and stimulating attitude while teaching.

I would also like to thank to my colleagues at the Naval Postgraduate School who, by their graciousness and hospitality, helped me feel comfortable while I have been far away from my home country.

I wish to express my thankfulness to my family.

THIS PAGE INTENTIONALLY LEFT BLANK

I. INTRODUCTION

A. MOTIVATION

In modern warfare, world navies are using guided missiles to protect their valuable units and to attack other navies. These missiles can be launched from an aircraft and/or a helicopter. One of the challenges with these guided missiles is the ability to hit moving targets. These moving targets can be on land or on the sea. To increase the probability of an accurate hit, pilots must be able to predict the position of the target. Previously, a study focused on moving land vehicles, but no target estimation study has been conducted for sea vehicles.

In littoral seas and gulfs, the U.S. Navy can encounter high-speed boats, which are a threat to aircraft carriers. In recent years, incidents with high-speed craft have been more common. In 2012, during tensions with Iran, U.S. Navy and Coast Guard ships had two close encounters in the Persian Gulf [1]. Foreign navies have installed mobile coastal missile batteries and modern anti-ship missiles on these high-speed boats to address asymmetric threats. Figure 1 shows a high-speed craft with anti-ship missiles [2].



Figure 1. Bradstone Challenger with Missiles, from [3]

Sea vehicles have different maneuvering abilities than land vehicles. Ship maneuvering is the response motion of the rudder angle change. Maneuvering characteristics of a vessel depend on vessel characteristic, steering characteristics, operation conditions, and hydrodynamic coefficients. Prediction methods for the maneuvering capabilities of displacement vessels have existed since 1960s. These prediction methods and simulations are used in ship design. However, there are a limited number of prediction methods for high-speed crafts [4].

This thesis focuses on the maneuverability estimation for high-speed craft and high-speed boats. With this estimation, the aim is to find the maneuvering characteristics of high-speed craft such as turning circle, advance, and transfer values with given speed and given rudder angle. The goal of this thesis is to develop a maneuvering model for small boats that can be used to provide predictive targeting information. This model analyzes the motions of such boats under a variety of assumed evasive actions and sets realistic bounds on the expected position of the boat within a specified time. This is accomplished through computer simulation.

B. BACKGROUND AND THESIS OVERVIEW

1. Background

Related studies have focused on land vehicles and are based on different road types. The roads were specified according to their standard deviation in curvature that limited the speed of the land vehicle. The speed and the motion of the land vehicles could be estimated according to road type. Since there are no roads and no specific restrictions at sea, boats can move in any direction and at any speed. However, the maneuverability of the vessel restricts its movements and can be used to estimate its maneuvers.

Maneuverability standards for displacement ships have existed since 1960. The goal of these standards was to have a universal maneuvering standard for all ships. The criteria of maneuvering were proposed in 1991, and these standards were adopted in 1993 by IMO (International Maritime Organization). In 2002, these standards were revised and introduced by IMO again. They examined basic maneuvering qualities:

turning ability, initial turning ability, course keeping ability, yaw-checking ability, and stopping ability. According to the Standards for Ship Maneuverability, a ship is considered satisfactory if it complies with the IMO criteria that are listed in Appendix A [5]. However, there are no specific maneuvering standards for high-speed crafts [4].

High-speed crafts are generally used in shallow waters and areas where ship traffic exists. Therefore, it has been expected that these crafts have better maneuverability than other ships [4]. For this reason, there was no need to set maneuvering standards or to develop prediction methods. *High-speed* is defined as the speed at which the effects of dynamic lift become significant. Lewandowski proposed that high-speed occurs when the volumetric Froude number (F_{∇}) of the craft is above 0.7–0.8 [6] where

$$F_{\nabla} = \frac{U}{\sqrt{g\nabla^{1/3}}} \quad (1)$$

U = Approach Speed

∇ = Underwater Volume

g = Gravity of Earth

Figure 2 shows a high-speed craft in a turn.



Figure 2. High-Speed Craft in Turning, from [7]

The static and dynamic equations of the equilibrium of high-speed craft have been developed for public domain by Lewandowski [6]. Dynamic effects are significant with high speed, and there is a closely coupled motion around all six degrees of freedom [4]. The degrees of freedoms are shown in Figure 3.

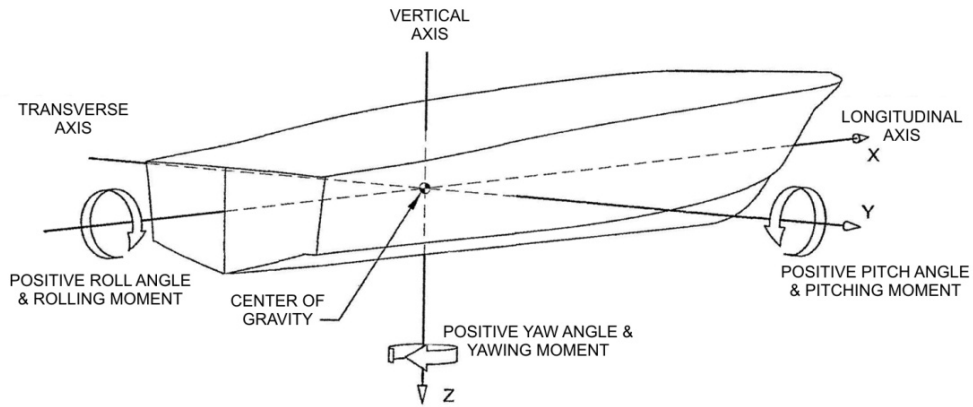


Figure 3. Six Degrees of Freedom with Positive Angles and Moments, from [4]

This thesis focuses on the hydrodynamic equations which are derived by Lewandowski. For the sample high-speed crafts, these equations are solved in a MATLAB program. A simulation program is developed in MATLAB Simulink in order to represent the motion of high-speed craft.

2. Thesis Overview

This thesis is focused on the problem of the maneuvering characteristic of high-speed crafts. The hydrodynamic coefficients are calculated with the equations presented in Lewandowski [6]. The mathematical model is developed based on Nomoto's first order model, which encapsulates the fundamental dynamics of turning on the horizontal plane. This model is going to be used for small boats to enhance the targeting accuracy of guided missiles.

This thesis is organized as follows:

Chapter II contains the literature review. Ship maneuverability and maneuvering characteristics are described in this chapter. An overview of equations of motion for sea vehicles is presented.

Chapter III presents the existing maneuvering programs and simulations. One of these programs is developed by the University of Michigan; the other one is developed at the Norwegian Institute of Technology. These models are analyzed for high-speed craft and the results of these programs are discussed.

Chapter IV introduces a new maneuvering model which is derived from equations by Lewandowski, Denny-Hubble, and Nomoto. A MATLAB Simulink program is used in order to predict continuous motion on the horizontal plane in time domain.

Chapter V presents an analogy with animal predators attempting to capture their prey and investigates the kinematics of their interactions. These interactions are then investigated in missile and high-speed craft interactions.

Chapter VI summarizes the conclusions from this study and offers recommendations for further studies.

THIS PAGE INTENTIONALLY LEFT BLANK

II. LITERATURE REVIEW

A. SHIP MOTIONS AND MANEUVERABILITY

Ship motions are presented in two groups: translations and rotations. Each group consists of three motions. Translation motions are surge, sway, and heave; they are presented in Figure 4. *Surge* is the translation motion along the longitudinal axis, *sway* is the motion in the transverse direction, and *heave* is the vertical motion. Rotation motions are roll, pitch, and yaw; they are presented in Figure 5. *Roll* is the rotation motion about the longitudinal axis, *pitch* is the rotation motion about the transverse axis, and *yaw* is rotation about the vertical axis [8].

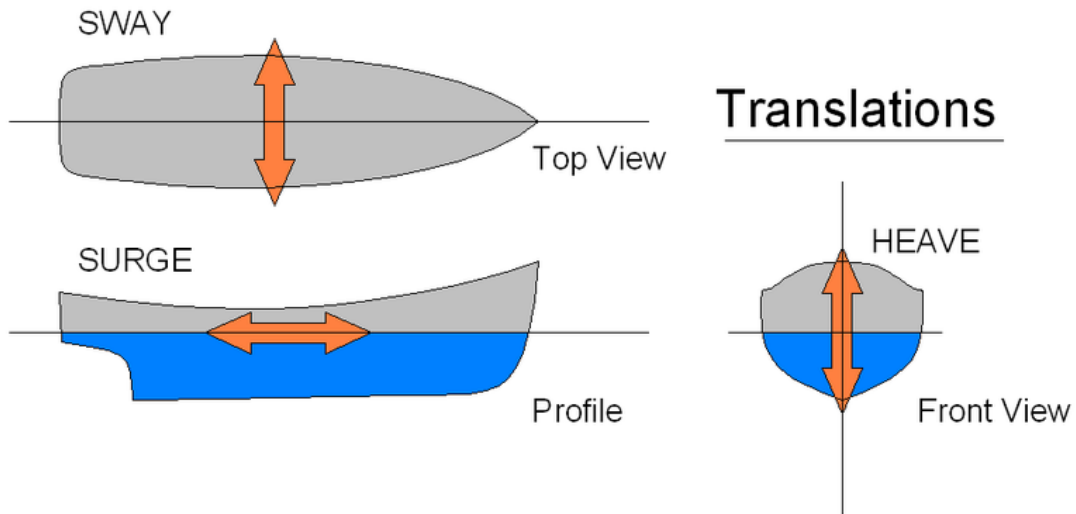


Figure 4. Ship Translation Motions, from [9]

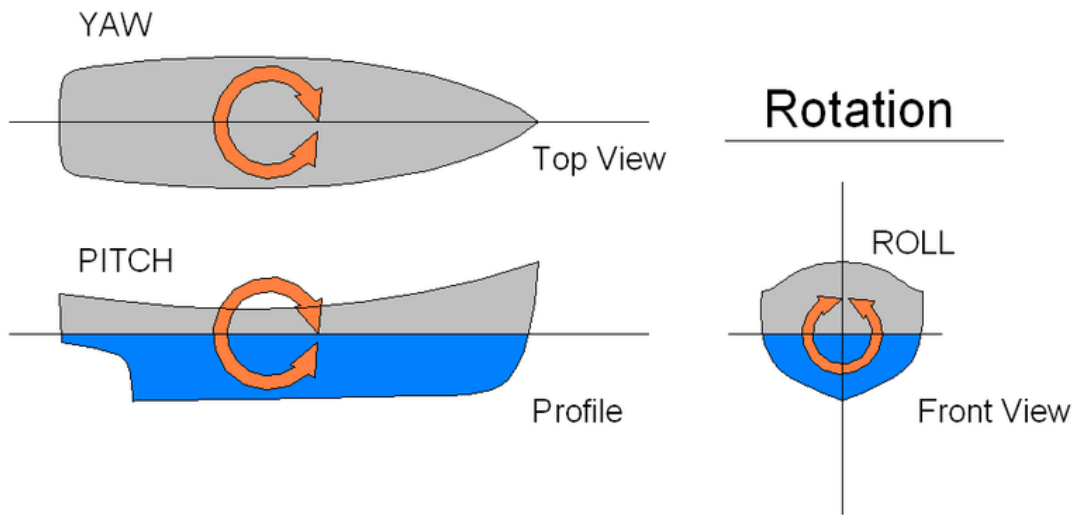


Figure 5. Ship Rotation Motion, from [9]

Maneuvering is the behavior of a ship in a horizontal plane: longitudinal and transverse direction. It is the response of motion which is a result of rudder angle change [5]. In other words, maneuverability includes sway, surge, and yaw motions. *Ship maneuverability* is defined as the ability of a ship to change its direction according to the intention of the helmsman.

Ship maneuverability has a close relationship with navigation safety and economy. Marine collisions may occur if the ship doesn't have enough maneuverability under emergency conditions and/or in restricted water. It is important for a ship to have adequate maneuverability in order to ensure a safe navigation. In this chapter, the concepts of ship maneuverability and an overview of equation of motions for marine vehicles are introduced.

Professor Zou Zaojian [5] stated in his notes that ship maneuverability includes the following abilities:

Straight Line Stability

Straight line stability is defined as the ability of a ship to be able to have a new course after a small disturbance. The final path is going to be straight but the direction has changed. The magnitude and period of the disturbance affect the change of direction. Straight line stability is shown in Figure 6.

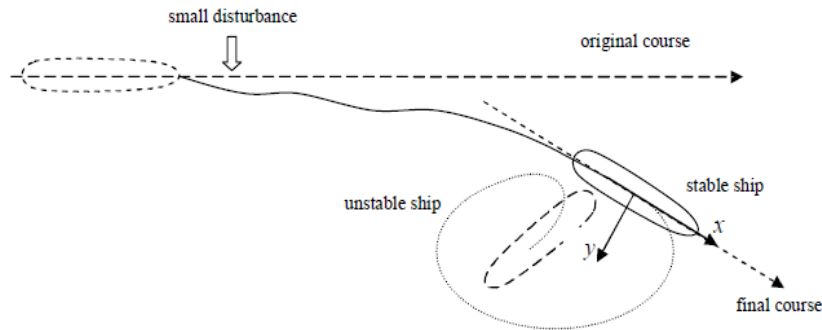


Figure 6. Straight Line Stability, from [5]

Course-Keeping Ability (Directional Stability)

Course-keeping ability is the ability of a ship to maintain a straight path in a determined course with course control action. Figure 7 shows the course-keeping ability.

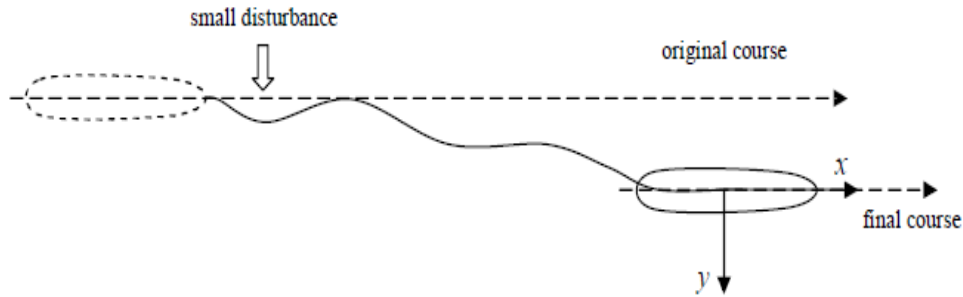


Figure 7. Course-Keeping Ability, from [5]

Initial Turning/Course-Changing Ability

Initial turning/course-changing ability is the ability to change the heading of the ship with a control action. A ship with a good course-changing ability will quickly change its heading to a new direction with a control action.

Yaw-Checking Ability

Yaw-checking ability is defined as the ability of a vessel to respond to the applied counter rudder action in a turning.

Turning Ability

Turning ability is defined as the ability of a ship to turn using maximum rudder angle. The results are “advance” at 90-degree change of heading and “tactical diameter” at 180-degree change of heading. Figure 8 shows the turning ability of a ship.

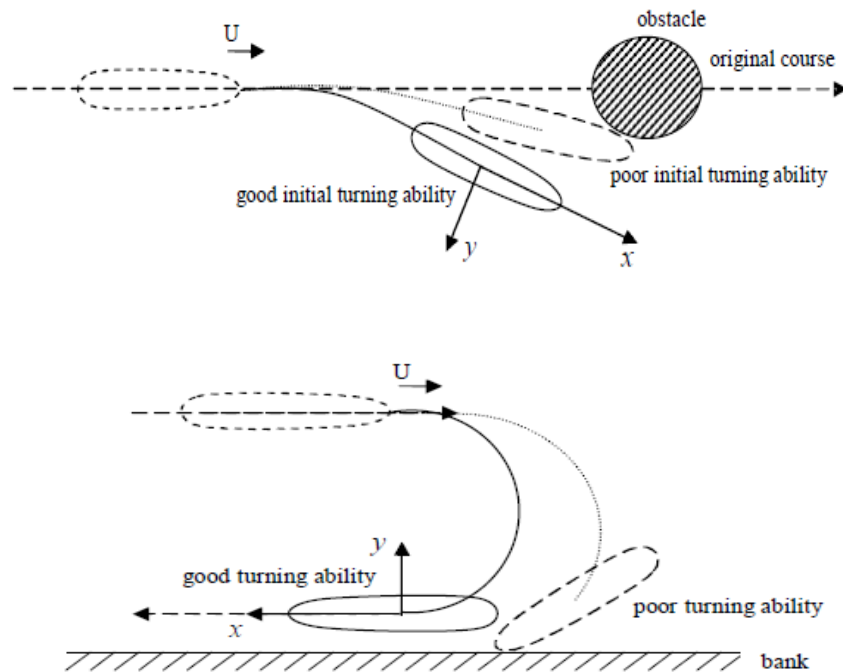


Figure 8. Turning Ability, from [5]

Stopping Ability

Stopping ability is defined as the ability of a ship to stop after engines are stopped or at full astern.

B. EQUATIONS OF MOTION

1. Coordinate Systems

In ship maneuvering, two different types of coordinate systems are generally used; one is earth-fixed with x_0, y_0, z_0 axes where the origin is fixed and the other one is body-fixed with x, y, z axes which move with the vessel. The earth-fixed coordinate system is shown in Figure 9. In the body-fixed coordinate system, the origin is on the center of gravity of the vessel with the z -axis downward and the x -axis forward. Generally, the body-fixed system is used to analyze hydrodynamic forces and equations of motion [10].

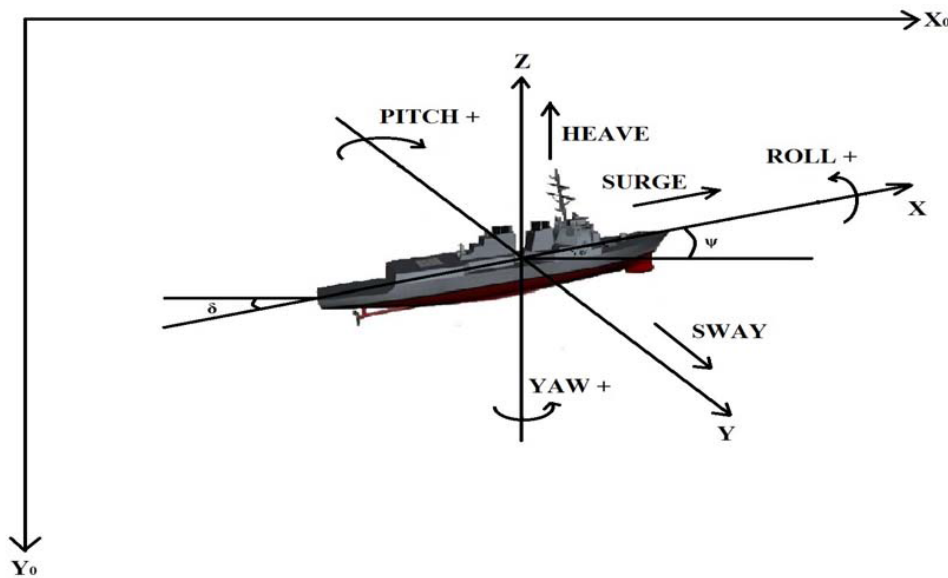


Figure 9. The Earth-Fixed Coordinate System and The Body-Fixed Coordinate System, from [11]

The hydrodynamic forces at the x -axis and y -axis are called X and Y . The hydrodynamic turning (yaw) moment about the z -axis is N . The longitudinal and lateral

components of the ship velocity are u and v , and the yaw angle is ψ . The yaw velocity is r : $r = \dot{\Psi}$

According to Newton's second law, the forces that affect the maneuverability of the vessel in the earth-fixed coordinate system are as follows:

$$\begin{aligned} m\ddot{x}_0 &= X_0 \\ m\ddot{y}_0 &= Y_0 \\ I_z\ddot{\Psi} &= N \end{aligned} \quad (2)$$

The X_0 and Y_0 are the components of forces that acting on the vessel in x_0 and y_0 direction and N is the moment about the Z_0 axis. Ψ is the yaw angle.

The motion can be transformed from earth-fixed coordinate system to body-fixed coordinate system to express the motion of the ship in a convenient way [5].

$$\begin{aligned} x_{0G} + x \cos \psi - y \sin \psi &= x_0 \\ y_{0G} + x \sin \psi + y \cos \psi &= y_0 \\ z &= z_0 \end{aligned} \quad (3)$$

The components of total force in x and y directions are replaced with X_0 and Y_0 , and the components of the vessel speed in x and y directions are replaced with u_G and v_G in the equation,

$$\begin{aligned} X_0 \cos \psi + Y_0 \sin \psi &= X \\ -X_0 \sin \psi + Y_0 \cos \psi &= Y \end{aligned} \quad (4)$$

$$\begin{aligned} u_g \cos \psi - v_g \sin \psi &= \dot{x}_{0G} \\ u_g \sin \psi + v_g \cos \psi &= \dot{y}_{0G} \end{aligned} \quad (5)$$

Equation (5) is differentiated with respect to time in order to get the following equation:

$$\begin{aligned} \dot{u}_G \cos \psi - u_G \dot{\psi} \sin \psi - \dot{v}_G \sin \psi - v_g \dot{\psi} \cos \psi &= \ddot{x}_{0G} \\ \dot{u}_G \sin \psi - u_G \dot{\psi} \cos \psi + \dot{v}_G \cos \psi - v_g \dot{\psi} \sin \psi &= \ddot{y}_{0G} \end{aligned} \quad (6)$$

The equations of motion in the body-fixed coordinate system can be found as in equation (7) by substituting equation (6) and equation (2) into equation (4)

$$\begin{aligned}
m\dot{u}_G - mv_G r &= X \\
m\dot{v}_G + mu_G r &= Y \\
I_z \dot{r} &= N
\end{aligned} \tag{7}$$

In practice, it becomes more convenient when the origin of the body-fixed coordinate was put into amidships. The center of gravity is on the $(x_G, 0, z_G)$, assuming that the ship is symmetrical along the x-axis. The components of the vessel speed can be expressed as follows:

$$\begin{aligned}
u_G &= u \\
v_G &= v + x_G \dot{\psi} \\
I_z &= I_{zG} + mx_G^2
\end{aligned} \tag{8}$$

The equations of motion for the body-fixed coordinate system are expressed in equation (9):

$$\begin{aligned}
m(\dot{u} - vr - x_G r^2) &= X \\
m(\dot{v} + ur + x_G \dot{r}) &= Y \\
I_z \dot{r} + mx_G (\dot{v} + ur) &= N
\end{aligned} \tag{9}$$

In the equations, u is the surge, v is the sway and r is the yaw velocity; x_G is the distance between the origin and the center of the gravity.

2. Hydrodynamic Forces

The total forces and the moment (X, Y, N) that act on the vessel include the hydrodynamics forces and moments. These forces and moments can be created by different environmental effects such as wind forces, wave forces, rudder and propeller forces, and so forth.

Hydrodynamic force and moment were analyzed with two different types of approaches. One is introduced by Martin A. Abkowitz from the Massachusetts Institute of Technology in the United States, and the other one is from the Maneuvering Mathematical Modelling Group (MMMG) from Japan [5].

In 1964, Abkowitz used the Taylor expansion series to find an expression for this hydrodynamic force and moment [5].

$$\begin{aligned}
X &= X(u, v, r, \dot{u}, \dot{v}, \dot{r}, \delta) \\
Y &= Y(u, v, r, \dot{u}, \dot{v}, \dot{r}, \delta) \\
N &= N(u, v, r, \dot{u}, \dot{v}, \dot{r}, \delta)
\end{aligned} \tag{10}$$

A Taylor series about the initial steady state forward motion with constant speed is listed, as follows.

$$\begin{aligned}
X &= X_0 + \frac{\partial X}{\partial u}(u-U) + \frac{\partial X}{\partial v}v + \frac{\partial X}{\partial r}r + \frac{\partial X}{\partial \dot{u}}\dot{u} + \frac{\partial X}{\partial \dot{v}}\dot{v} + \frac{\partial X}{\partial \dot{r}}\dot{r} + \frac{\partial X}{\partial \delta}\delta \\
&\quad + \frac{1}{2} \left[\frac{\partial}{\partial u}(u-U) + \frac{\partial}{\partial v}v + \frac{\partial}{\partial r}r + \frac{\partial}{\partial \dot{u}}\dot{u} + \frac{\partial}{\partial \dot{v}}\dot{v} + \frac{\partial}{\partial \dot{r}}\dot{r} + \frac{\partial}{\partial \delta}\delta \right]^2 X \\
&\quad + \dots + \frac{1}{n!} \left[\frac{\partial X}{\partial u}(u-U) + \frac{\partial}{\partial v}v + \frac{\partial}{\partial r}r + \frac{\partial}{\partial \dot{u}}\dot{u} + \frac{\partial}{\partial \dot{v}}\dot{v} + \frac{\partial}{\partial \dot{r}}\dot{r} + \frac{\partial}{\partial \delta}\delta \right]^n X \\
Y &= Y_0 + \frac{\partial Y}{\partial u}(u-U) + \frac{\partial Y}{\partial v}v + \frac{\partial Y}{\partial r}r + \frac{\partial Y}{\partial \dot{u}}\dot{u} + \frac{\partial Y}{\partial \dot{v}}\dot{v} + \frac{\partial Y}{\partial \dot{r}}\dot{r} + \frac{\partial Y}{\partial \delta}\delta \\
&\quad + \frac{1}{2} \left[\frac{\partial Y}{\partial u}(u-U) + \frac{\partial}{\partial v}v + \frac{\partial}{\partial r}r + \frac{\partial}{\partial \dot{u}}\dot{u} + \frac{\partial}{\partial \dot{v}}\dot{v} + \frac{\partial}{\partial \dot{r}}\dot{r} + \frac{\partial}{\partial \delta}\delta \right]^2 Y \\
&\quad + \dots + \frac{1}{n!} \left[\frac{\partial Y}{\partial u}(u-U) + \frac{\partial}{\partial v}v + \frac{\partial}{\partial r}r + \frac{\partial}{\partial \dot{u}}\dot{u} + \frac{\partial}{\partial \dot{v}}\dot{v} + \frac{\partial}{\partial \dot{r}}\dot{r} + \frac{\partial}{\partial \delta}\delta \right]^n Y \\
N &= N_0 + \frac{\partial N}{\partial u}(u-U) + \frac{\partial N}{\partial v}v + \frac{\partial N}{\partial r}r + \frac{\partial N}{\partial \dot{u}}\dot{u} + \frac{\partial N}{\partial \dot{v}}\dot{v} + \frac{\partial N}{\partial \dot{r}}\dot{r} + \frac{\partial N}{\partial \delta}\delta \\
&\quad + \frac{1}{2} \left[\frac{\partial N}{\partial u}(u-U) + \frac{\partial}{\partial v}v + \frac{\partial}{\partial r}r + \frac{\partial}{\partial \dot{u}}\dot{u} + \frac{\partial}{\partial \dot{v}}\dot{v} + \frac{\partial}{\partial \dot{r}}\dot{r} + \frac{\partial}{\partial \delta}\delta \right]^2 N \\
&\quad + \dots + \frac{1}{n!} \left[\frac{\partial N}{\partial u}(u-U) + \frac{\partial}{\partial v}v + \frac{\partial}{\partial r}r + \frac{\partial}{\partial \dot{u}}\dot{u} + \frac{\partial}{\partial \dot{v}}\dot{v} + \frac{\partial}{\partial \dot{r}}\dot{r} + \frac{\partial}{\partial \delta}\delta \right]^n N
\end{aligned} \tag{11}$$

The derivatives in Taylor series expansions are called hydrodynamic derivatives; they are usually expressed as

$$\frac{\partial X}{\partial u} = X_u, \quad \frac{\partial X}{\partial v} = X_v, \quad \frac{\partial X}{\partial r} = X_r, \quad \frac{\partial X}{\partial \dot{u}} = X_{\dot{u}}, \quad \frac{\partial X}{\partial \dot{v}} = X_{\dot{v}}, \quad \frac{\partial X}{\partial \dot{r}} = X_{\dot{r}}, \quad \frac{\partial X}{\partial \delta} = X_{\delta} \tag{12}$$

The Maneuvering Mathematical Modelling Group (MMMG), which was founded by a Japanese research group, analyzes hydrodynamic force and moment

acting on the ship hull, propeller, and rudder, as well as the interaction between them. These expressions are presented in equation (13).

$$\begin{aligned} X &= X_H + X_P + X_R \\ Y &= Y_H + Y_P + Y_R \\ N &= N_H + N_P + N_R \end{aligned} \tag{13}$$

The subscripts H, P, and R refer to the hull, the propeller, and the rudder. By plugging equation (13) into equation (9), we will obtain the equation of ship maneuvering motion [5]. Two approaches become identical when the MMMG equations are expressed in Taylor series expansions [11]. The forces on a ship in a turn are shown in Figure 10.

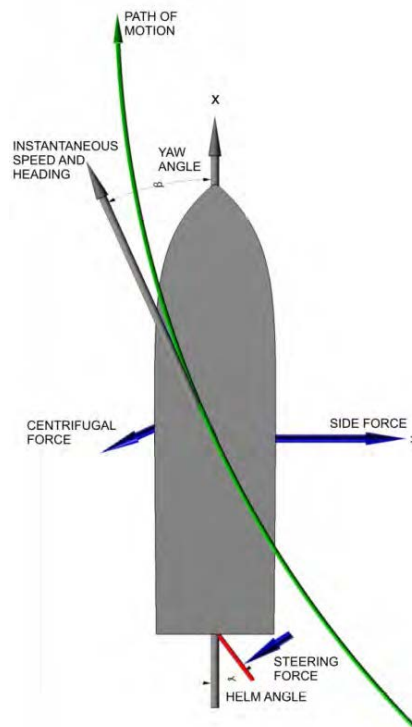


Figure 10. Free Body Diagram in a Steady Turn, from [4]

C. MANEUVERING CHARACTERISTICS

Maneuvering characteristics are developed in order to have a complete picture of the ship's maneuverability. These characteristics are based on ship-turning ability and include tactical diameter, advance, and transfer distances.

Tactical diameter is defined as the distance gained to the left or right of the original course after a turn of 180 degrees is completed. In a turning circle maneuver, the rudder angle must be a maximum design rudder angle at the test speed. *Advance* is the amount of distance run on the original course until the ship steadies on the new course. It is measured from the point where the rudder is first put over. *Transfer* is the amount of distance gained toward the new course. These motions are presented in Figure 11.

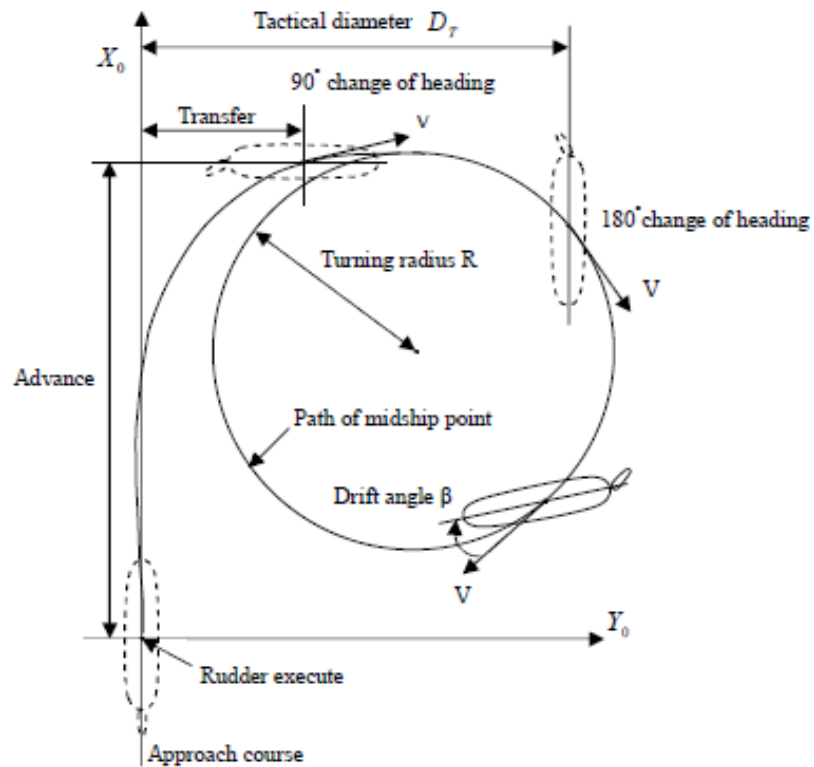


Figure 11. Advance, Transfer, and Tactical Diameter, from [5]

III. ANALYZING EXISTING MANEUVERING MODELS

A. INTRODUCTION

In ship construction, shipbuilding companies are using maneuvering models and simulations in design stage in order to meet IMO maneuvering standards. These models are generally used for displacement vessels because they should have adequate maneuverability to ensure a safe navigation.

In this chapter, these models are analyzed in order to understand the challenges and problems in maneuverability estimation of high-speed crafts. I am going to use these models for high-speed crafts to find reasonable maneuvering characteristics values that can be used in maneuvering predictions.

B. MANEUVERING PREDICTION PROGRAM (UNIVERSITY OF MICHIGAN)

1. Program Information

The Maneuvering Prediction Program (MPP) was developed by the University of Michigan's Department of Naval Architecture and Marine Engineering to support the teaching of conceptual ship design [12]. This program applies methods to find the hydrodynamic coefficients, turning ability, and controllability of a surface marine vehicle. We can find the estimated maneuvering characteristics of the given ship by using the basic parameters.

In order to run the program, input information of the vessel characteristics, steering characteristics, operation conditions, and water properties are needed.

The first input page is for vessel characteristics. Figure 12 shows the window in the program. The vessel characteristics are listed with units in Table 1.

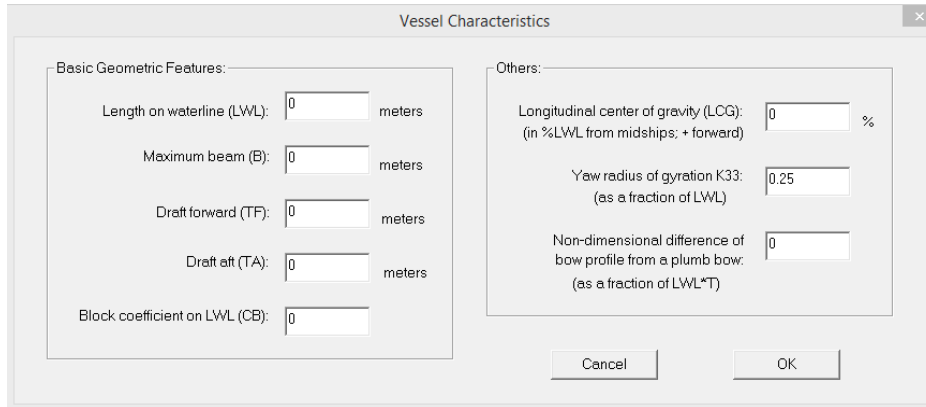


Figure 12. Vessel Characteristics at Input Page

Table 1. Vessel Characteristics with Units

Vessel Characteristics	
Length on waterline (LWL)	[meters]
Maximum Beam (B)	[meters]
Draft forward (TF)	[meters]
Draft aft (B)	[meters]
Block coefficient on LWL (CB)	Dimensionless

Length on Waterline (LWL): LWL is the length that goes along on the designed waterline from the forepart of the stern to the afterpart. Figure 13 shows the overall length of a vessel.

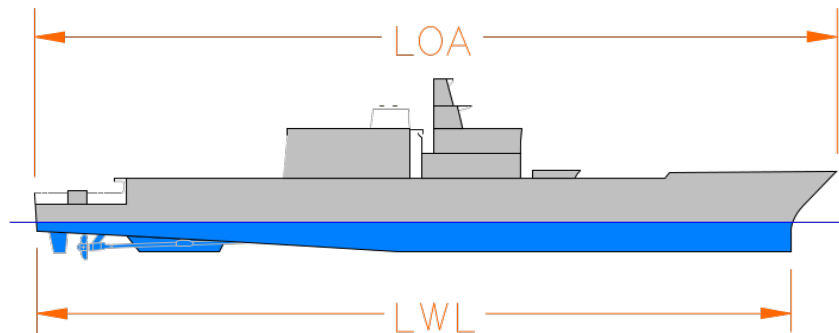


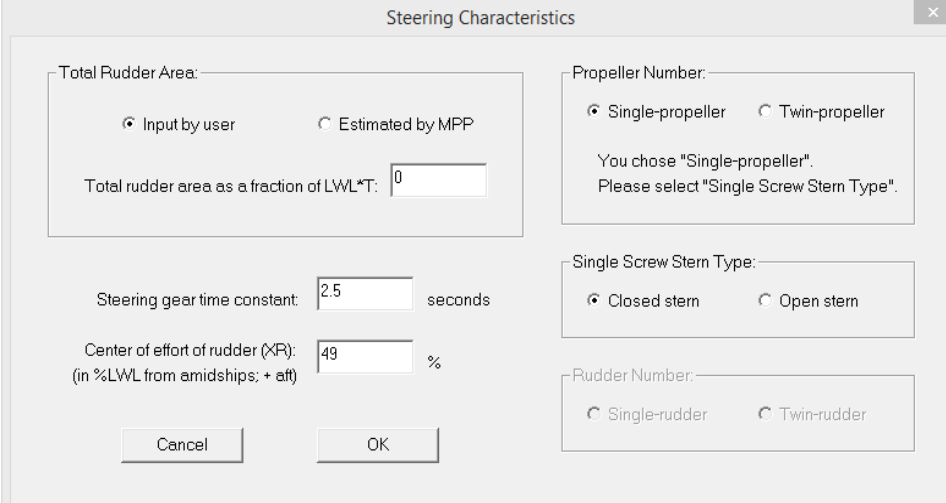
Figure 13. Length on Waterline of a Vessel, from [13]

Beam (B): *Beam* is the transverse dimension at the outside of hull amidships, or the greatest breadth.

Draft (T): *Draft* is the vertical measurement from the waterline to the bottom of the ship. Drafts are typically measured to the keel.

Block Coefficient: *Block coefficient* is the ratio of the immersed volume of the hull to the volume of a block made of the length, beam, and draft [14].

In the next input page, the program needs steering characteristics (see Figure 14). Since I couldn't find the rudder areas for every specific ship, I let the program estimate it. The propeller number was selected to be two because most of them have two propellers (see Figure 15).



The image shows a software dialog box titled "Steering Characteristics". It contains several input fields and radio button options. On the left, there are two radio buttons: "Input by user" (selected) and "Estimated by MPP". Below them is a text input field for "Total rudder area as a fraction of LWL*T" with the value "0". Further down are two more input fields: "Steering gear time constant" with the value "2.5" and the unit "seconds", and "Center of effort of rudder (XP): (in %LWL from amidships; + aft)" with the value "49" and the unit "%". At the bottom left are "Cancel" and "OK" buttons. On the right side, there are two radio buttons: "Single-propeller" (selected) and "Twin-propeller". Below them is a message: "You chose 'Single-propeller'. Please select 'Single Screw Stern Type'." This is followed by two radio buttons: "Closed stern" (selected) and "Open stern". At the bottom right, there are two radio buttons: "Single-rudder" (selected) and "Twin-rudder".

Figure 14. Steering Characteristics of the Vessel

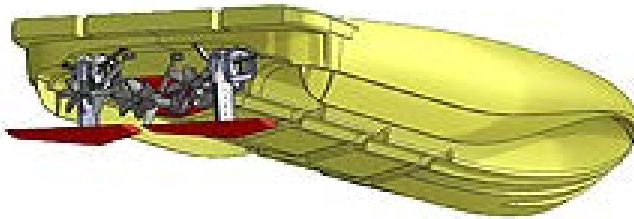


Figure 15. Typical Hull of the High-Speed Craft, from [15]

In operating conditions (see Figure 16), the water depth was selected to be deep waters because the high-speed boats are being used in deep waters such as the Mediterranean Sea and Persian Gulf. The initial or reference speed depends on the vessel. We are going to analyze the maneuvering characteristics for maximum speed.

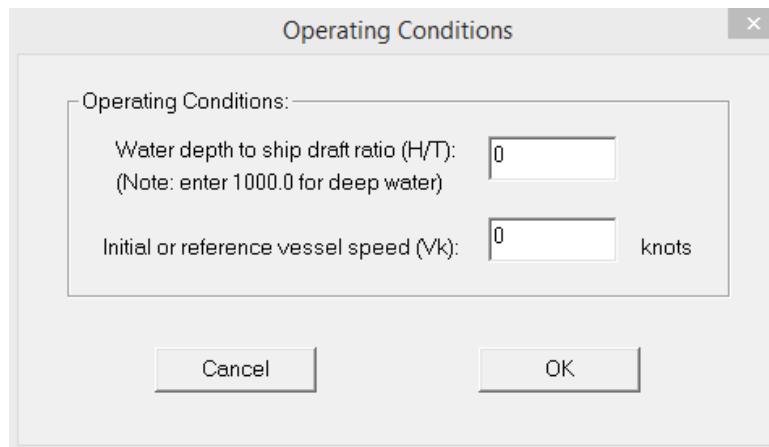


Figure 16. Operating Conditions

Water property is selected to be salt water at 15 degrees Celsius (see Figure 17).

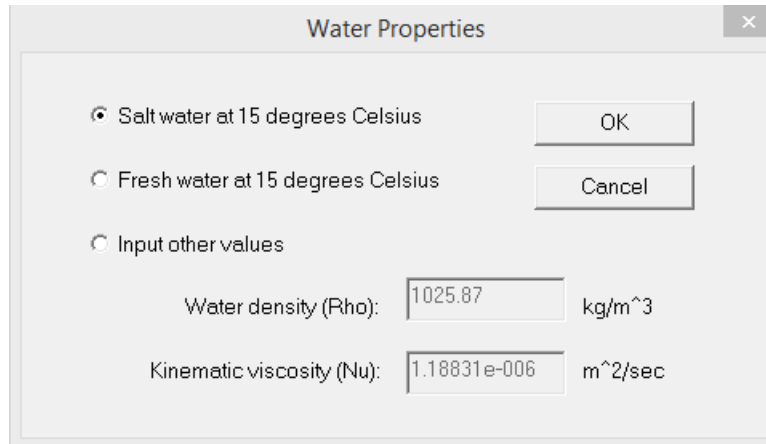


Figure 17. Water Properties

After I entered all of the input information into the Maneuvering Prediction Program, I could run the program for different rudder angles (see Figure 18).

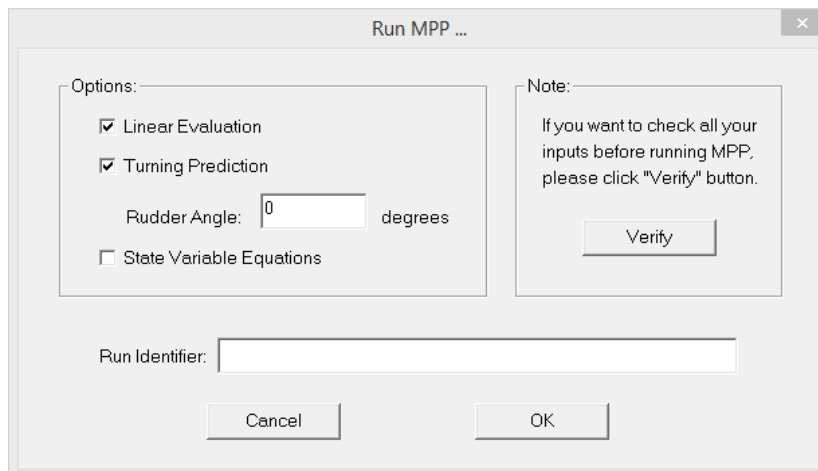


Figure 18. The Analysis Page

After introducing the program, I need vessel characteristics for specific high-speed crafts in order to run the program properly. Jane's Fighting Ship is a good source to get the data that needed. Since I am analyzing high-speed crafts, vessels in Table 2 were selected based on their length and maximum speed. The lengths of the ships are between 10 and 30 meters; their maximum speeds are between 43 and 72 knots.

Table 2. Basic Characteristics of the High-speed Crafts

Number	Country	Vessel Type	Length (meters)	Beam (meters)	Draft (meters)	Displacement (tons)	Max Speed (knots)
1	Iran	MIL 55 Class	16.43	2.85	0.84	15.5	72
2	Iran	MIL 40 Class	12.90	2.64	0.82	6	62
3	UAE	MRTP 16 Fast Intervention Craft	17.75	4.19	1.20	22	60
4	Oman	Fast Patrol Craft	27.40	5.50	1.50	55	45
5	Turkey	Kaan 20 Class	22.55	4.76	1.30	38	50
6	Mexico	Isla Class	25.00	5.40	1.20	53	50
7	Italy	V 2000 Class	13.20	3.40	0.90	11	45
8	Italy	V 600 Falco	10.20	2.80	0.80	4	54
9	Israel	Shaldag Class	24.80	6.00	1.20	59	50
10	USA	Riverine Boats	16.10	3.78	0.90	22.8	43
11	Kuwait	Victory Team P 46 Class	14.00	3.23	0.80	9	52

However, the block coefficients of sample vessels are missing in the table. I can find the volume and block coefficients with equation (14).

$$\nabla = \frac{\Delta}{g}$$

$$C_B = \frac{\nabla}{L.B.T} \quad (14)$$

where

g = Density of Salt Water, L = Length on waterline, B = Beam, T = Draft

The block coefficients for the ships are listed in Table 3.

Table 3. Block Coefficients of the High-Speed Crafts

Number	Country	Vessel Name	Disp. (tons)	Volume (m ³)	Block Coefficient
1	Iran	MIL 55 Class	15.5	15.12	0.38
2	Iran	MIL 40 Class	6	5.85	0.21
3	UAE	M RTP 16 Fast Intervention Craft	22	21.46	0.24
4	Oman	Fast Patrol Craft	55	53.66	0.24
5	Turkey	Kaan 20 Class	38	37.07	0.27
6	Mexico	Isla Class	53	51.71	0.32
7	Italy	V 2000 (N 61) class	11	10.73	0.27
8	Italy	V 600 Falco	4	3.90	0.17
9	Israel	Shaldag Class	59	57.56	0.32
10	United States	Riverine Command Boats	22.8	22.24	0.41
11	Kuwait	Victory Team P 46 Class	9	8.78	0.24

The MPP is used to find the maneuvering characteristics of the ships in the table. The program was run for maximum speed, and rudder angle was selected to be 30 degree as a maximum rudder angle.

2. Results and Discussions

The results of MPP are presented in Table 4.

Table 4. Results of the MPP

Number	Country	Vessel Name	Speed (knots)	Rudder Angle	Steady Turning Diameter (meters)	Steady Speed in Turn (knots)	Turning Radius to Length Ratio
1	Iran	MIL 55 class (Bradstone Challenger)	72	30	566.58	110.1	34.5
2	Iran	MIL 40 class	62	30	441.55	94.51	34.2
3	UAE	MRTP 16 Fast Intervention Craft	60	30	509.65	82.02	28.7
4	Oman	Fast Patrol Craft	45	30	523.21	49.15	19.1
5	Turkey	Kaan 20 class	50	30	500.93	59.07	22.2
6	Mexico	Isla class	50	30	523.3	57.24	20.9
7	Italy	V 2000 (N 61) class	45	30	331.11	56.85	25.1
8	Italy	V 600 Falco	54	30	336.82	80.46	33.0
9	Israel	Shaldag class	50	30	514.23	56.96	20.7
10	United States	Riverine command boats	43	30	345.55	49.88	21.5
11	Kuwait	Victory Team P 46 class	52	30	393.26	70.16	28.1

The results show that the turning-diameters-to-length ratios are over 20. The real sea trials that are presented by Denny and Hubble show that the results should be around 10–20 [16]. The program estimated higher standard turning radiuses than real values.

Both displacement ships and high-speed crafts have two common characteristics of a turn: the loss of speed in a turn and the presence of a drift or yaw angle [4]. I should expect a speed loss in turn. However, the results in Table 4 show that the steady speed in turning becomes even higher than the approach speed. This doesn't match with the phenomena that the speed of the vessel decreases in turn. Moreover, the speed cannot be higher than the maximum speed.

In order to find the reasons of this anomaly, I analyzed the formula to calculate turning speed. It is calculated with the empirical formula given by C. A. Lyster and H. L. Knights [17].

$$\frac{V_T}{V_A} = 0.543 + \frac{\text{TurningDiameter}}{\text{Length}} \quad (15)$$

After the equation was plotted for the higher turning-diameter-to-length ratios in Figure 19, we see that the ratio of turning speed to approach speed becomes bigger than one. Most of the turning-diameter-to-length ratios are bigger than 15.

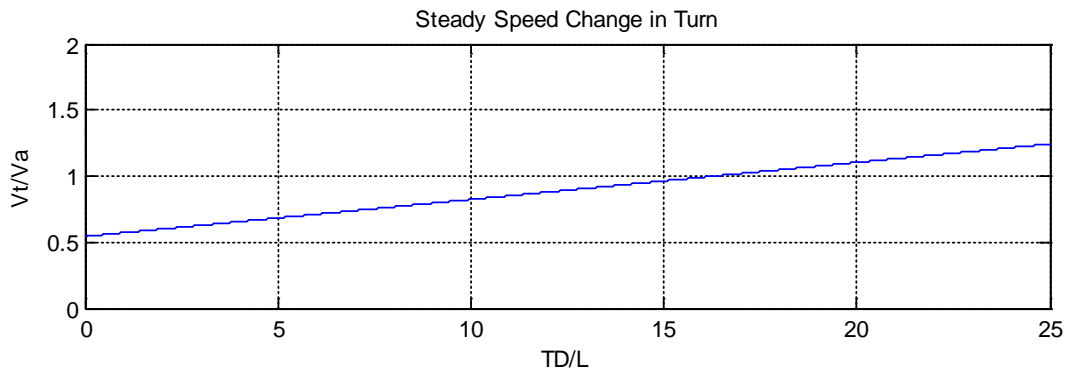


Figure 19. Turning Speed Ratio vs. Normalized Turning Diameter

The results show that the Maneuvering Prediction Program is not good enough to evaluate maneuvering characteristics of the type of small boats of interest to this study.

C. MATLAB SIMULATIONS BY FOSSEN

1. Program Information

According to equations in the *Handbook of Marine Craft Hydrodynamics and Motion Control*, a simulation program was developed in a MATLAB program [18]. The program includes several mathematical models of marine and flight vehicles intended for a course at the Norwegian Institute of Technology [19]. These vehicles are listed in Figure 20.

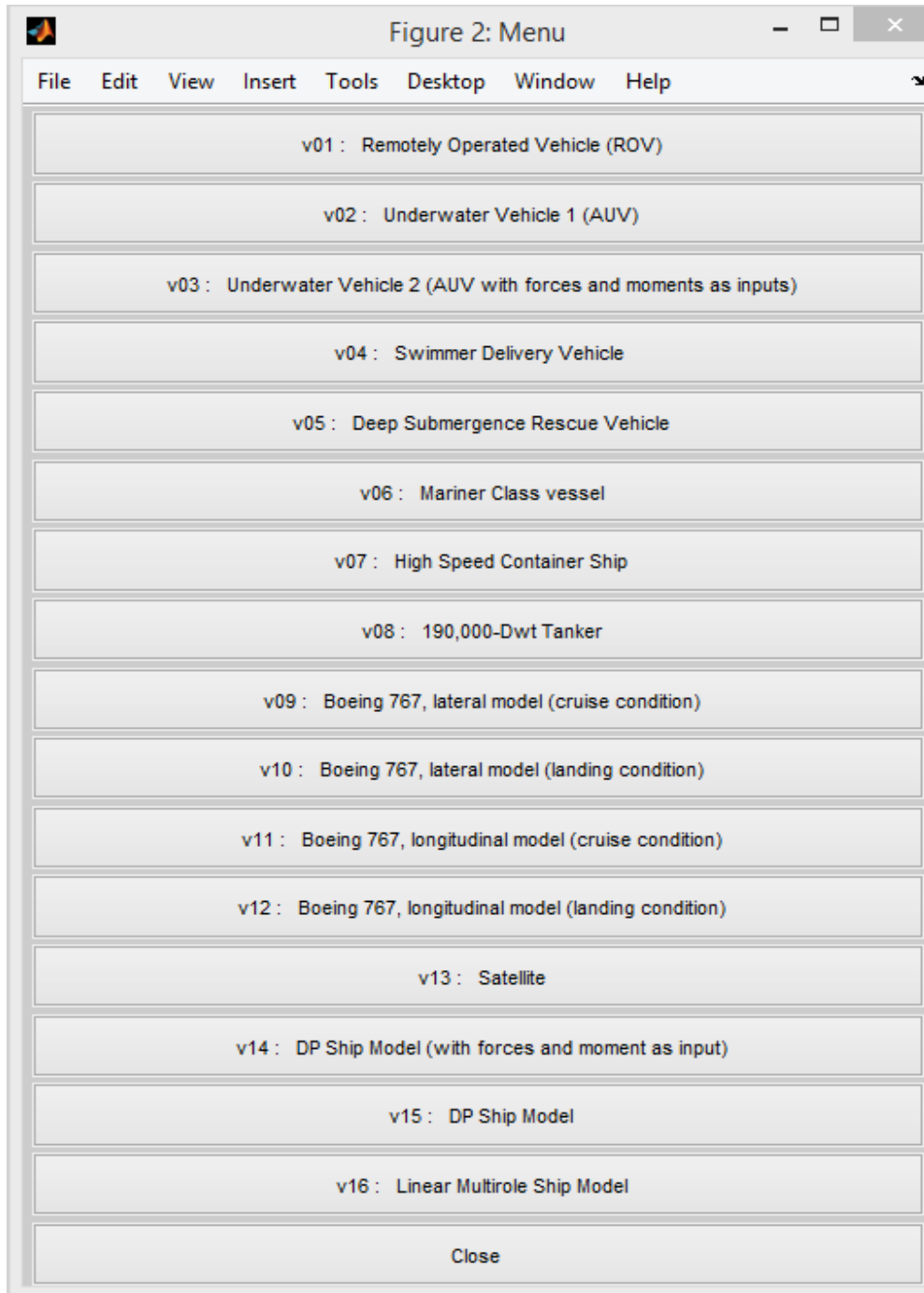


Figure 20. The Vehicles in MATLAB Program

Mariner Class Vessel, High-speed Container Ship, and Linear Multirole Ship Model simulations can be used for determining maneuvering characteristics. The vessel characteristics are listed in the following tables.

Table 5. The Vessel Characteristics of Mariner Class Ship

Marine Class Ship Characteristics	
Length	160.93 meters
Speed	7.7175 [m/sec] 15 [knots]

Table 6. The Vessel Characteristics of High-speed Container

Marine Class Ship Characteristics	
Length	175 meters
Speed	7.7175 [m/sec] 15 [knots]

Table 7. The Vessel Characteristics of Multirole Naval Ship

Marine Class Ship Characteristics	
Length	48 meters
Beam	8.6 meters
Draft	2.2 meters
Displacement	350 tons

Each vessel in the program has different vessel characteristics. Among these vessels, the Multirole Naval Ship Model has the most similar vessel characteristics with the high-speed craft of study. So I used Multirole Naval Ship Model for my analysis.

2. Results and Discussions

I can run the program for different speeds for the Multirole Naval Ship Model. One of the best features of this program is visualizing the motion in the horizontal plane. The results in x_0 - y_0 coordinates are shown in Figures 21–24.

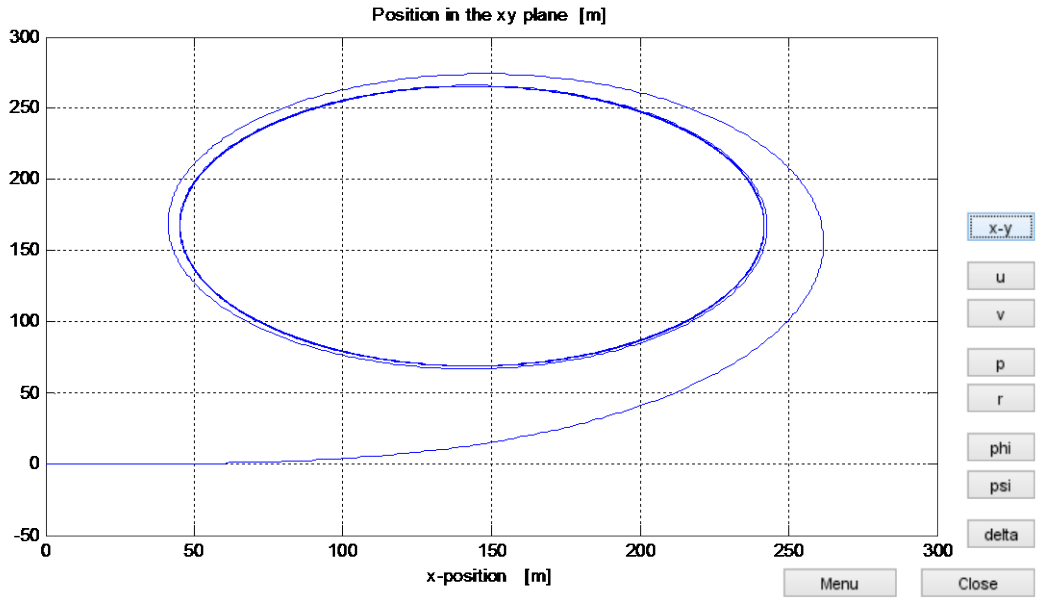


Figure 21. Turning Motion of Multirole Naval Ship with 15.43 m/s [30 knots]

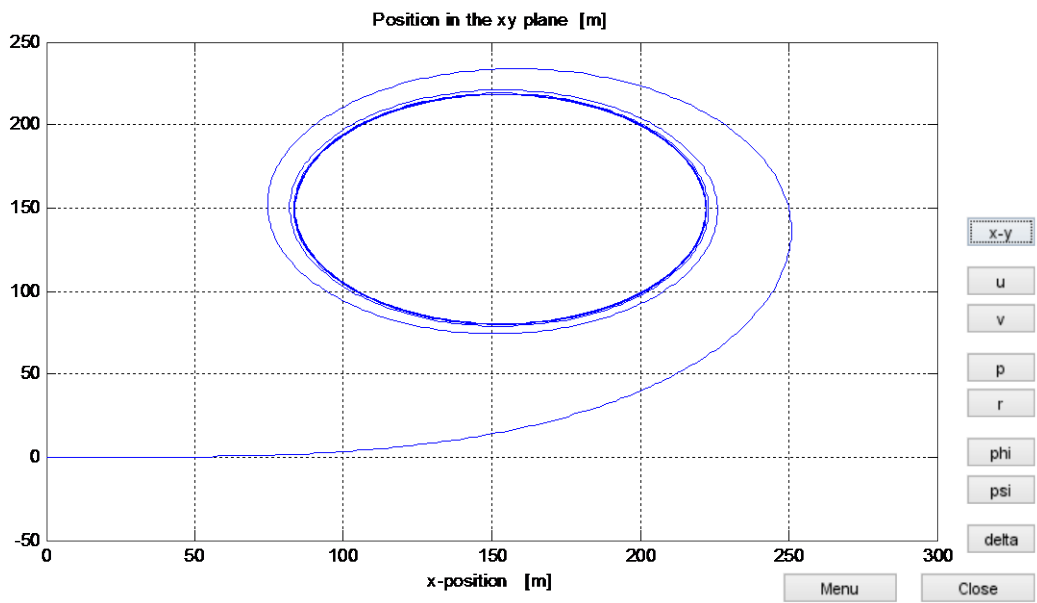


Figure 22. Turning Motion of Multirole Naval Ship with 20.57 m/s [40 knots]

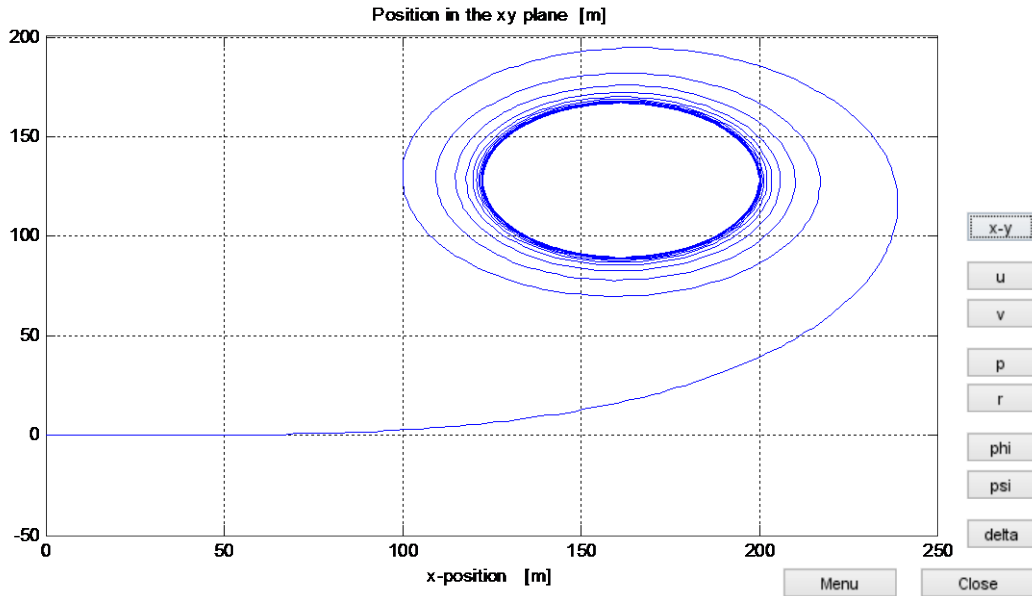


Figure 23. Turning Motion of Multirole Naval Ship with 25.72 m/s [50 knots]

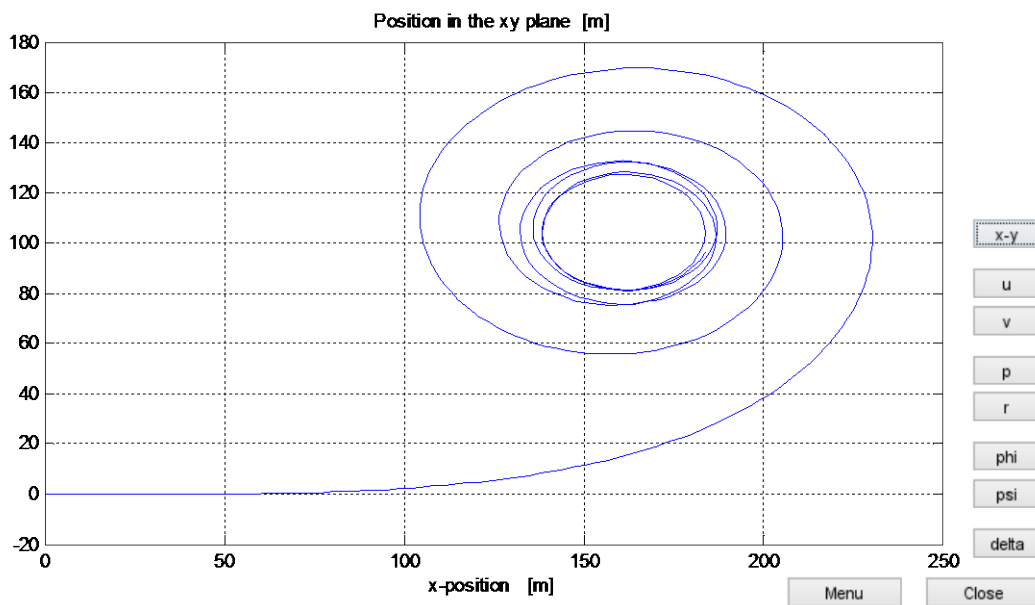


Figure 24. Turning Motion of Multirole Naval Ship with 30.86 m/s [60 knots]

The results show that as the speed is increased in MATLAB simulation, the turning radius of the vessel decreases. The turning diameter decreases about 50 meters at 60 knots, which cannot be possible in real conditions. According to Denny-Hubble, the turning radius increases with speed in sea trials. [16]

The steady speed in turn is stayed the same in all simulations. However, I should expect a speed decrease in turning. For illustration, the speed change is shown just for 60 knots (30.86 m/s) in Figure 25, and it is the same for every speed.

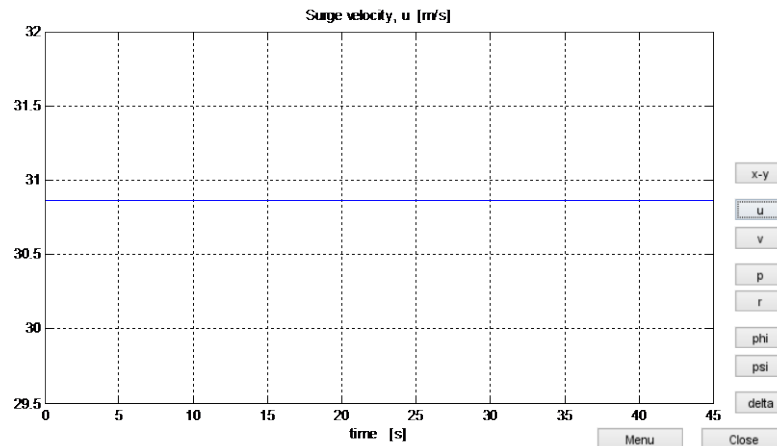


Figure 25. Steady Speed Change in Time for 30.86 m/s [60 knots]

The program does not let us evaluate other vessels properly even if I change the length, beam, or other vessel characteristics. This is because the hydrodynamic coefficients stay fixed. The results show that the MATLAB simulation by Fossen is not appropriate for our application to evaluate maneuvering characteristics.

In conclusion, the existing maneuvering models that are analyzed in this chapter are generally used for evaluating maneuvering characteristics of displacement vessels. These models cannot be applied to small high-speed boats, so a new model must be developed.

THIS PAGE INTENTIONALLY LEFT BLANK

IV. MODEL DEVELOPMENT & SIMULATION MODEL

A. INTRODUCTION

A mathematical model for the maneuvering characteristics of high-speed craft is derived in this chapter. The objective of the mathematical model is to provide motion profiles for the boat which will then lead to predictable targeting information.

The forces and moments of high-speed craft will not be in balance when the vessel enters a turning with some angle of helm. The vessel will slow down because the craft is exposed to added drag in a turn. This speed loss is significant when compared to displacement vessels. The other phenomenon for high-speed craft is roll motion. It is generally neglected for displacement vessels but it is significant for high-speed crafts in turns [6].

Static and dynamic forces affect the accuracy of calculations; the force coefficients are non-linear with speed. However, high-speed craft show similar behaviors to a displacement ship at a slow speed, because the dynamics effects are at a minimum level at these speeds and yaw angle is not big enough to develop a steady roll angle [4].

B. EQUATIONS BY LEWANDOWSKI

The most recent study about turning characteristics of high-speed crafts was done by Lewandowski in 2004. The static and dynamic equations of equilibrium of high-speed crafts have been developed and presented. According to the study, the prediction of the turning performance of high-speed crafts becomes difficult for the following reasons [6]:

The hydrodynamic coefficients are highly speed-dependent.

Motions are strongly coupled.

In calm weather, the heave and pitch characteristics are insignificant to turning ability. For traditional maneuvering and seakeeping analysis, it is assumed that the geometry of the wetted hull surface is constant; however, for high-speed craft, dynamic

lift is developed which results in a reduction in draft compared to static conditions [6]. Therefore, all hydrodynamic coefficients are strongly dependent on speed [4].

For these hydrodynamic coefficients, Lewandowski derived and proposed empirical equations. The equations are based on quantities that are listed in Table 8 which are dependent on speed. The quantities are illustrated in Figure 26.

Table 8. Variables in the Lewandowski Equations

Quantities	
C_v	Speed Coefficient
τ	Dynamic Trim (positive bow up)
L_k	Wetted length of keel
L_c	Wetted length of chine
T	Transom draft

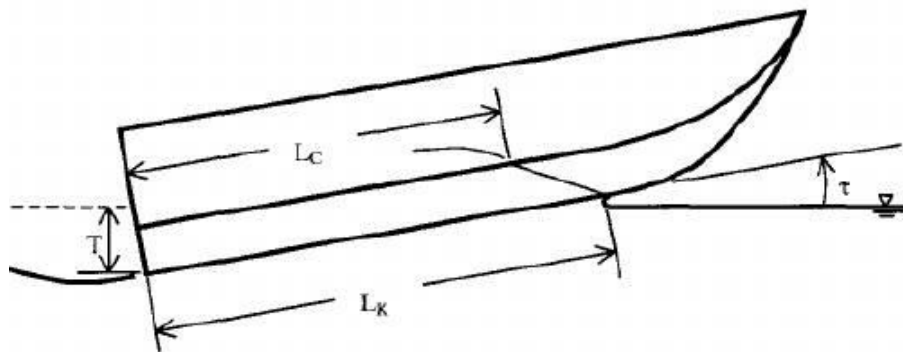


Figure 26. L_k and L_c of the Vessel, from [6]

However, a simple expression to estimate the approximate turning radius of high-speed craft is derived by Lewandowski [6] from the full-scale data and sea trials in Denny and Hubble's [16] work. According to this equation, the turning radius depends on length, volume, volumetric Froude number, and rudder angle.

$$\frac{STD}{L} \approx \left[1.7 + 0.0222 F_{\nabla} \left(\frac{L}{\nabla^{1/3}} \right)^{2.85} \right] \left(\frac{30}{\delta} \right) \quad (16)$$

For

$$\begin{aligned} 0.3 < F_{\nabla} < 4 \\ 4.5 \leq L/\nabla^{1/3} \leq 7 \end{aligned} \quad (17)$$

where

$$F_{\nabla} = \frac{U}{\sqrt{g\nabla^{1/3}}} \quad (18)$$

U = approach speed, L = the length on waterline, δ = rudder angle

Since dimensional data had already been collected from Jane's Fighting Ships, I can calculate volumetric Froude numbers and volumetric coefficients in order to see if the Lewandowski equations are applicable. These values are listed in Table 9.

Table 9. Volume Coefficients and Volumetric Froude Number of The Vessels

Number	Vessel Type	Length on Waterline (LWL) (meters)	Disp. (Tons)	Volume (m ³)	Max Speed (knots)	Max Speed (m/sec)	Vol. Coef	Froude Number
1	V 600 Falco	10.2	4	3.9	54.0	27.8	6.5	7.1
2	MIL 40 class	12.9	6	5.9	62.0	31.9	7.2	7.6
3	V 2000 (N 61) class	13.2	11	10.7	45.0	23.1	6.0	5.0
4	Victory Team P 46 class	14.0	9	8.8	52.0	26.7	6.8	5.9
5	Riverine command boats	16.1	22.8	22.2	43.0	22.1	5.7	4.2
6	MIL 55 class	16.4	15.5	15.1	72.0	37.0	6.6	7.5
7	MRTP 16 Fast Intervention Craft	17.8	22	21.5	60.0	30.9	6.4	5.9
8	Kaan 20 class	22.6	38	37.1	50.0	25.7	6.8	4.5
9	Shaldag class	24.8	59	57.6	50.0	25.7	6.4	4.2
10	Isla class	25.0	53	51.7	50.0	25.7	6.7	4.3
11	Fast Patrol Craft	27.4000	55	53.7	45.0	23.1	7.3	3.8

All volumetric coefficients are in the specified range and the volumetric Froude numbers are close to the upper limit of its specified range. As a result, I am going to use the Lewandowski equations to evaluate maneuvering characteristics of high-speed crafts in Table 9.

However, the length isn't specified clearly in equation (15). Figure 26 shows that there are three different length values for high-speed crafts. These length values are the length on waterline, which is specified as LWL; wetted length of keel, which is specified as Lk; and wetted length of chine, which is Lc.

In order to make a better maneuvering estimation, I decided to calculate standard turning diameter for each different length (LWL, Lk, Lc), naming them STD, STDk, and STDc. However, the wetted length of chine and the wetted length of keel are functions of speed. As speed increases, Lc and Lk values decrease. Raju Datla [20] has Lc and Lk data for different speeds for a specific vessel, so I used this data to correlate Lc/L and Lk/L as a function of the volumetric Froude number.

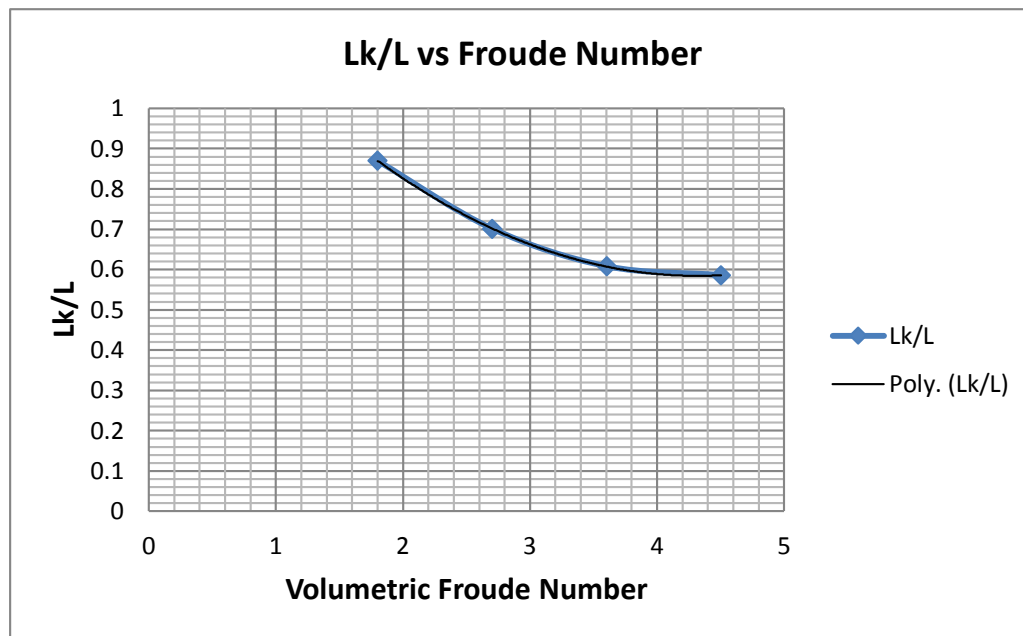


Figure 27. Lk/L vs. Volumetric Froude Number

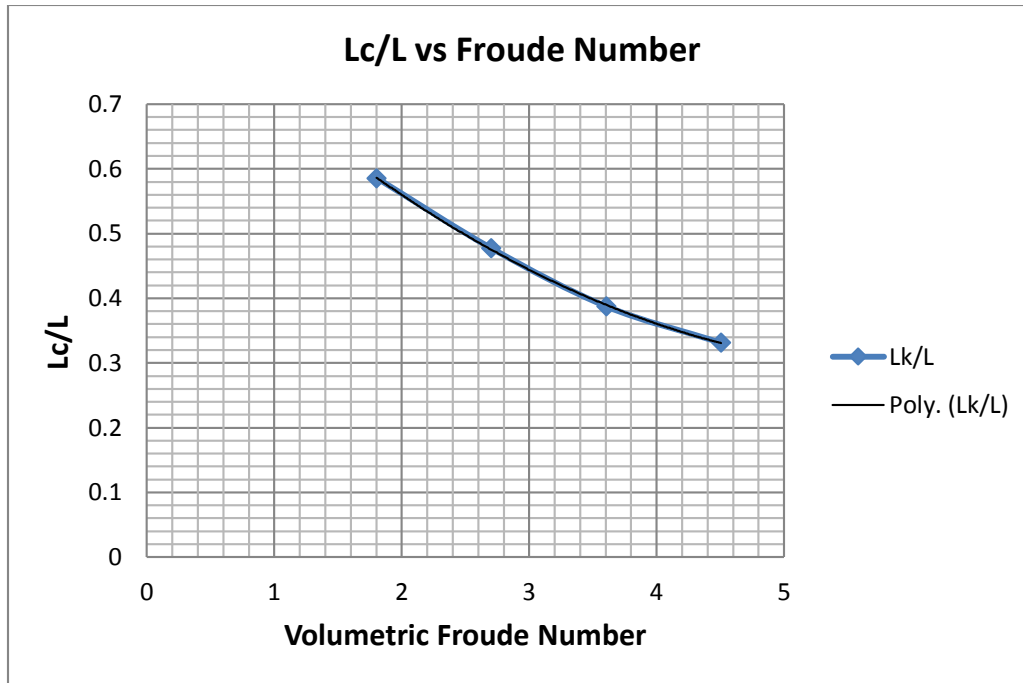


Figure 28. L_c/L vs. Volumetric Froude Number

The correlations between L_k/L & L_c/L and volumetric Froude number are presented in equation (19).

$$\begin{aligned} L_k / L &= 0.0452(\text{Vol. Froude Number})^2 - 0.3897(\text{Vol. Froude Number}) + 1.4251 \\ L_c / L &= 0.0161(\text{Vol. Froude Number})^2 - 0.1961(\text{Vol. Froude Number}) + 0.888 \end{aligned} \quad (19)$$

The next step is to make plots of standard turning diameters (STD, STD_k, and STD_c) versus LWL with the help of MATLAB. The first calculations are for 40 knots speed, 30-degree rudder angle, and different length values.

For standard turning diameter calculations, I need displacement data for any different lengths in order to find the volumetric Froude number and volumetric coefficient at each length. Since I have the displacement and length data for high-speed crafts, a correlation between the displacement and the length may be found. The data and the correlation are shown in Table 10 and Figure 29.

Table 10. Length and Displacement Data of the Vessels

Number	Vessel Characteristics	Country	Length on Waterline (LWL) (meters)	Displacement (tons)
1	V 600 Falco	Italy	10.2	4
2	MIL 40 class	Iran	12.9	6
3	V 2000 (N 61) class	Italy	13.2	11
4	Victory Team P 46 class	Kuwait	14.0	9
5	Riverine command boats	United States	16.1	22.8
6	MIL 55 class	Iran	16.4	15.5
7	MRTP 16 Fast Intervention Craft	UAE	17.8	22
8	Kaan 20 class	Turkey	22.6	38
9	Shaldag class	Israel	24.8	59
10	Isla class	Mexico	25.0	53

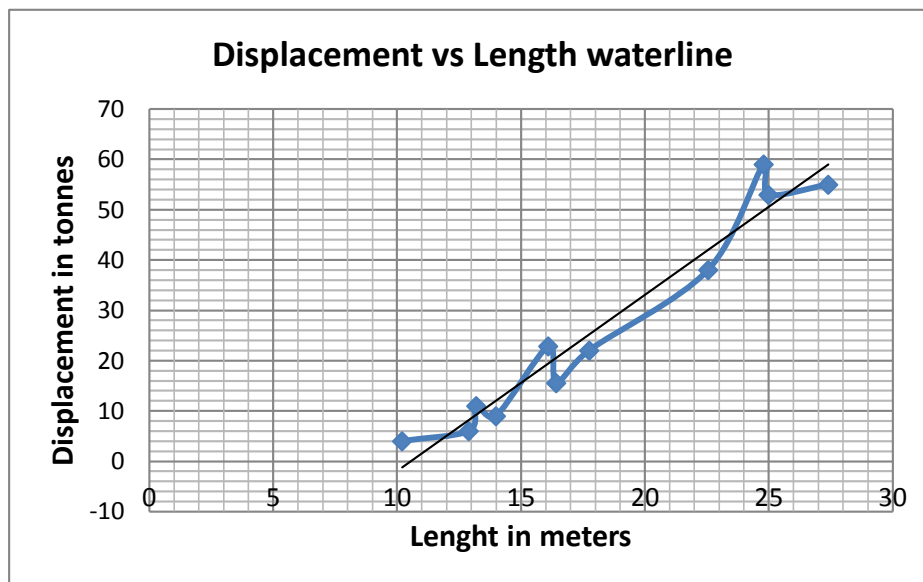


Figure 29. The Correlation Between Length and Displacement

The correlation between displacement and length is presented in equation (20).

$$Displacement = 3.5011xLength - 36.916 \quad (20)$$

Plots are generated for STD, STDk, and STDc as a function of length on waterline in one figure in order to compare them easily (see Figure 30 and Figure 31).

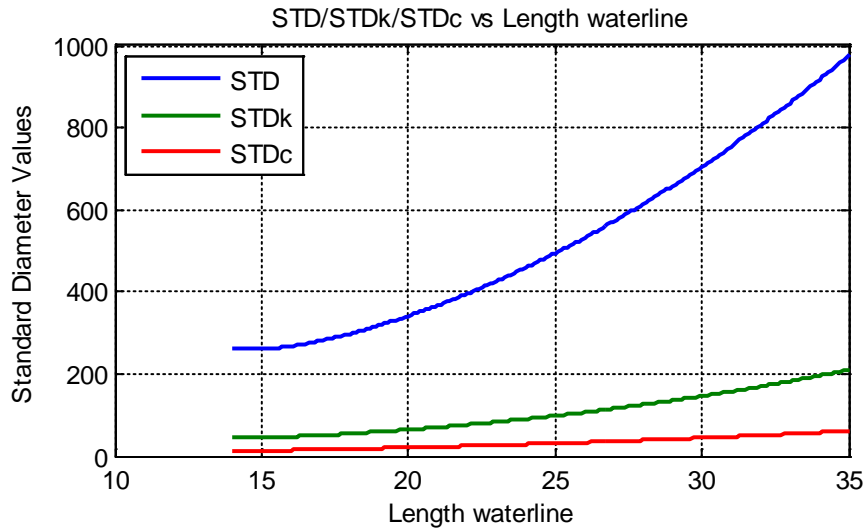


Figure 30. Standard Turning Diameter vs. Length

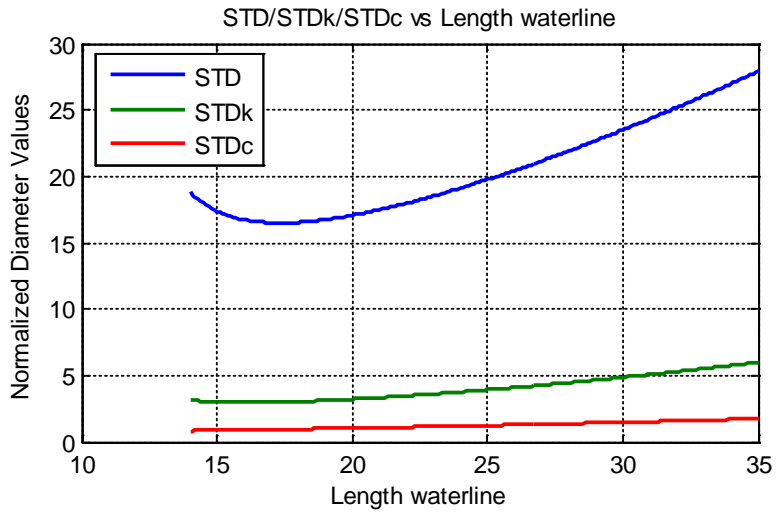


Figure 31. Normalized Turning Diameter vs. Length

The normalized turning diameters calculated with LWL (STD) are reasonable. Jeffrey Bowles made a comparison with test data and predicted results in his study [4]. The test and predicted TD/LWL (turning diameter/length ratio) results in his study are between 10 and 20 which are consistent with the predicted normalized STD results in my study. However, Figure 31 shows that normalized STDc stays around 2–3, and normalized STDk stays around 4–5. These values cannot satisfy Figure 32, so they are not reasonable.

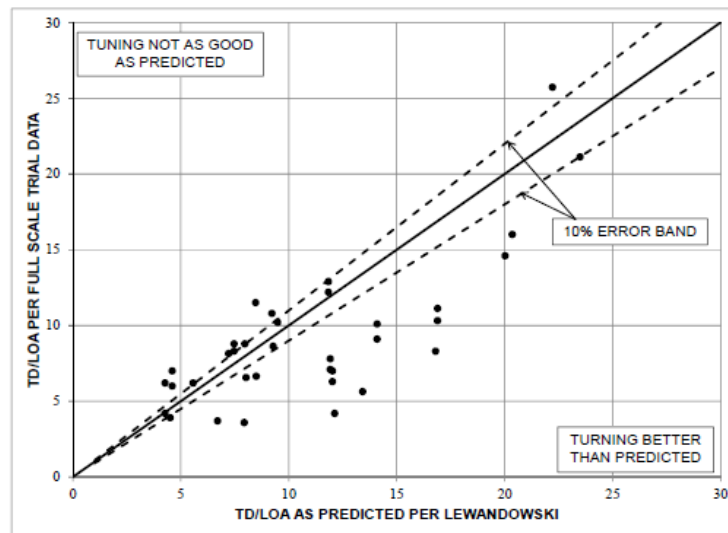


Figure 32. TD/LOA Comparison Between Full Scale Data and Prediction By Lewandowski, from [4]

In the next step, the normalized turning diameter is plotted against rudder angle values in order to see the rudder angle effect. The speed is selected to be 40 knots. The results are shown in Figure 33.

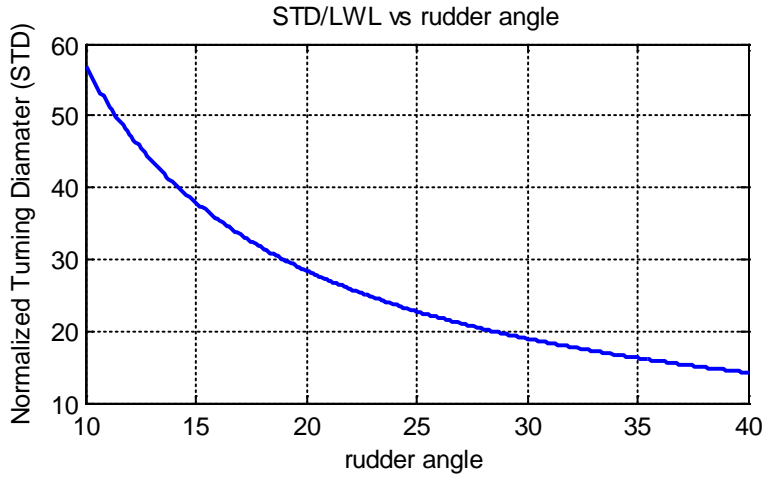


Figure 33. Normalized Turning Diameter vs. Rudder Angle for MRTP 16 Fast Intervention Craft

The normalized turning diameter versus different speed is plotted in Figure 34. Here we can also see that STD/LWL is more reasonable than others, since as I increase the speed, the normalized turning radius increases.

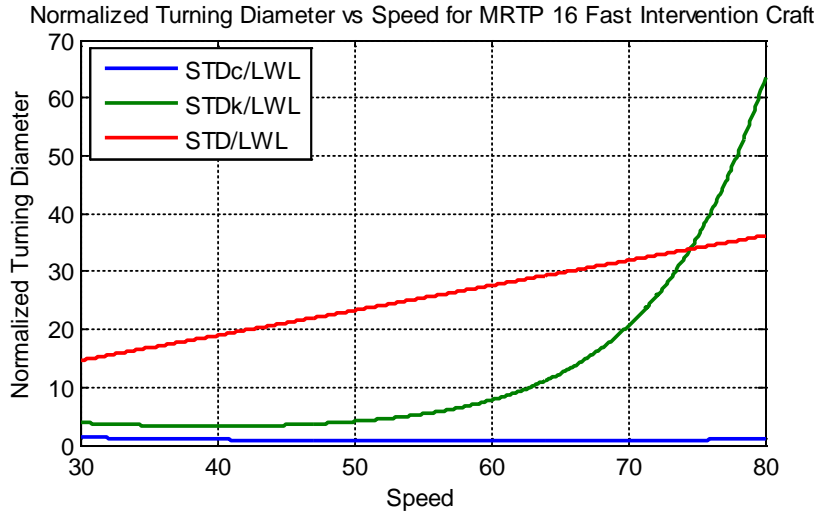


Figure 34. Normalized Turning Diameter vs. Speed for MRTP 16 Fast Intervention Craft

C. EQUATIONS BY DENNY AND HUBBLE

A study for predicting turning radius and turning rate of high-speed crafts is presented by Hubble [16]. The predictions can be used for crafts up to 33.52 meters (100 feet) length, which fits well with my study case. Since I am analyzing high-speed craft, I can find the speed decrease during the turn by using equations presented by Hubble after calculating the standard turning radius. These equations are listed below.

$$(U_c / U_A)^2 = 1 / \left[1 + K_c (L / R_c)^2 \right] \quad (21)$$

where L = length on waterline, Kc = empirical constant, Ua = approach speed, and Uc = steady speed in a turn.

The ratio of steady speed in a turn to approach speed becomes as follows:

$$U_c / U_a = \sqrt{\left(1 / \left[1 + K_c (L / R_c)^2 \right] \right)} \quad (22)$$

where

$$K_c = F_v^2 \times 30 / \delta \quad (23)$$

The turning radius equation based on Uc/Ua was presented by Hubble.

$$L / R_c = \left[(U_A^2 - U_c^2) / (K_c U_c^2) \right]^{1/2} \quad (24)$$

Rearranging the equation, the normalized turning radius becomes

$$\frac{R_c}{L} = \left[\frac{1}{\left(\frac{U_A}{U_c} \right)^2 - 1} \right]^{1/2} F_v \left(\frac{30}{\delta} \right) \quad (25)$$

The normalized turning radiuses are plotted for different Uc/Ua values in Figure 35.

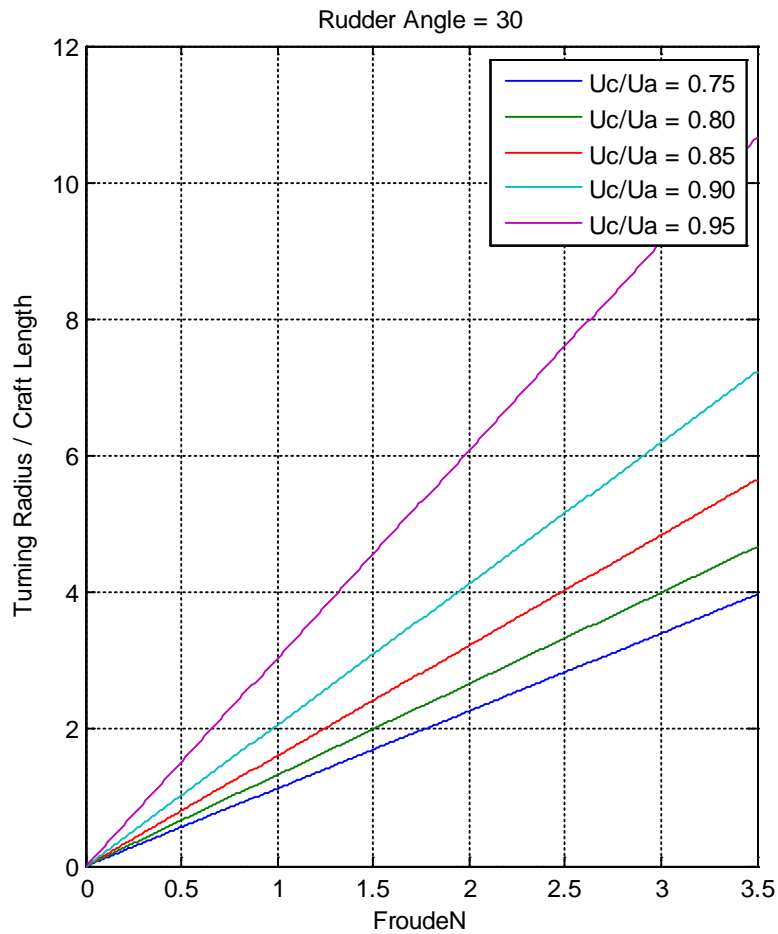


Figure 35. The Plots of Turning Radius for Different U_c/U_a Values, from [16]

In order to see consistency of Lewandowski equations and Denny-Hubble equations, I compare the predictions for normalized turning diameter of Shaldag class vessels in Figure 36. The predicted normalized turning diameters values from the paper “Prediction of Craft Turning Characteristics” [16] matches with the predicted results that are from Lewandowski equations when I use LWL (STD). From the results, it is clear that the Lewandowski equation is using length on waterline.

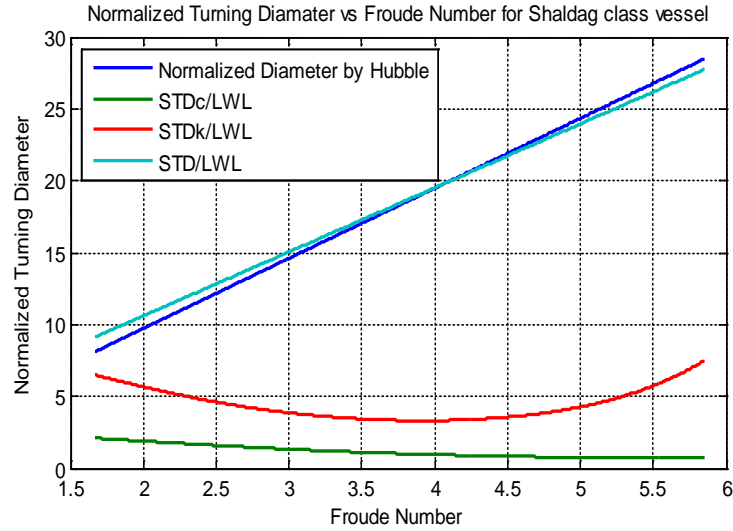


Figure 36. Comparison of Turning Diameter of Shaldag Class Vessel

The speed reduction formula was developed in equation (22), using the formula and plotted speed reduction versus rudder angle. As expected, speed reduction increases with a higher rudder angle. We can see the result in Figure 37.

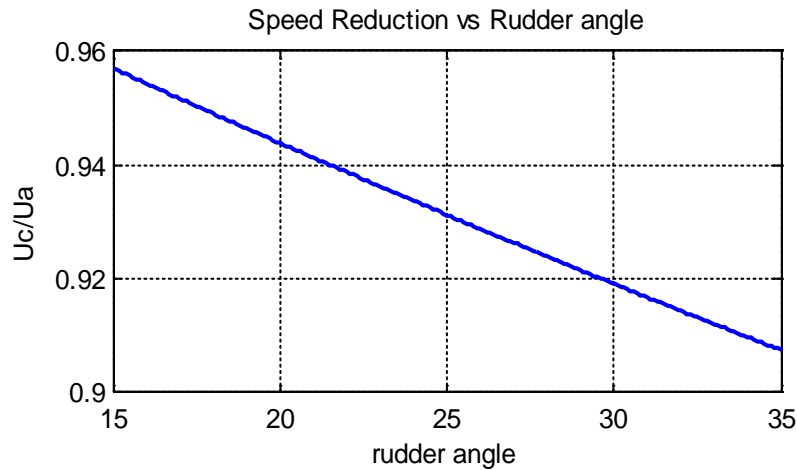


Figure 37. Speed Reduction with Given Rudder Angle

D. NOMOTO EQUATIONS (STABILITY AND CONTROL)

Several simplified models have been developed to evaluate the stability of a ship in a preliminary design stage. Nomotos's K-T model is one of the most notable ones. This model is used for comparing course-keeping and turning abilities [21].

In order to run the model in time domain, I use Nomoto's equations. The linear sway-yaw equations are transformed into the Nomoto equations in second and first order [22].

Nomoto's second order transfer function is

$$\frac{r}{\delta} = \frac{K + T_3 s}{T_1 T_2 s^2 + (T_1 + T_2) s + 1} \quad (26)$$

This equation can be expressed in time domain as

$$T_1 T_2 \ddot{r} + (T_1 + T_2) \dot{r} + r = K(\delta + T_3 \dot{\delta}) \quad (27)$$

Nomoto's first order transfer function is

$$\frac{r}{\delta} = \frac{K}{1 + TS} \quad (28)$$

This equation can be expressed in time domain as

$$T\dot{r} + r = K\delta \quad (29)$$

where

$$\begin{aligned} r &= \dot{\psi} \\ T &= \frac{\text{yaw inertia coefficient}}{\text{yaw damping coefficient}} \\ K &= \frac{\text{Turning moment coefficient}}{\text{yaw damping coefficient}} \end{aligned} \quad (30)$$

T = Course Stability, 1/T = Responsiveness to rudder, K = Turning ability

For simplicity, I am going to use Nomoto's first order equations. As an assumption, I choose yaw inertia coefficient (T) zero, in order to start the calculations.

$$K\delta_{\max} = \frac{U_R}{R} \quad (31)$$

$$K = \frac{U}{R\delta} \quad (32)$$

where R is the turning radius and δ is the rudder angle. I have calculated turning radius before. Because I can find K constant, this helps us to define the r value. By integration, I can find the ψ values.

$$\dot{\psi} = r = k\delta \quad (33)$$

I assume the T to be zero; however, I need to find a coefficient to satisfy the Lewandowski equations. Both the turning radius from Lewandowski and from the model should be consistent. The correction coefficient is found to be $\eta = 0.909$. The correction coefficient is the ratio between turning radiuses; in this way, the results become consistent.

$$\dot{\psi} = r = k\delta\eta \quad (34)$$

$$\psi = \int K\delta(t)\eta dt \quad (35)$$

Since I have calculated the speed for different rudder angles, I can transform the motion into an x-y coordinate system.

$$\begin{aligned} \dot{x} &= U(t)\sin(\psi) \\ \dot{y} &= U(t)\cos(\psi) \end{aligned} \quad (36)$$

With MATLAB integrator, I can find the x and y portion of the vessel at any time with any initial conditions.

E. MODEL IN MATLAB SIMULINK

Simulink is a modeling program that is integrated with MATLAB. It enables us to create block diagrams for simulations and designs. It supports plotting the motions for time-based continuous equations, and with it, we can model linear and nonlinear systems. The program has a library that can provide predefined and definable blocks.

After I found the equations to determine maneuvering characteristics, I could create a Simulink model to run these equations in the time domain. Nomoto's equation is used to create this Simulink model. First I made the basic schematic diagram of the mathematical model in Figure 38. The Motion 1 block shows us the motion for constant speed and given rudder angle. After the instant speed can be calculated according to

rudder angle, the Motion 2 block shows us the motion with instant speed and rudder angle.

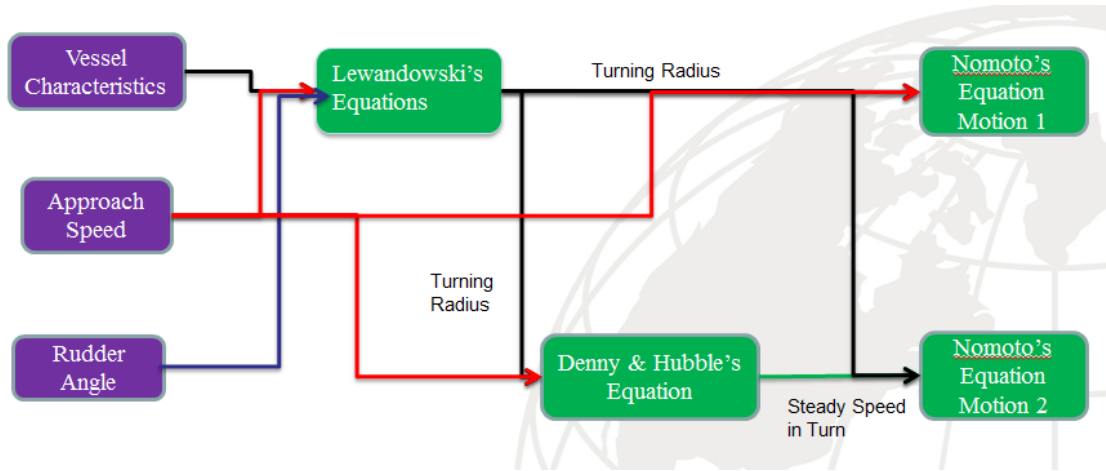


Figure 38. The Basic Diagram of the Mathematical Model

The mathematical model is presented in Figure 39. The blocks in this Simulink model are listed in this section; the functions in these blocks are written in MATLAB and presented in Appendix B.

Volumetric Froude Number Block: This block calculates the volumetric Froude number with speed and volume input.

Kc Block: In this block, Kc value is calculated using with the rudder angle and volumetric Froude number. Kc is going to be used to calculate the speed according to rudder angle.

Lewandowski Equation: This block finds the normalized turning radius according to speed, volumetric coefficient, and rudder angle.

Hubble Block: This block calculates the instant speed of the vessel during the simulation.

Nomoto Equation Block: The instant speed and the turning radius are used to make a continuous motion.

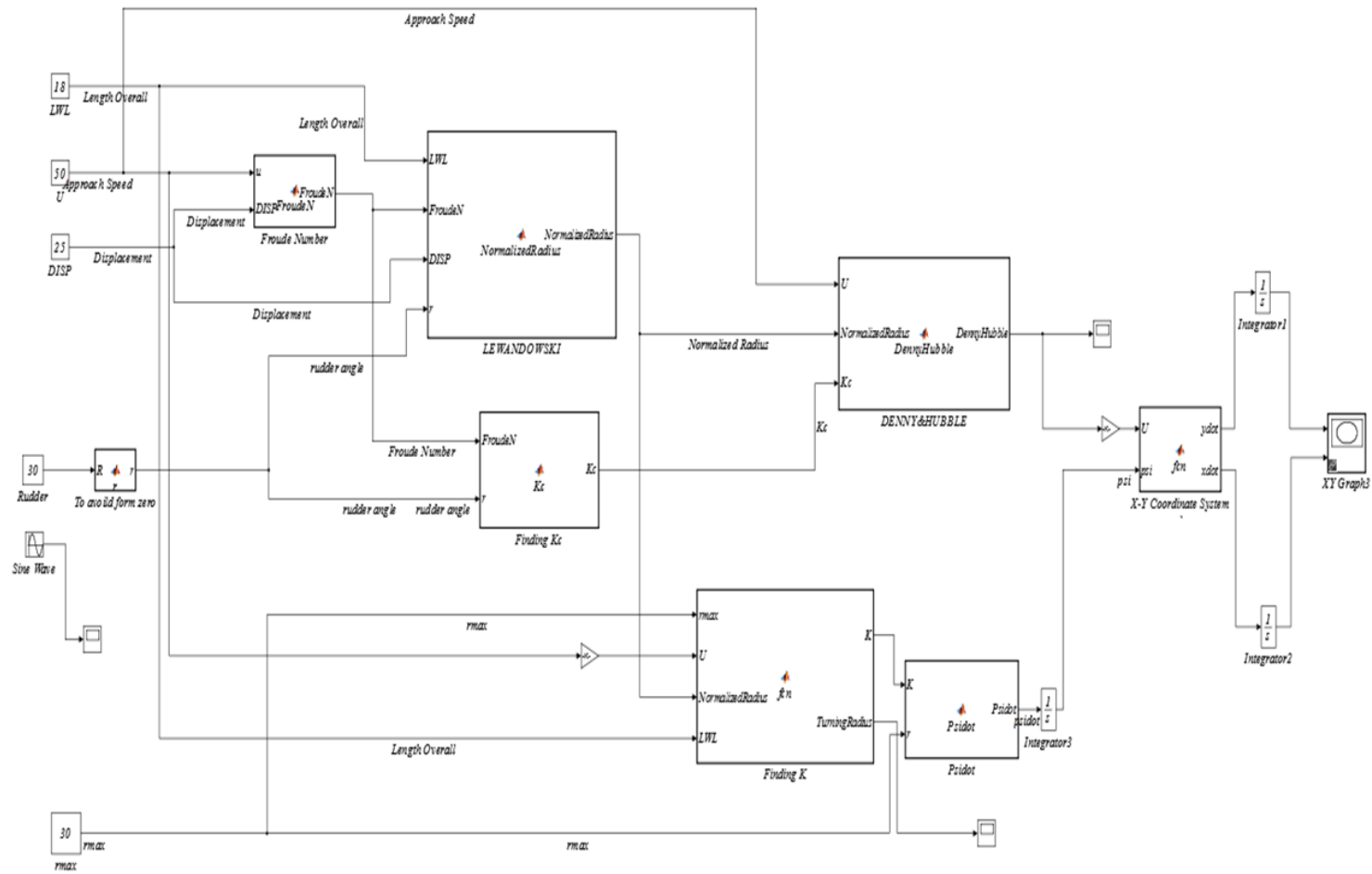


Figure 39. The Block Diagram of the Mathematical Model

F. RESULTS AND DISCUSSION

In the MATLAB Simulink model, I need to input the vessel characteristics, including length on waterline and displacement, and the operating characteristics, including speed and rudder angle. The model estimates the turning radius and steady speed in turn with the equations presented previously. With the help of Nomoto's first order equation, the motion is presented on the horizontal plane.

The sample model inputs (MRTP 16 Fast Intervention Craft) are as follows:

- LWL = 17.8 meters
- Displacement = 22 tons
- Rudder angle = 0, 30
- Approach Speed = 40 knots, 50 knots, 60 knots

To see the reactions for different speeds, lengths, and rudder angle, I make some sample runs. The results are shown in Figures 40–44.

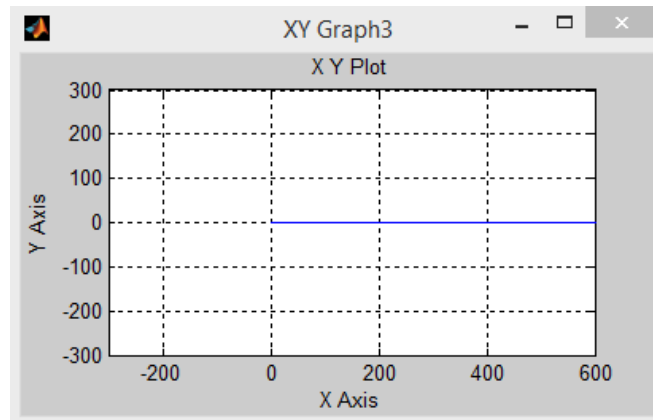


Figure 40. Vessel Movement with 40 Knots and 0 Rudder Angle

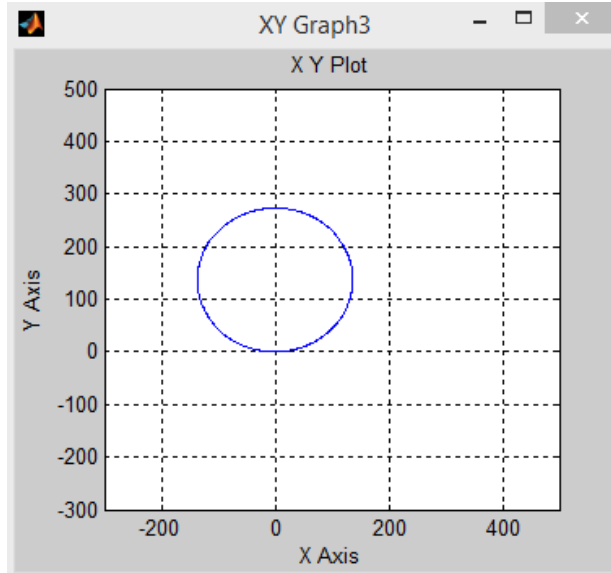


Figure 41. Turning Radius of a Vessel with 40 Knots and 30 Rudder Angle

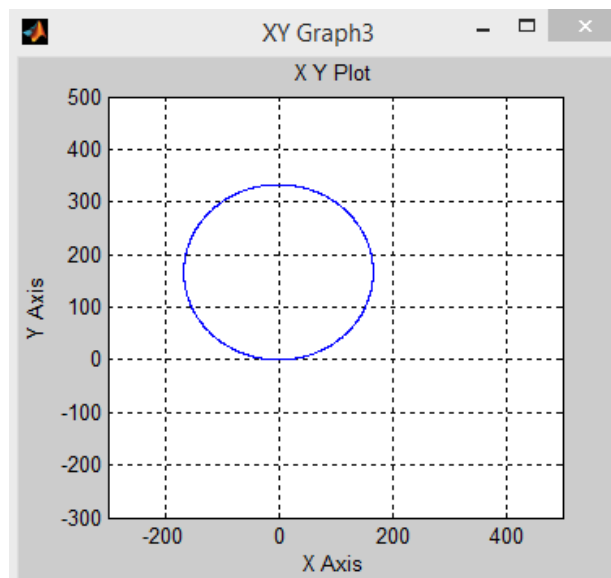


Figure 42. Turning Radius of a Vessel with 50 Knots and 30 Rudder Angle

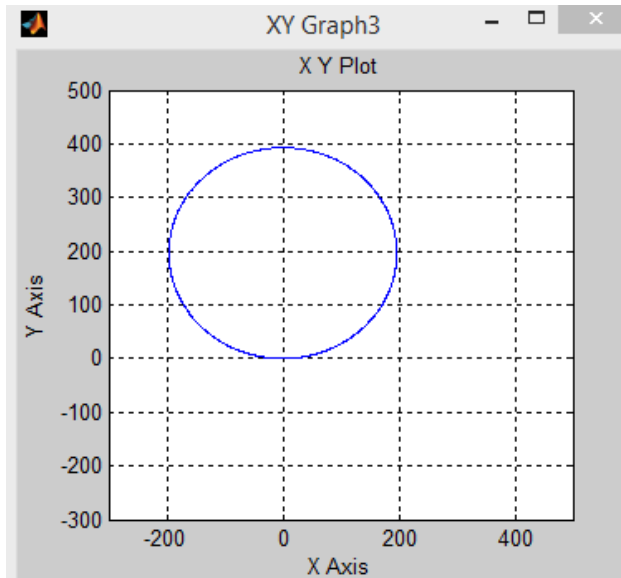


Figure 43. Turning Radius of a Vessel with 60 Knots and 30 Rudder Angle

The standard turning diameter increases as I increase the speed of the vessel. The length and the rudder angle also affect the turning diameter. The turning radius values increase as the length of the vessel increases, and the turning radius values decrease as the rudder angle increases.

In order to see consistency in turning radius, I compared the standard turning radius from Lewandowski equations and the standard turning radius in simulation. We can take the information with a scope from the block diagram for 50 knots speed. The results are shown in Figure 44 and Figure 45.

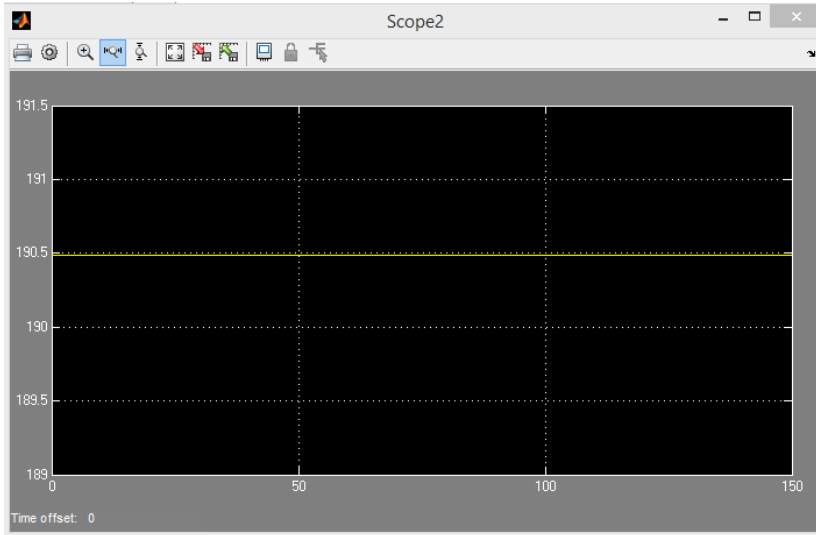


Figure 44. Standard Turning Radius from Lewandowski Equation

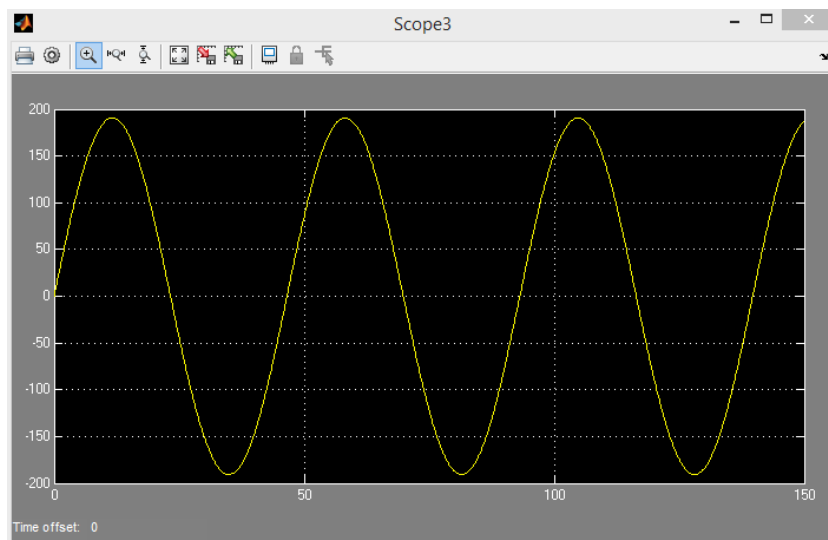


Figure 45. Turning Radius in Nomoto's Equation

We see that in both cases, the turning radius values stay the same (STR = 190.5 meters).

I can analyze for sinusoidal rudder inputs as well. With a sinusoidal rudder angle, the ship motion is presented in Figure 46. The motion pattern depends on rudder angle frequency and the maximum rudder angle.

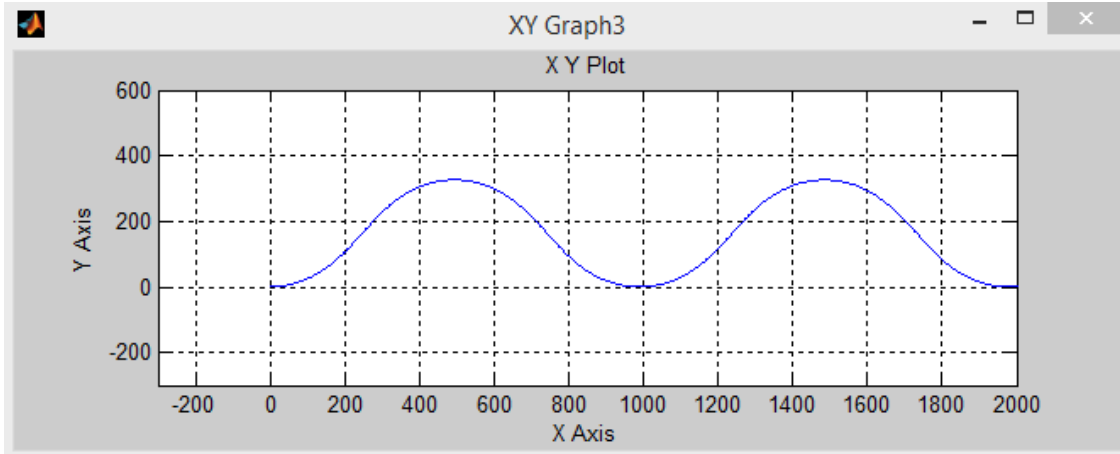


Figure 46. The Motion of the Vessel on the Horizontal Plane with Time

The change in speed depends on the rudder angle. The speed becomes approach speed when the rudder angle gets to zero and it has minimum speed values at the turn at maximum rudder angle. The speed change and rudder angle change are shown in Figure 47 and Figure 48.

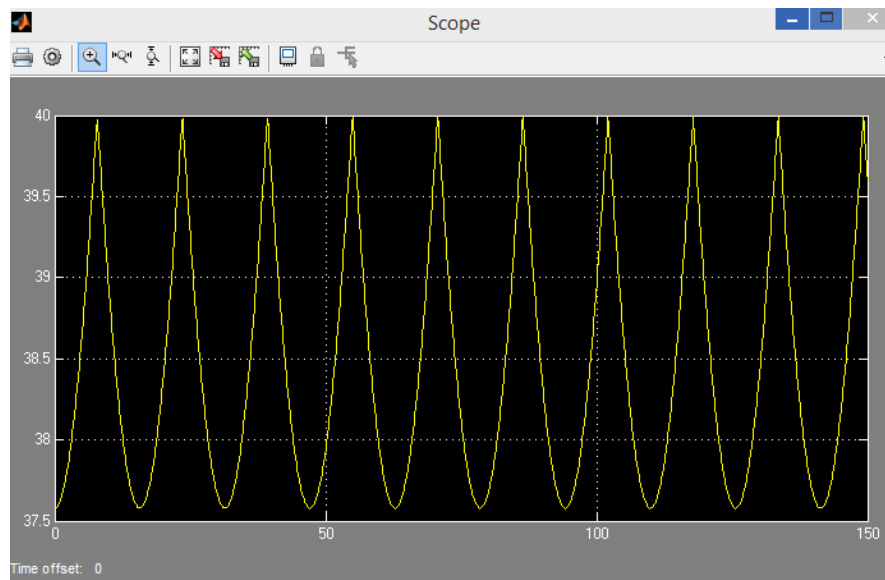


Figure 47. Speed Change vs. Time

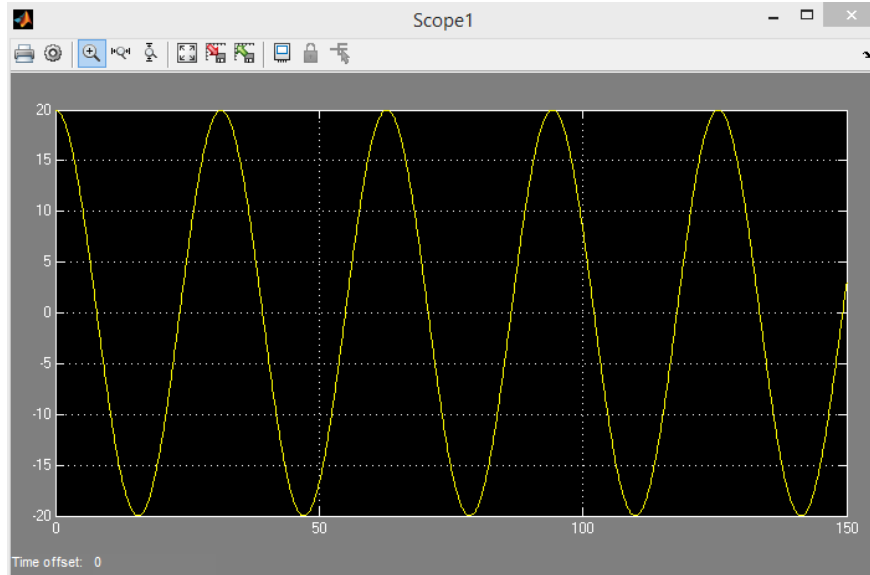


Figure 48. Rudder Angle Change vs. Time

The results show that the mathematical model can be used to find maneuvering characteristics and can also be used for simulation of vessel motion if I know the speed and rudder angle change with time.

THIS PAGE INTENTIONALLY LEFT BLANK

V. ATTACK AND AVOIDANCE

A. INTRODUCTION

After developing the maneuvering model of high-speed boats, the next step is to estimate how the helmsman will react when the boat is being attacked by a missile. In order to make this estimation, I can analyze prey-predator interactions in nature as an analogy to the missile-boat problem, because over centuries, predators and preys generate new tactics in order to find food and survive.

Howland analyzed the optimal strategies for predator avoidance based on the relative speed and maneuverability of the predator versus the prey. The dynamics of the prey and predator are presented [23]. Howland's study proposed the basic fundamentals for many studies that have been done after it. D. Weihs and P. W. Webb produced optimal avoidance tactics for different cases, including avoidance and evasion [24].

B. PREY AND PREDATOR INTERACTIONS IN NATURE

Weihs and Webb suggest that there are two different situations in prey-predator interactions: avoidance and evasion.

Avoidance: A predator may be observed first by prey, in which case the prey may decide to take an avoidance action to reduce the probability of detection, or to enhance its future chances of escape.

In missile-vessel interactions, an avoidance action can't be expected. Since a missile is fired first, this action will lead to an attack, so the vessel has to make an evasion move to escape from the missile.

Evasion: A successful search by a predator leads to an attack. In this case, the prey decides to take evasive action. In my problem, I search for the optimal escape maneuvers once a missile has started attacking the vessel.

The evasion actions basically depend on the maneuverability of the prey and the predator. The prey has the maneuverability advantage and the predator has the speed advantage.

In pursuit situation analysis, the turning radius and the speed of the predator are R and V ; the turning radius and the speed of the prey are r and v . The distance between prey and predator is called x_0 distance, when the predator begins to move along the x -axis towards the prey. Figure 49 shows a pursuit situation on the horizontal plane. The speed of the predator and prey are assumed to stay constant during the process.

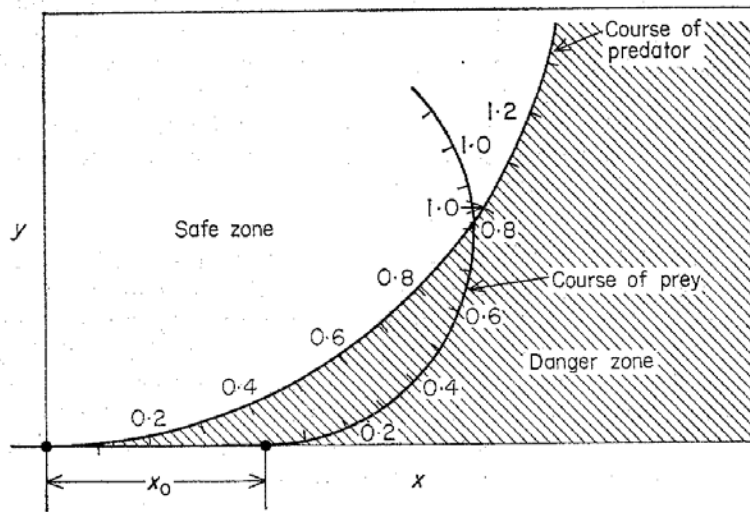


Figure 49. The Prey-Predator Interactions in a Pursuit Situation, from [23]

C. CATCH/ESCAPE CONDITIONS AND GENERALIZED CIRCLE INTERSECTION POINTS

Howland suggests the escape/catch criterion, which is based on the comparison of y values when the x values are equal to each other. This criterion is presented in this section. V_2 = speed of prey, V_1 = speed of predator, R_2 = turning radius of prey, R_1 = turning radius of predator, and T = time.

The normalization of speed, radius, and time is shown in the following equations:

$$v = V_2 / V_1 \quad (37)$$

$$r = R_2 / R_1 \quad (38)$$

$$t = TV_1 / R_1 \quad (39)$$

The normalization of x and y coordinates of predator and prey are as follows:

$$\begin{aligned} x_1 &= X_1 / R_1 \\ y_1 &= Y_1 / R_1 \\ x_2 &= X_2 / R_1 \\ y_2 &= Y_2 / R_1 \end{aligned} \quad (40)$$

The coordinates of predator and prey at any time can be found.

$$\begin{aligned} x_1 &= \sin(t) \\ y_1 &= 1 - \cos(t) \end{aligned} \quad (41)$$

$$\begin{aligned} x_2 &= x_0 + r \sin(vt / r) \\ y_2 &= r + r \sin(vt / r) \end{aligned} \quad (42)$$

The criterion depends on the comparison of y values when $x_1 = x_2$

$$\begin{aligned} y_2 &> y_1 \text{ (escape)} \\ y_2 &\leq y_1 \text{ (catch)} \end{aligned} \quad (43)$$

However, this criterion does not give the correct analysis every time. Because there are some conditions in which the intersection point is in a different quadrant, a revision is needed in escape/catch criterion. So I am going to make my own escape/catch criterion.

1. Generalized Circle Intersection

Both prey and predator make their turns at their minimum turning radius. According to their turning radius, I need to find the intersection point of two circles to determine the escape or catch condition of the prey. In pursuit attack, the predator starts from the origin of the coordinate system, and the prey is on the x axes at x_0 distance from the predator. When both predator and prey have started their turning maneuvers, the intersection points become important for both of them. A generalized circle intersection theorem is presented below.

The origins of the circles are x_0, y_0 and X_0, Y_0 , with radiuses r and R . Let x and y be the intersection points.

$$\begin{aligned}(x - x_0)^2 + (y - y_0)^2 &= r^2 \\ (x - X_0)^2 + (y - Y_0)^2 &= R^2\end{aligned}\tag{44}$$

With the expansion of equation (44), I get equation (45):

$$\begin{aligned}x^2 + x_0^2 - 2xx_0 + y^2 + y_0^2 - 2yy_0 &= r^2 \\ x^2 + X_0^2 - 2xX_0 + y^2 + Y_0^2 - 2yY_0 &= R^2\end{aligned}\tag{45}$$

Multiply the first equation by (-1):

$$\begin{aligned}-x^2 - x_0^2 + 2xx_0 - y^2 - y_0^2 + 2yy_0 &= -r^2 \\ x^2 + X_0^2 - 2xX_0 + y^2 + Y_0^2 - 2yY_0 &= R^2\end{aligned}\tag{46}$$

Then add them together in equation (47):

$$(X_0^2 - x_0^2) - 2x(X_0 - x_0) + (Y_0^2 - y_0^2) - 2y(Y_0 - y_0) = R^2 - r^2\tag{47}$$

Rearrange the equation as follows:

$$-2x(X_0 - x_0) = 2y(Y_0 - y_0) + (R^2 - r^2) + (y_0^2 - Y_0^2) + (x_0^2 - X_0^2)\tag{48}$$

Then I find the expression for the intersection point x in equation (49):

$$x = -y \frac{(Y_0 - y_0)}{(X_0 - x_0)} + \left[\frac{(R^2 - r^2) + (y_0^2 - Y_0^2) + (x_0^2 - X_0^2)}{2(X_0 - x_0)} \right]\tag{49}$$

For simplification, I use p and q in the expression of x ,

$$x = py + q\tag{50}$$

Substitute x into equation (44) in order to find an expression for y :

$$(py + q - x_0)^2 + (y - y_0)^2 = r^2\tag{51}$$

In an expansion of equation (51), I get equation (52):

$$p^2y^2 + (q - x_0)^2 + 2p^2(q - x_0)y + y^2 + y_0^2 - 2yy_0 = r^2\tag{52}$$

I can find a quadratic equation for y:

$$y^2(1+p^2) + y[2p(q-x_0) - 2y_0] + [(q-x_0)^2 + y_0^2 - r^2] = 0 \quad (53)$$

where

$$p = \frac{(Y_0 - y_0)}{(X_0 - x_0)} \quad (54)$$

$$q = \left[\frac{(R^2 - r^2) + (y_0^2 - Y_0^2) + (x_0^2 - X_0^2)}{2(X_0 - x_0)} \right]$$

Therefore,

$$\begin{aligned} a &= (1+p^2) \\ b &= [2p(q-x_0) - 2y_0] \\ c &= [(q-x_0)^2 + y_0^2 - r^2] \end{aligned} \quad (55)$$

Finally, I can find the x and y values of the intersection points in equation (56).

$$y = \frac{-b \pm \sqrt{b^2 - 4ac}}{2a} \quad (56)$$

$$x = py + q$$

My criterion for escape or capture of the prey depends on time. After I find the intersection point, I compare the time of prey and predator to determine which of them reaches the intersection point first. The speed of the prey and predator are assumed to stay constant during the analysis. If the prey reaches the intersection point first, then the prey will escape from the predator. Otherwise, the prey will be caught by the predator. These calculations are presented below.

The chord length has been found in order to find the angle between the starting point and intersection point. The chord lengths are illustrated in Figure 50.

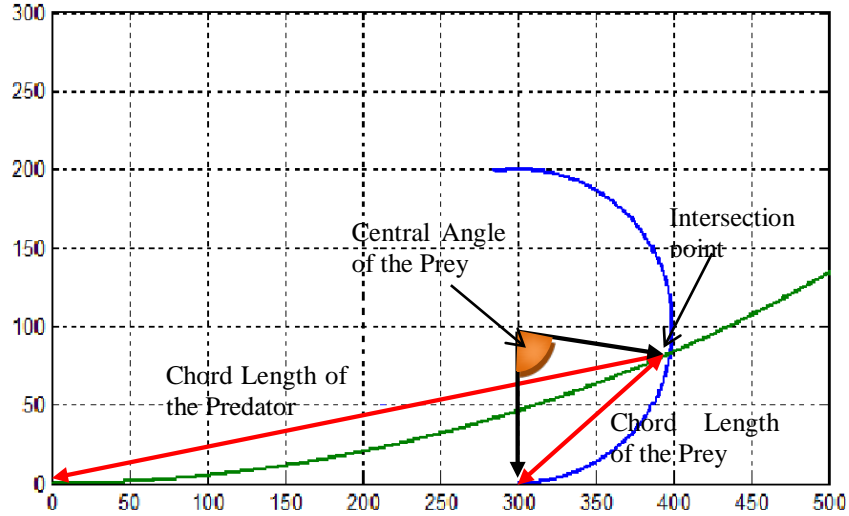


Figure 50. Chord Lengths of the Predator and Prey

$$\begin{aligned}
 \text{Chord Length of the Predator} &= \sqrt{x^2 + y^2} \\
 \text{Chord Length of the Prey} &= \sqrt{(x - x_0)^2 + y^2}
 \end{aligned}
 \tag{57}$$

Then I can find central angle with equation (58).

$$\begin{aligned}
 \text{Central Angle of the Predator} &= 2 \sin^{-1} \left(\frac{\text{Chord Length of the Predator}}{2R} \right) \\
 \text{Central Angle of the Prey} &= 2 \sin^{-1} \left(\frac{\text{Chord Length of the Prey}}{2r} \right)
 \end{aligned}
 \tag{58}$$

Then I can calculate arc length.

$$\begin{aligned}
 \text{Arc Length of the Predator} &= \text{Central Angle of the Predator} \times R \\
 \text{Arc Length of the Prey} &= \text{Central Angle of the Prey} \times r
 \end{aligned}
 \tag{59}$$

The time that passed until prey and predator reached the intersection point is calculated as follows:

$$\begin{aligned}
 \text{Time Predator} &= \frac{\text{Arc Length of the Predator}}{V} \\
 \text{Time Prey} &= \frac{\text{Arc Length of the Prey}}{v}
 \end{aligned}
 \tag{60}$$

2. Escape/Catch Analysis for Different Situations in Missiles-Ships Interactions

After determining the catch/escape conditions for prey for specific x_0 distance above, I investigate general missile-ship interactions for different x_0 distances. Three different scenarios are investigated. Sample values are $R = 3000$ meter, $r = 200$ meters, $V = 300$ meters/sec, and $v = 100$ meters/sec. These values do not relate to specific missile or ship characteristics, but are generic values used for illustrative purposes.

a. *Escape/Catch Analysis in Pursuit Attack Situation*

It is crucial for the prey to decide at what distance it should start its maneuver, so I am looking for an optimum distance to maximize the chance to escape. First, I am going to analyze the pursuit attack situation.

In a pursuit situation, the predator is at the origin of the coordinate system, so the center of the turning circle for the predator is $(0, R)$ and the center of the turning circle for the prey is $(x_0 \text{ distance}, r)$; see Figure 51).

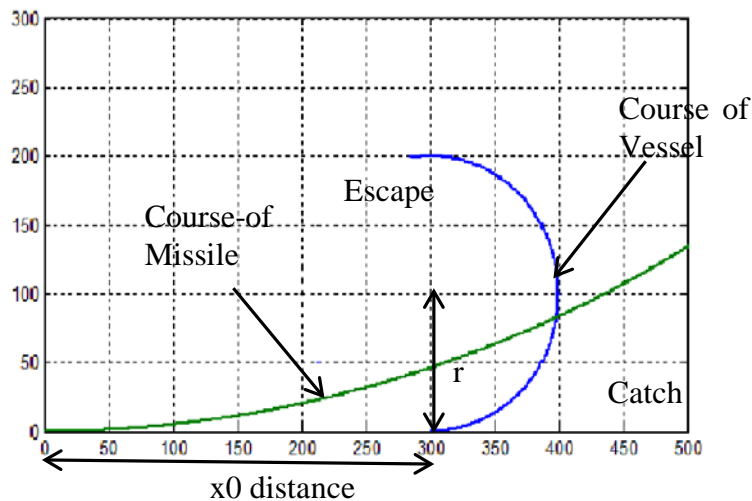


Figure 51. Vessel-Missile Interactions in Pursuit Attack Situation

After catch/escape condition analysis, Figure 52 shows that the prey has a chance to escape if it starts its maneuvers when x_0 distance gets smaller than 1300 meters.

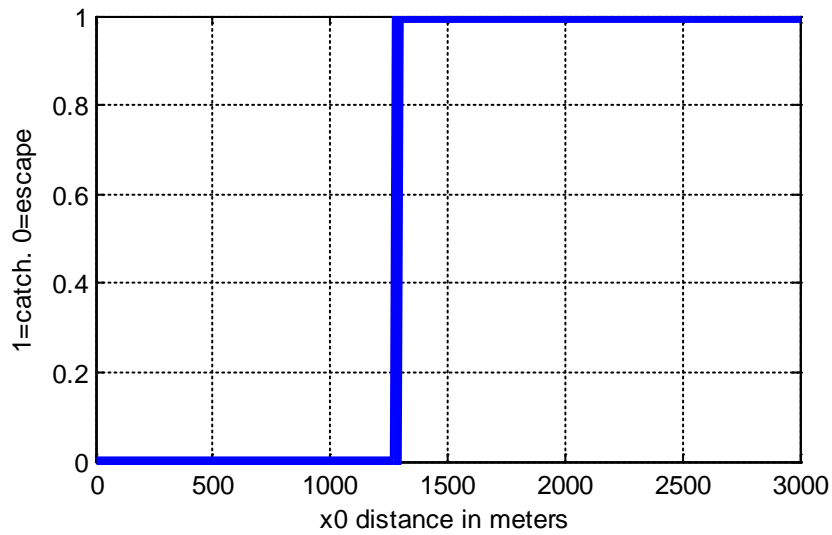


Figure 52. Catch/Escape Conditions vs. x_0 Distance in Pursuit Attack

For escape conditions, I can calculate the miss distances between predator and prey as a function of x_0 distance. The miss distances are defined as the direct distances between prey and predator when prey reaches the intersection point. The miss distance for $x_0 = 300$ meter was illustrated in Figure 53. Figure 54 shows that for evasion analysis, there is an optimum x_0 distance to maximize the miss distance.

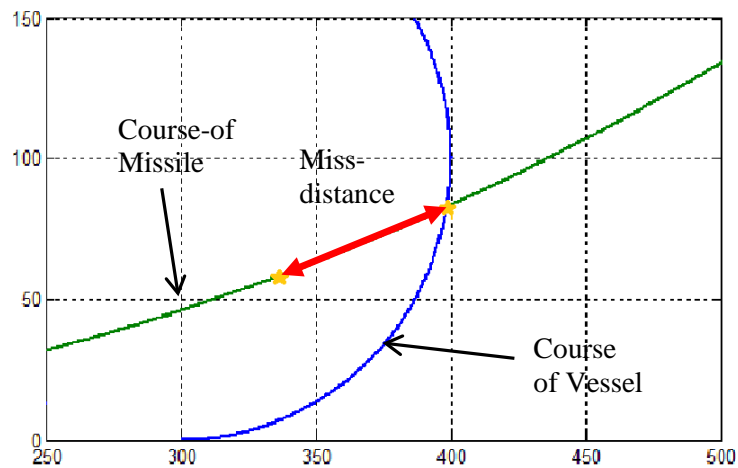


Figure 53. Miss Distance Illustration in Pursuit Attack

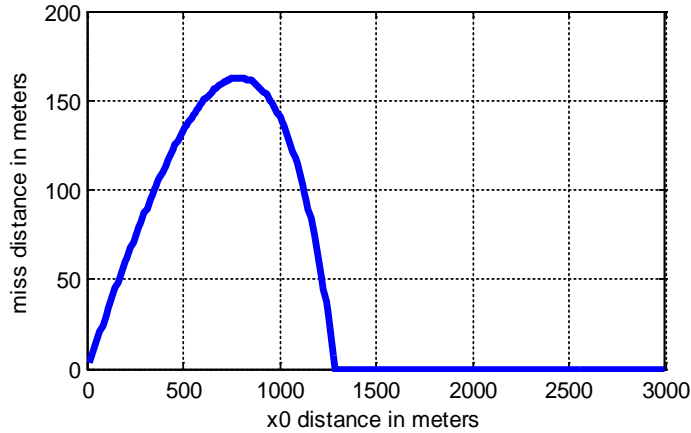


Figure 54. Miss Distances vs. x_0 Distances in Pursuit Attack

In addition to miss distance, I also calculate the closest approach distance, which is not necessarily the same as the miss distance. Closest approach is illustrated in Figure 55. Closest approach is an important parameter for the missile-vessel interaction since the missile may not need to hit the boat to damage it. A proximity fuse would sense the closest approach, detonate, and damage the boat with its warhead lethal radius. In order to calculate the closest approach distance, I increase the time by increments for each x_0 distance, and calculate the distance between prey and predator at each time. These calculations are done with MATLAB codes that are presented in Appendix E. Figure 56 shows the change of miss distance versus time for x_0 distance = 500. The closest approach is the minimum value of the distances between missile and vessel.

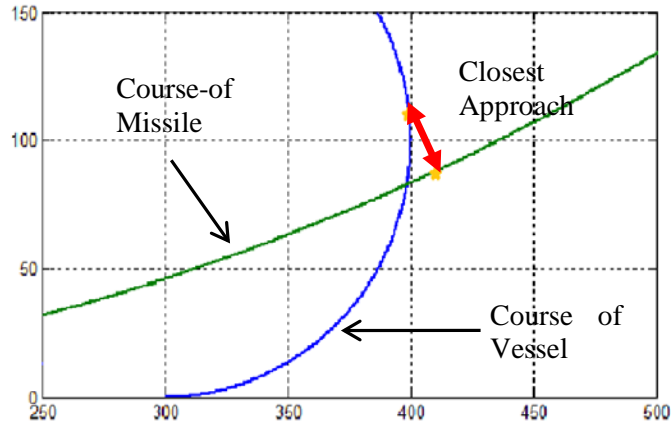


Figure 55. Closest Approach Illustration in Pursuit Attack

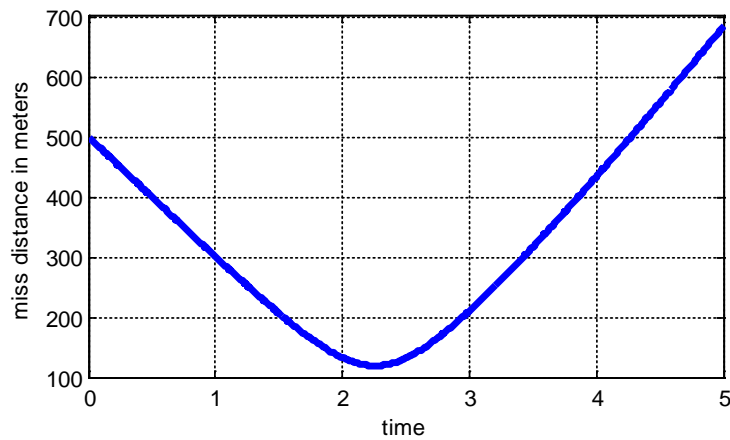


Figure 56. Miss Distance vs. Time in Pursuit Attack

I can find the closest approach distances by varying x_0 over the range for which escape is possible, as shown in Figure 57. As we can see from this figure and as expected, the closest approach distances are smaller than miss distances.

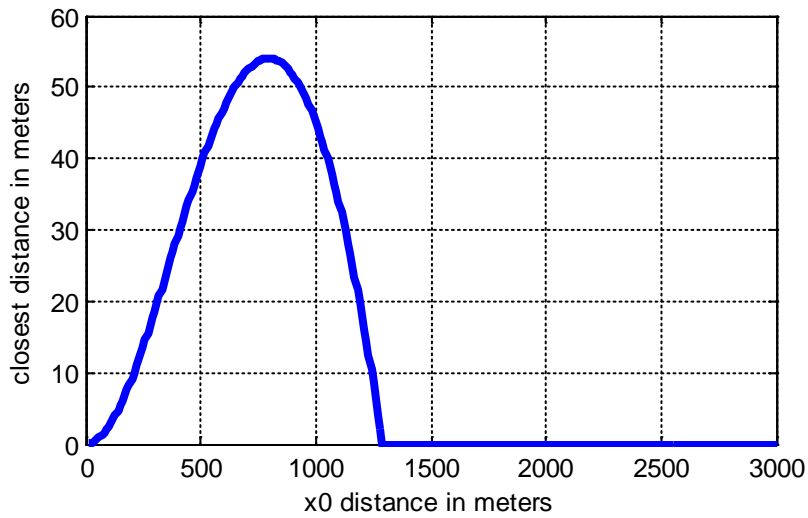


Figure 57. Closest Approach Distances vs. x_0 Distances in Pursuit Attack

b. Escape/Catch Analysis in Beam Attack Situation

After pursuit analysis, I am going to analyze the beam attack for generic missile/ship values. In this case, the prey is travelling vertically to the x axes. The center of the turning circle for the predator stays in the same position $(0, R)$, but the center of the turning circle for the prey is $(x_0 \text{ distance}-r, 0)$. Next, I carried out the same procedure that I did in pursuit analysis. The beam attack situation is illustrated in Figure 58.

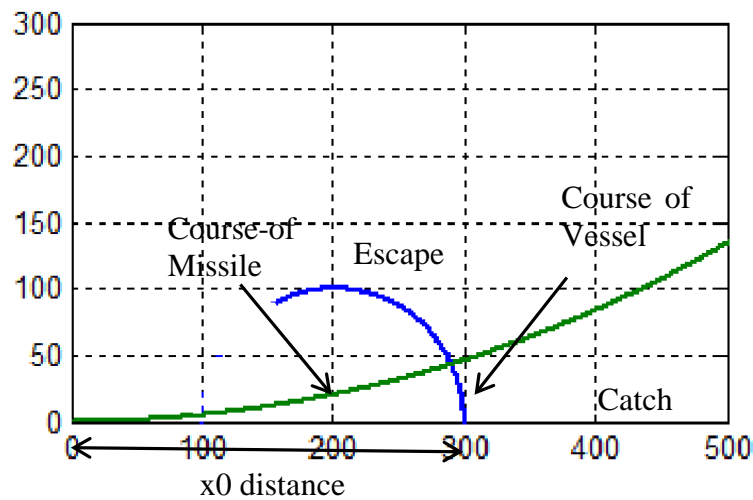


Figure 58. Vessel-Missile Interactions in Beam Attack Situation

Catch/escape conditions are drawn for different distances in Figure 59. The prey has to start its maneuver at a similar distance with a pursuit attack.

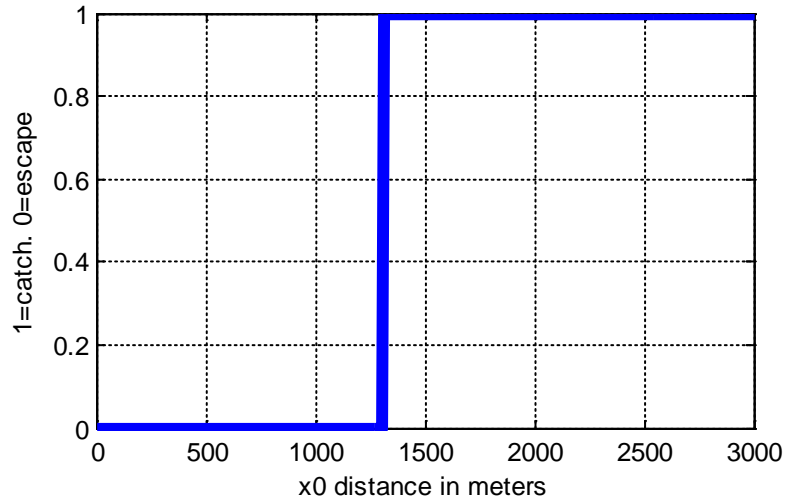


Figure 59. Catch/Escape Conditions for x_0 Distances in Beam Attack

However, the miss distances and the closest approach distances are higher than the pursuit case for the same conditions. The closest approach distance becomes important for the missiles with lethal radius. Figure 60 shows the miss distances, and Figure 61 shows the closest approach distances for different x_0 distances.

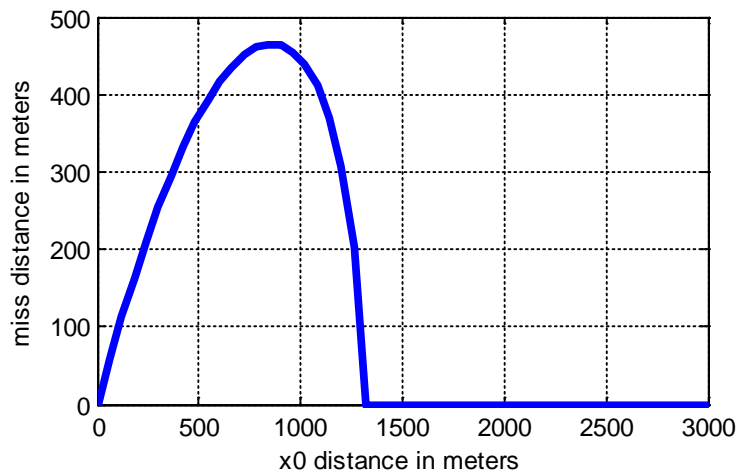


Figure 60. Miss Distances vs. x_0 Distance in Beam Attack

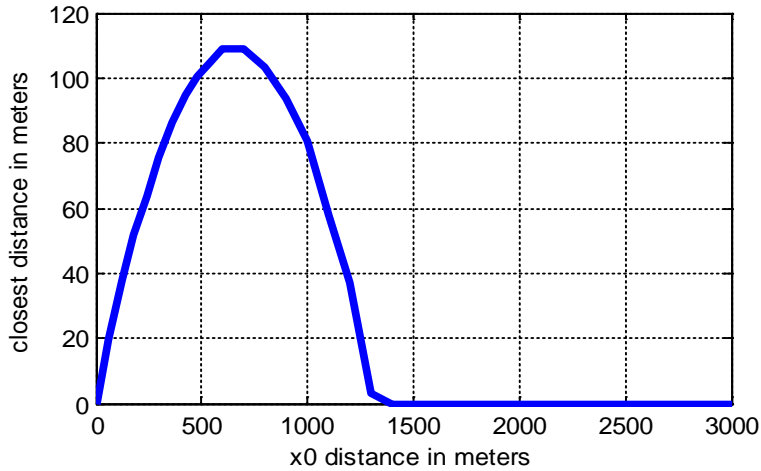


Figure 61. Closest Approach vs. x_0 Distance in Beam Attack

c. Escape/Catch Analysis in Head-to-Head Attack Situation

In the last scenario, I am going to analyze when vessel moves towards the missile and start its maneuvering at a certain distance before collision. Again, I assume they execute their maneuvers at their maximum speed and minimum turning radius. The same procedures are being followed to determine the escape/catch condition for generic missile/ship values. The head-to-head attack situation is illustrated in Figure 62.

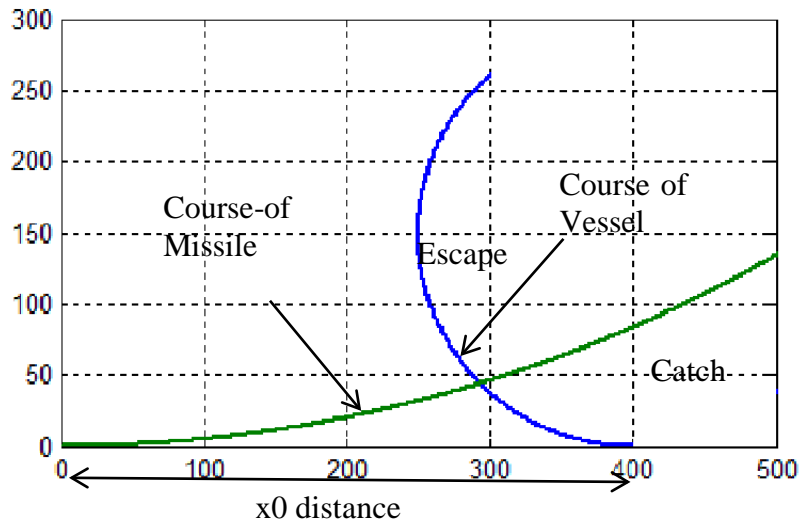


Figure 62. The Vessel-Missile Interactions in Head-to-Head Situation

Next I performed the analysis for the same sample speed and turning radius conditions. This situation leads the prey to start its maneuver earlier. Figure 63 shows the escape/catch conditions for different x_0 distances.

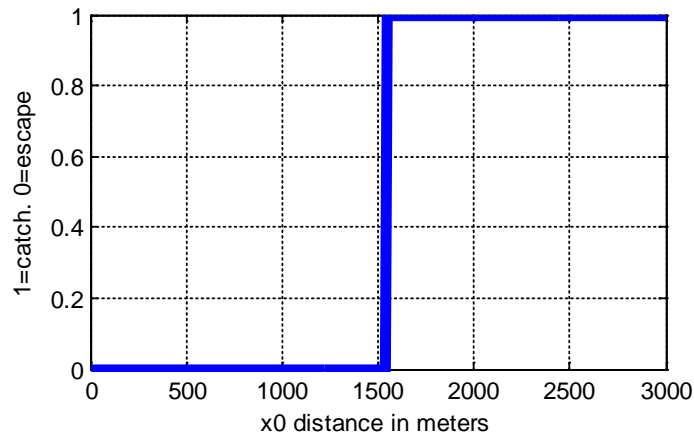


Figure 63. Catch/Escape Conditions for x_0 Distances in Head-to-Head Attack

The miss distances and the closest approach distances are calculated in the same way as the pursuit attack situation. The results are smaller than the beam scenario values but similar to pursuit scenario values. Figure 64 shows the miss distances, and Figure 65 shows the closest approach distances for different x_0 distances.

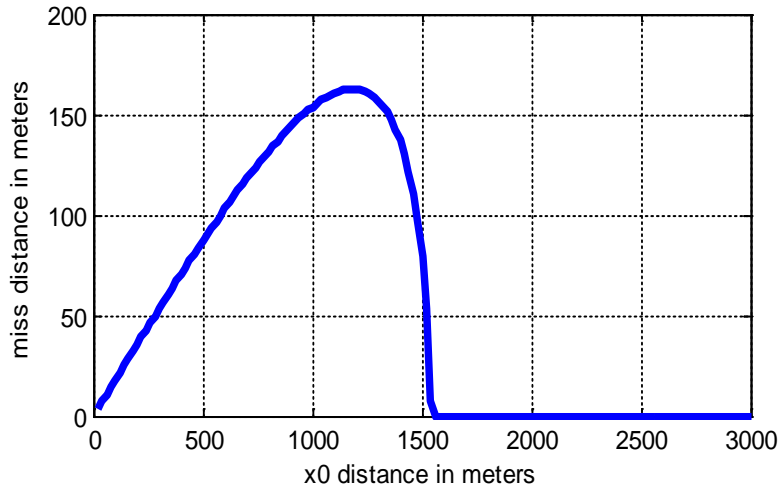


Figure 64. Miss Distances vs. x_0 Distance in Head-to-Head Attack

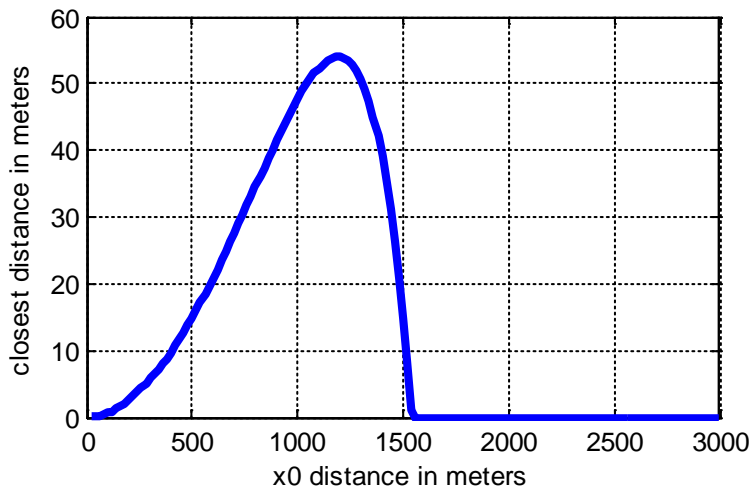


Figure 65. Closest Approach vs. x_0 Distance in Head-to-Head Attack

D. ANALYZING SPECIFIC MISSILE-VESSEL INTERACTIONS

In Chapter IV, the maneuverability of the vessel has been found in the mathematical model as a function of length, displacement, and maximum speed. After discussing the general missile-vessel situations previously, I am going to analyze more detailed missile-vessel conditions. I used a representative sample high-speed boat to determine the turning radius, and set the speed to 60 knots. The characteristics of the sample boat are listed in Table 11. The turning radius becomes 200 meters and the

speed becomes 30 m/sec. I assumed the missile travels at 300 m/sec and sustains a maximum of 2 g during a turn. The turning radius has been found to be 4500 meters with equation (60). Different speeds and g-forces can be analyzed with a MATLAB program that is presented in Appendix C.

$$g \text{ force } \times g = \frac{V^2}{R}$$

$$R = \frac{V^2}{g \text{ force } \times g} \tag{60}$$

where $g = 9.81 \text{ m/s}^2$ (Gravity of Earth).

Table 11. Sample High-Speed Boat Characteristics

Sample High-Speed Boat Characteristics	
Length	17 meters
Displacement	23 tons
Speed	60 knots
Rudder Angle	30 degrees

So the analysis has been done for pursuit attack, beam attack, and head-to-head attack situations. The missile hits the vessel at every x_0 distance in pursuit and head-to-head situations. Figure 66 shows the escape/catch condition for the pursuit situation, and Figure 67 shows the escape/catch condition for the head-to-head situation.

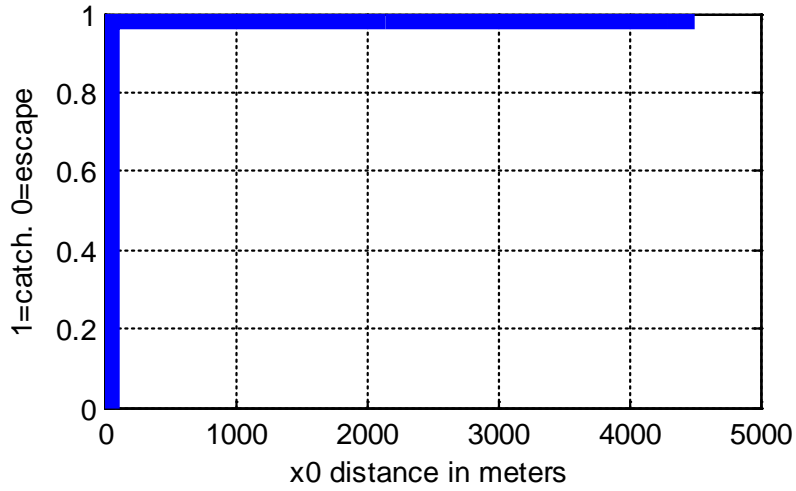


Figure 66. Catch/Escape Conditions for x_0 Distances in Pursuit Attack

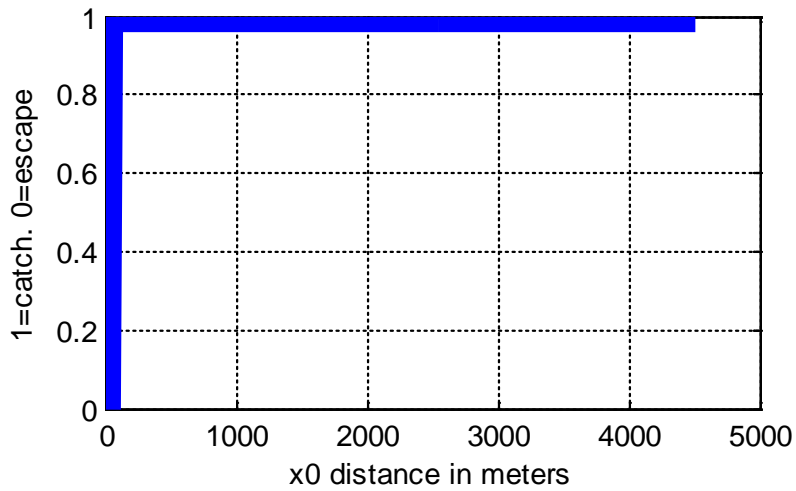


Figure 67. Catch/Escape Conditions for x_0 Distances in Head-to-Head Attack

However, in beam attack, the vessel has a chance to escape from a missile for a specific distance. Figure 68 shows the catch/escape conditions. The miss distances and closest approach distances are plotted in Figure 69 and Figure 70.

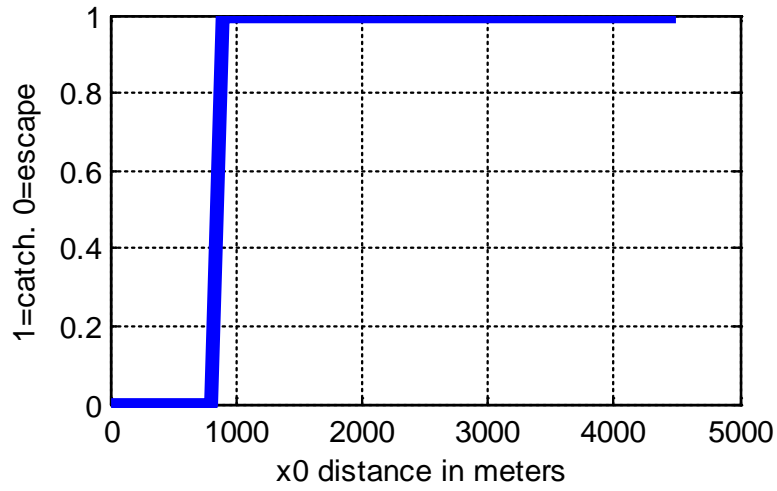


Figure 68. Catch/Escape Conditions for x_0 Distances in Beam Attack

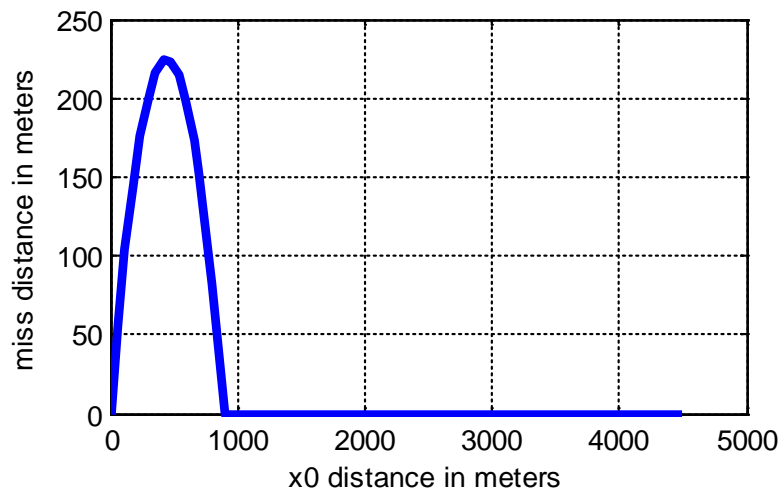


Figure 69. Miss Distances vs. x_0 Distances in Beam Attack

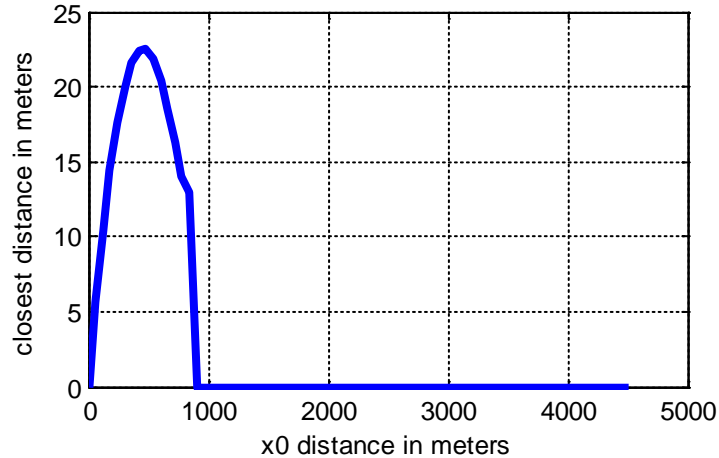


Figure 70. Closest Approach Distance vs. x_0 Distances in Beam Attack

E. THE CRITICAL G-FORCE FOR THE MISSILE

Let us assume the missile can carry different g-forces. The air-to-surface missile (Penguin anti-ship missile, AGM-114B/K/M Hellfire missile) has a maximum speed around Mach 1.2. I assume the missile is travelling with same speed at 300 meters/sec, and its turning radius depends on how many g-forces the missile can sustain. However, this information may be classified for the specific missiles. For high-speed craft, I am going to use the same numbers: $v = 30$ m/sec and $r = 200$ meters.

I find a critical g-force that the missile should sustain to make a successful hit as a function of the maneuver initiation distance x_0 . Let us assume this distance to be 500 meters, because that distance is suitable for a high-speed boat to start its maneuver. I can find the critical g-forces with different x_0 distances with the help of the MATLAB program shown in Appendix D.

I plotted catch/escape conditions versus g-force for the missile. The Figures 71-73 show the minimum sustainable g-force in order for the missile to intercept the target for the pursuit, beam, and head-on attack scenarios, respectively.

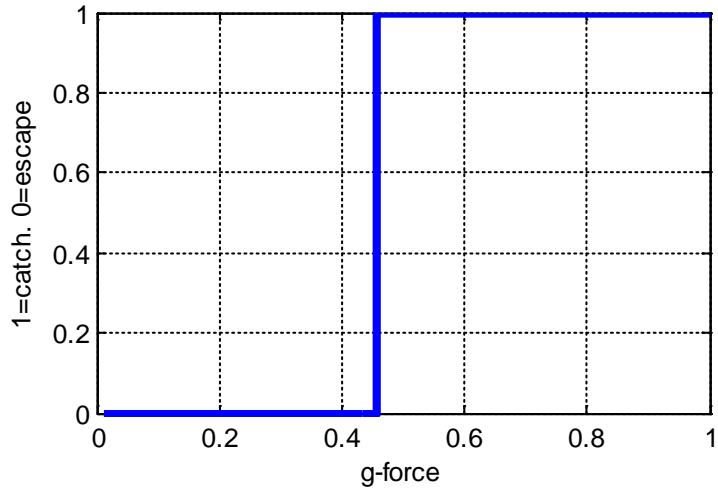


Figure 71. Catch/Escape Conditions vs. g-force in Pursuit Attack

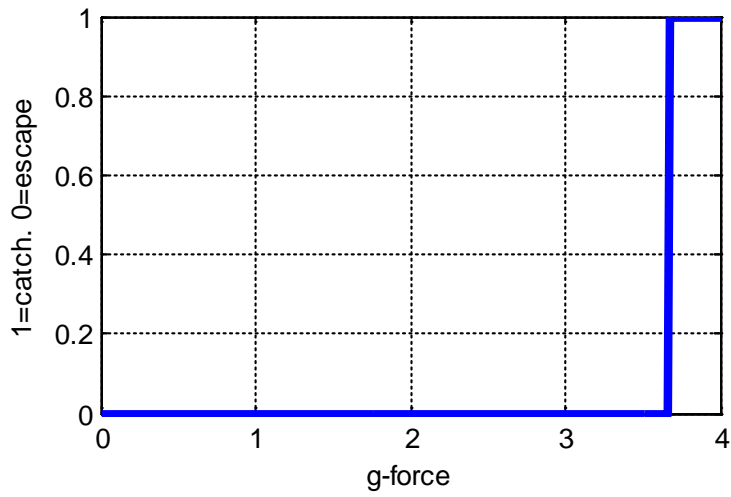


Figure 72. Catch/Escape Conditions vs. g-force in Beam Attack

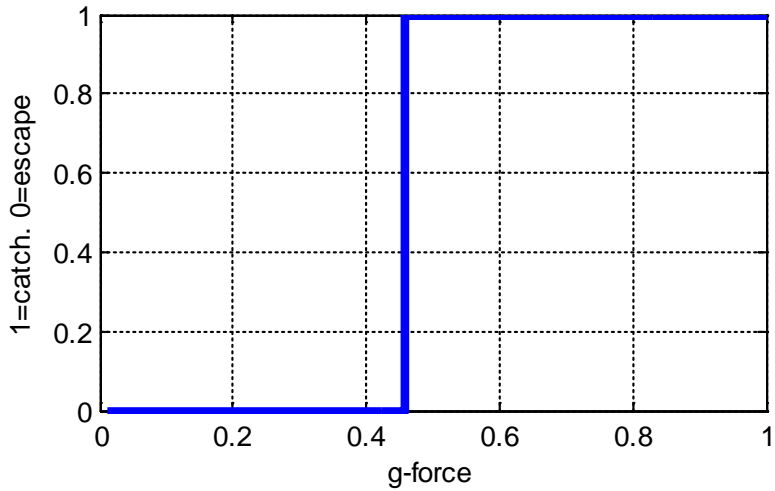


Figure 73. Catch/Escape Conditions vs. g-force in Head-to-Head Attack

The closest approach distances are important if the missile has a lethal radius of its warhead. For those attacks resulting in the boat escaping the attack, the closest approach distances are calculated for different g-forces. The closest approach distances are very small in pursuit and head-to-head attack situations. However, in beam attack situations, these distances are higher than in the other situations.

For the pursuit situation, the miss distances and the closest approach distances are shown in Figure 74 and Figure 75 for different g-forces.

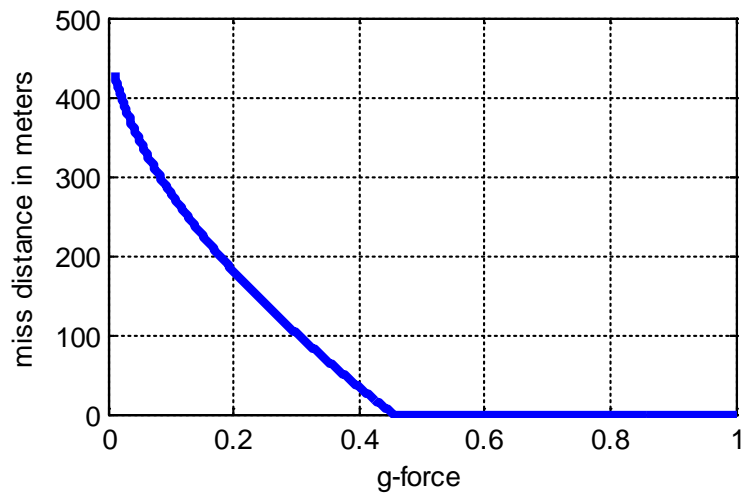


Figure 74. Miss Distances vs. g-force in Pursuit Situation

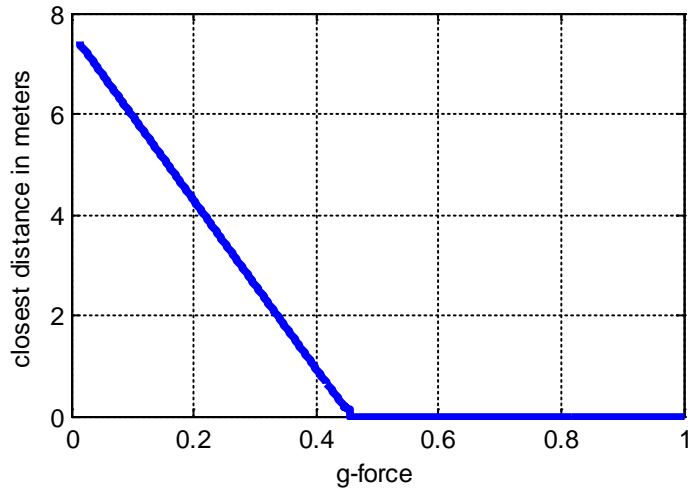


Figure 75. Closest Approach Distances vs. g-force in Pursuit Situation

For the beam situation, the miss distances and the closest approach distances are shown in Figure 76 and Figure 77 for different g-forces.

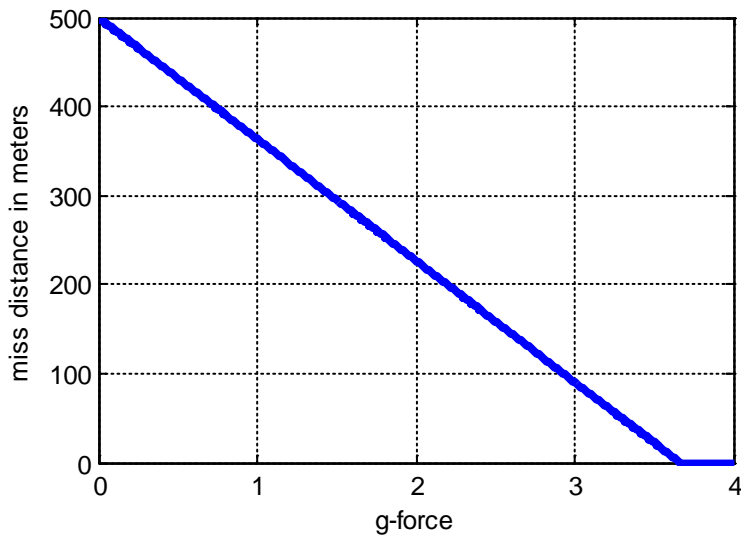


Figure 76. Miss Distances vs. g-force in Beam Situation

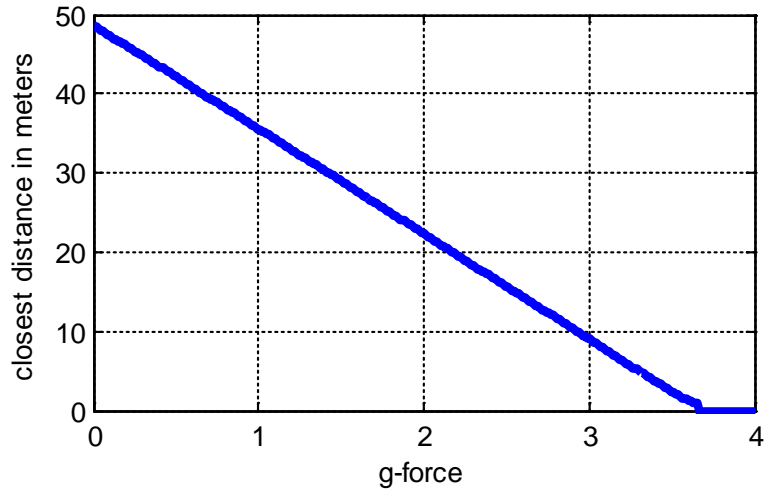


Figure 77. Closest Approach Distances vs. g-force in Beam Situation

For the head-to-head situation, the miss distances and the closest approach distances are shown in Figure 78 and Figure 79 for different g-forces.

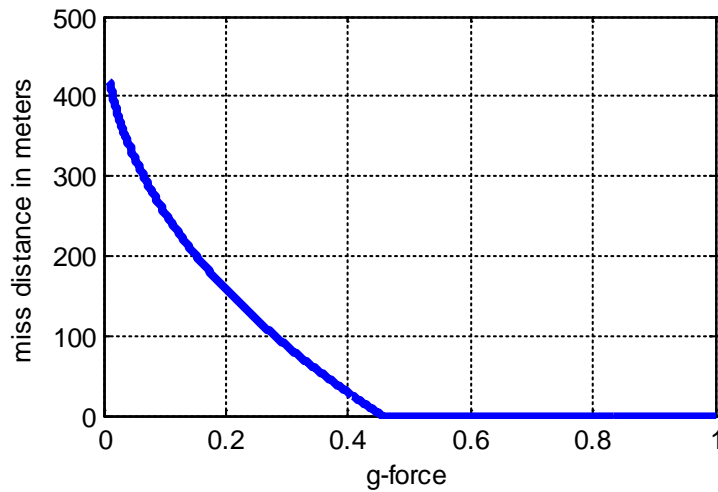


Figure 78. Miss Distances vs. g-force in Head-to-Head Situation

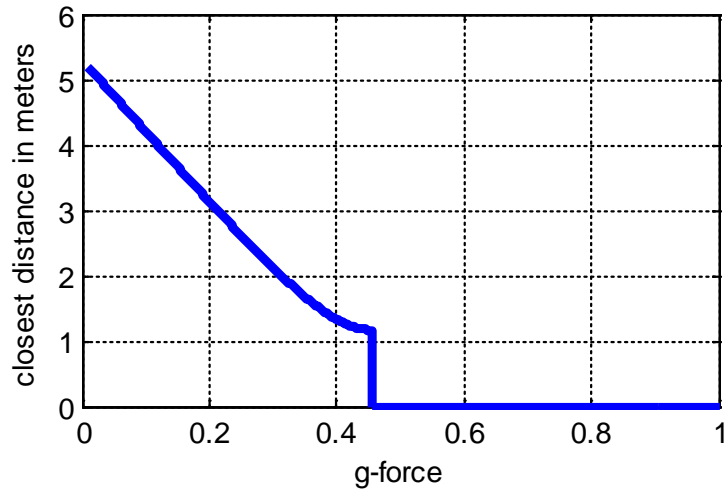


Figure 79. Closest Approach Distances vs. g-force in Head-to-Head Situation

VI. CONCLUSION AND RECOMMENDATIONS

A. CONCLUSION

This thesis addressed the problem of the maneuverability estimation of high-speed craft, including the interaction between a high-speed craft and an attacking missile. The maneuverability characteristics problem was solved with the help of the MATLAB Simulink model; prey-predator interactions were analyzed to understand the missile-vessel interactions.

The main work and results are summarized as follows:

1. The Maneuvering Prediction Program and MATLAB Simulations by Fossen are used for displacement vessels, and these models cannot be applied to small high-speed boats.
2. A small, high-speed boat maneuverability model was derived based on equations by Lewandowski and Hubble.
3. The model was developed in the MATLAB Simulink model in time domain with the help of Nomoto's first order equation, and the motion is visualized on the horizontal plane.
4. Using this maneuverability model, the possibility of such a craft evading a missile attack was analyzed using an analogous concept from animal predator-prey kinematics. A model was developed allowing the effect of speed ratio, turning circle radius ratio, missile g-loading, and evasion initiation to be investigated.
5. It was found that for pursuit and head-on attacks, with representative data for missile and target, the missile usually hit the target. For a beam attack, however, there are some ranges of parameters for which escape is possible.

B. RECOMMENDATIONS

This study can be extended and developed into several areas, which are summarized as follows:

1. The results of the Lewandowski equations should be compared with full-scale trial data to create a higher confidence in the equation.

2. The critical g-forces should be analyzed during the missile's design stage in order to make an accurate hit assessment in various situations.
3. Ship design requirements and operational tactics can be developed for a vessel to escape from a missile according to the model presented for optimum escape conditions.

APPENDIX A. IMO REQUIREMENTS

TABLE 1
Overview of Standards and Criteria

<i>Measure of Maneuverability</i>	<i>Criteria and Standard</i>	<i>Maneuver</i>	<i>IMO Standard</i>	<i>ABS Guide Requirement</i>
<i>Required for Optional Class Notation</i>				
Turning Ability	Tactical Diameter	Turning Circle	$TD < 5L$	Rated $Rtd \geq 1$
	Advance		$Ad < 4.5L$	Not rated $Ad < 4.5L$
Course Changing and Yaw Checking Ability	First Overshoot Angle	10/10 Zig-zag test	$\alpha 10_1 \leq f_{101}(L/V)$	Rated $Rt\alpha_{10} \geq 1$
	Second Overshoot Angle		$\alpha 10_2 < f_{102}(L/V)$	Not rated $\alpha 10_2 < f_{102}(L/V)$
	First Overshoot Angle	20/20 Zig-zag test	$\alpha 20_1 \leq 25$	Rated $Rt\alpha_{20} \geq 1$
Initial Turning Ability	Distance traveled before 10-degree course change	10/10 Zig-zag test	$\ell_{10} \leq 2.5L$	Rated $Rti \geq 1$
Stopping Ability	Track Reach	Crash stop	$TR < 15L^{(1)}$	Not rated $TR < 15L^{(1)}$
	Head Reach		None	Rated $Rts \geq 1$
<i>Recommended, Not Required for Optional Class Notation</i>				
Straight-line Stability and Course Keeping Ability	Residual turning rate	Pull-out test	$r \neq 0$	Not rated $r \neq 0$
	Width of instability ⁽²⁾ loop	Simplified spiral	$\alpha_U \leq f_u(L/V)$	Not rated $\alpha_U \leq f_u(L/V)$

Notes:

- 1 For large, low powered vessels, $TR < 20L$.
- 2 Applicable only for path-unstable vessels.

THIS PAGE INTENTIONALLY LEFT BLANK

APPENDIX B. MODEL BLOCKS

```

% VOLUMETRIC FROUDE NUMBER CALCULATION
function FroudeN = FroudeN(u,DISP) % u is the approach speed and DISP
                                   is displacement
RHO = 1.025                         % The Density of the Sea Water
v = u/1.944;                       % Converting the speed from knots
                                   to meter/sec
VOL = DISP/RHO;                    % Finding the Volume
G = 9.81;                          % Gravity
FroudeN = (v/sqrt(G*VOL^(1/3)));    % Volumetric Froude Number
end

% FINDING TURNING RADIUS WITH LEWANDOWSKI EQUATION
function NormalizedRadius = NormalizedRadius(LWL,FroudeN,DISP,r)
RHO = 1.025;                        % Density of the Sea Water
VOL = DISP/RHO;                    % Finding Volume
STD = LWL*(1.7 + 0.0222*FroudeN*((LWL/(VOL^(1/3)))^(2.85)))*(30/r);
NormalizedRadius = 0.5*STD/LWL;    % Normalized Turning Radius
end

% FINDING Kc VALUES IN DENNY AND HUBBLE'S EQUATIONS
function Kc = Kc(FroudeN,r)
Kc = (FroudeN^2)*(30/abs(r));
end

% FINDING THE SPEED IN TURN
function DennyHubble = DennyHubble(U,NormalizedRadius,Kc)
UcUa = (1/(1+Kc*(1/NormalizedRadius)^2))^(0.5);
DennyHubble = UcUa*U % Finding The Speed In a Turn
end

% FINDING K CONSTANT IN NOMOTO'S EQUATIONS
function [K,TurningRadius]= fcn(rmax,U,NormalizedRadius,LWL)
TurningRadius = NormalizedRadius*LWL
K = U/(TurningRadius*rmax);
end

% FINDING THE PSIDOT, THE CORRECTION FACTOR IS 0.909
function Psidot = Psidot(K,r)
Psidot = K*r*0.909;
end

% FINDING THE MOTION IN THE HORIZONTAL PLANE
function [ydot,xdot]= fcn(U,psi)
xdot = U*sin(psi);
ydot= U*cos(psi);
end

```

THIS PAGE INTENTIONALLY LEFT BLANK

APPENDIX C. MATLAB CODES FOR OPTIMUM X0 DISTANCE IN PURSUIT ATTACK, BEAM ATTACK, AND HEAD-TO-HEAD ATTACK SITUATIONS

```

%% NAZMI ASLAN MATLAB CODE
% OPTIMUM X0 DISTANCE IN MISSILE-VESSEL INTERACTIONS IN PURSUIT ATTACK
clc; clear all; close all;

r=200;
R=4500;
v=30;
V=300;

x0 = [0:10:R];
y0 = r;
X0 = 0;
Y0 = R;

p = -1*(Y0 - y0)./(X0-x0);
q = ((R.^2-r.^2)+(y0.^2-Y0.^2)+(x0.^2-X0.^2))./(-2.*(X0-x0));
a = 1+p.^2;
b = 2.*p.*(q-x0) - 2.*y0;
c = (q-x0).^2 + y0.^2 - r.^2;

% INTERSECTION POINT
y = (-b+sqrt(b.^2-4.*a.*c))./(2.*a);
x = (p.*y)+q;

k = abs(imag(x))<=0; % Checking if the intersection point is imaginary

% PREDATOR CALCULATIONS
chordL = sqrt(y.^2 + x.^2);
centralAngle = 2.*(asin(chordL/(2*R)));
arcL = centralAngle.*R;
time = arcL./V;

% PREY CALCULATIONS;
chordLPrey = sqrt((y).^2 + (x-x0).^2);
centralAnglePrey = 2.*(asin(chordLPrey./(2.*r)));
arcLPrey = centralAnglePrey.*r;
timePrey = arcLPrey./v;

% Predator position when the prey reaches to intersection point
arcL1 = timePrey*V;
circumferencel = 2*pi*R;
centralAngle1 = 2*pi*arcL1/circumferencel;
xpred = X0 + R*sin(centralAngle1);
ypred = Y0 - R*cos(centralAngle1);

```



```

%comparing the time of Prey and Predator to find catch/escape
conditions
timeratio = time./timePrey;
result = timeratio<=1; % 1=catch, 0=escape

N = length(x0);

% miss distances are found for escape conditions
missdistance = zeros(1,N);

for i=1:N;
    if k(i)==0; % checking imaginary
        missdistance(i) = 0;
        result(i) = 1;
    else if result(i)==0; % miss distance calculations if it's an
escape
        missdistance(i) = sqrt((x(i)-xpred(i)).^2+(y(i)-
ypred(i)).^2);
        end
    end
end

% closest approach distances are found for escape conditions
closestpoint = zeros(1,N);
for i=1:N
    if k(i)==0; %check imaginary
        closestpoint(i) = 0;
    else if result(i)==0
        closestpoint(i) =
closestpoint1_pursuitcase(x0(i),x(i),y(i),r,R,v,V,timePrey(i));
        end
    end
end

figure(1);
graph1 = plot(x0,result); grid on; set(graph1,'Linewidth',10);
title('catch/escape vs x0 distance'); xlabel('x0 distance');
ylabel('1=catch. 0=escape');
figure(2);
graph2 = plot(x0,missdistance); grid on; set(graph2,'Linewidth',3);
title('miss-distance vs x0 distance'); xlabel('x0 distance');
ylabel('miss distance in meters');
figure(3)
graph3 = plot(x0,closestpoint); grid on; set(graph3,'Linewidth',3);
title('closest-distance vs x0 distance'); xlabel('x0 distance');
ylabel('closest distance in meters');

```

```

%% NAZMI ASLAN MATLAB CODE
% OPTIMUM X0 DISTANCE IN MISSILE-VESSEL INTERACTIONS IN BEAM ATTACK
clc; clear all; close all;

r=200;
R=4500;
v=30;
V=300;

distance = [0:60:R];
N = length(distance);

x0 = distance-r;
y0 = 0;
X0 = 0;
Y0 = R;

p = -1*(Y0 - y0)/(X0-x0);
q = ((R.^2-r.^2)+(y0.^2-Y0.^2)+(x0.^2-X0.^2))/(-2.*(X0-x0));
a = 1+p.^2;
b = 2.*p.*(q-x0) - 2.*y0;
c = (q-x0).^2 + y0.^2 - r.^2;

% INTERSECTION POINT
for i=1:N;
if distance(i)<=r;
    y(i) =(-b(i)-sqrt(b(i).^2-4.*a(i).*c(i)))/(2.*a(i));
else distance(i)>=r;
    y(i) =(-b(i)+sqrt(b(i).^2-4.*a(i).*c(i)))/(2.*a(i));
end
end

x = (p.*y)+q;

k = abs(imag(x))<=0; % checking imaginary

% PREDATOR CALCULATIONS
chordL = sqrt(y.^2 + x.^2);
centralAngle = 2.*(asin(chordL/(2*R)));
arcL = centralAngle.*R;
time = arcL./V;

% PREY1 CALCULATIONS;
chordLPrey = sqrt((y-y0).^2 + (distance-x).^2);
centralAnglePrey = 2.*(asin(chordLPrey./(2.*r)));
arcLPrey = centralAnglePrey.*r;
timePrey = arcLPrey./v;

% Predator position when the prey reaches to intersection point
arcL1 = timePrey*V;
circumferencel = 2*pi*R;
centralAngle1 = 2*pi*arcL1/circumferencel;
xpred = X0 + R*sin(centralAngle1);
ypred = Y0 - R*cos(centralAngle1);

```

```

%comparing the time of Prey and Predator to find catch/escape
conditions
timeratio = time./timePrey;
result = timeratio<=1; % 1=catch, 0=escape
N = length(distance);

% miss distances are found for escape conditions
missdistance = zeros(1,N);
for i=1:N;
    if k(i)==0; %check imaginary
        missdistance(i) = 0;
        result(i) = 1;
    else if result(i)==0; % miss distances
        missdistance(i) = sqrt((x(i)-xpred(i)).^2+(y(i)-
ypred(i)).^2);
    end
end
end

% closest approach distances are found for escape conditions
closestpoint = zeros(1,N);
for i=1:N
    if k(i)==0; %check imaginary
        closestpoint(i) = 0;
    else if result(i)==0
        closestpoint(i) =
closestpoint1_beamcase(x0(i),x(i),y(i),r,R,v,V,timePrey(i));
    end
end
end

figure(1);
graph1 = plot(distance,result);grid on; set(graph1,'Linewidth',5);
title('catch/escape vs x0 distance'); xlabel('x0 distance');
ylabel('1=catch. 0=escape');
figure(2)
graph2 = plot(distance,missdistance);grid on;
set(graph2,'Linewidth',3);
title('miss-distance vs x0 distance'); xlabel('x0 distance');
ylabel('miss distance in meters');
figure(3)
graph3 = plot(distance,closestpoint);grid on;
set(graph3,'Linewidth',3);
title('closest-distance vs x0 distance'); xlabel('x0 distance');
ylabel('closest distance in meters');

```

```

%% NAZMI ASLAN MATLAB CODE
% OPTIMUM X0 DISTANCE IN MISSILE-VESSEL INTERACTIONS IN HEAD TO HEAD
% ATTACK
clc; clear all; close all;

r=200;
R=4500;
v=30;
V=300;

distance = [0:20:R];
x0 = distance;
y0 = r;
X0 = 0;
Y0 = R;

p = -1*(Y0 - y0)/(X0-x0);
q = ((R.^2-r.^2)+(y0.^2-Y0.^2)+(x0.^2-X0.^2))./(-2.*(X0-x0));
a = 1+p.^2;
b = 2.*p.*(q-x0) - 2.*y0;
c = (q-x0).^2 + y0.^2 - r.^2;

% INTERSECTION POINT
y = (-b-sqrt(b.^2-4.*a.*c))./(2.*a);
x = (p.*y)+q;

k = abs(imag(y))<=0;

% PREDATOR CALCULATIONS
chordL = sqrt(y.^2 + x.^2);
centralAngle = 2.*(asin(chordL/(2*R)));
arcL = centralAngle.*R;
time = arcL./V;

% PREY CALCULATIONS;
chordLPrey = sqrt((y).^2 + (x-x0).^2);
centralAnglePrey = 2.*(asin(chordLPrey./(2.*r)));
arcLPrey = centralAnglePrey.*r;
timePrey = arcLPrey./v;

% Predator position when the prey reaches to intersection point
arcL1 = timePrey*V;
circumferencel = 2*pi*R;
centralAngle1 = 2*pi*arcL1/circumferencel;
xpred = X0 + R*sin(centralAngle1);
ypred = Y0 - R*cos(centralAngle1);

%comparing the time of Prey and Predator to find catch/escape
conditions
timeratio = time./timePrey;
result = timeratio<=1; % 1=catch, 0=escape

N = length(x0);

```

```

% miss distances are found for escape conditions
missdistance = zeros(1,N);
for i=1:N;
    if k(i)==0; %check imaginary
        missdistance(i) = 0;
        result(i) = 1;
    else if result(i)==0; % miss distance
        missdistance(i) = sqrt((x(i)-xpred(i)).^2+(y(i)-
ypred(i)).^2);
    end
end
end

% closest approach distances are found for escape conditions
closestpoint = zeros(1,N);
for i=1:N
    if k(i)==0; %check imaginary
        closestpoint(i) = 0;
    else if result(i)==0
        closestpoint(i) =
closestpoint1_headtohead(distance(i),x(i),y(i),r,R,v,V,timePrey(i));
    end
end
end

figure(1);
graph1 = plot(x0,result); grid on; set(graph1,'Linewidth',10);
title('catch/escape vs x0 distance'); xlabel('x0 distance');
ylabel('1=catch. 0=escape');
figure(2);
graph2 = plot(x0,missdistance);grid on; set(graph2,'Linewidth',3);
title('miss-distance vs x0 distance'); xlabel('x0 distance');
ylabel('miss distance in meters');
figure(3)
graph3 = plot(x0,closestpoint);grid on; set(graph3,'Linewidth',3);
title('closest-distance vs x0 distance'); xlabel('x0 distance');
ylabel('closest distance in meters');

```

APPENDIX D. MATLAB CODES FOR CRITICAL G-FORCE IN PURSUIT ATTACK, BEAM ATTACK, AND HEAD-TO-HEAD ATTACK SITUATIONS

```

%% NAZMI ASLAN MATLAB CODE
% MISSILE-VESSEL INTERACTIONS FOR CRITICAL g-force IN PURSUIT ATTACK
% SITUATION
clc; clear all; close all;

gforce = [0.01:0.0001:1];
g=9.81;

v=30;
V=300;
r=200;
R=(V.^2)./(gforce.*g);

x0 = 500;
y0 = r;
X0 = 0;
Y0 = R;

p = -1*(Y0 - y0)./(X0-x0);
q = ((R.^2-r.^2)+(y0.^2-Y0.^2)+(x0.^2-X0.^2))./(-2.*(X0-x0));
a = 1+p.^2;
b = 2.*p.*(q-x0) - 2.*y0;
c = (q-x0).^2 + y0.^2 - r.^2;

% INTERSECTION POINT
y = (-b+sqrt(b.^2-4.*a.*c))./(2.*a);
x = (p.*y)+q;

k = abs(imag(x))<=0;

% PREDATOR CALCULATIONS
chordL = sqrt(y.^2 + x.^2);
centralAngle = 2.*(asin(chordL./(2*R)));
arcL = centralAngle.*R;
time = arcL./V;

% PREY1 CALCULATIONS;
chordLPrey = sqrt((y).^2 + (x-x0).^2);
centralAnglePrey = 2.*(asin(chordLPrey./(2.*r)));
arcLPrey = centralAnglePrey.*r;
timePrey = arcLPrey./v;

% Predator position when the prey reaches to intersection point
arcL1 = timePrey*V;
circumferencel = 2*pi.*R;
centralAngle1 = 2*pi*arcL1./circumferencel;

```

```

xpred = X0 + R.*sin(centralAngle1);
ypred = Y0 - R.*cos(centralAngle1);

%comparing the time of Prey and Predator to find catch/escape
conditions
timeratio = time./timePrey;
result = timeratio<=1; % 1=catch, 0=escape

N = length(R);

% miss distances are found for escape conditions
missdistance = zeros(1,N);
for i=1:N;
    if k(i)==0; %check imaginary
        missdistance(i) = 0;
        result(i) = 1;
    else if result(i)==0; % miss distance
        missdistance(i) = sqrt((x(i)-xpred(i)).^2+(y(i)-
ypred(i)).^2);
    end
end
end

% closest approach distances are found for escape conditions
closestpoint = zeros(1,N);
for i=1:N
    if k(i)==0; %check imaginary
        closestpoint(i) = 0;
    else if result(i)==0
        closestpoint(i) =
closestpoint1_pursuitcase_g(Y0(i),x(i),y(i),r,R(i),v,V,timePrey(i));
    end
end
end

figure(1);
graph1 = plot(gforce,result); grid on; set(graph1,'Linewidth',3);
title('catch/escape vs g-force'); xlabel('g-force'); ylabel('1=catch.
0=escape');
figure(2);
graph2 = plot(gforce,missdistance); grid on;
set(graph2,'Linewidth',3);
title('miss-distance vs g-force'); xlabel('g-force'); ylabel('miss
distance in meters');
figure(3)
graph3 = plot(gforce,closestpoint); grid on;
set(graph3,'Linewidth',3);
title('closest-distance vs g-force'); xlabel('g-force');
ylabel('closest distance in meters');

```

```

%% NAZMI ASLAN MATLAB CODE
% MISSILE-VESSEL INTERACTIONS FOR CRITICAL g-force IN BEAM ATTACK
% SITUATION
clc; clear all; close all;

gforce = [0.01:0.01:4];
g=9.81;

v=30;
V=300;
r=200;
R= (V.^2)./(gforce.*g);

distance = 500;
N = length(R);

x0 = distance-r;
y0 = 0;
X0 = 0;
Y0 = R;

p = -1*(Y0 - y0)./(X0-x0);
q = ((R.^2-r.^2)+(y0.^2-Y0.^2)+(x0.^2-X0.^2))./(-2.*(X0-x0));
a = 1+p.^2;
b = 2.*p.*(q-x0) - 2.*y0;
c = (q-x0).^2 + y0.^2 - r.^2;

% INTERSECTION POINT
y = (-b+sqrt(b.^2-4.*a.*c))./(2.*a);
x = (p.*y)+q;

k = abs(imag(x))<=0;

% PREDATOR CALCULATIONS
chordL = sqrt(y.^2 + x.^2);
centralAngle = 2.*(asin(chordL./(2.*R)));
arcL = centralAngle.*R;
time = arcL./V;

% PREY1 CALCULATIONS;
chordLPrey = sqrt((y-y0).^2 + (distance-x).^2);
centralAnglePrey = 2.*(asin(chordLPrey./(2.*r)));
arcLPrey = centralAnglePrey.*r;
timePrey = arcLPrey./v;

% Predator position when the prey reaches to intersection point
arcL1 = timePrey*V;
circumferencel = 2*pi.*R;
centralAngle1 = 2*pi*arcL1./circumferencel;
xpred = X0 + R.*sin(centralAngle1);
ypred = Y0 - R.*cos(centralAngle1);

```



```

%comparing the time of Prey and Predator to find catch/escape
conditions
timeratio = time./timePrey;
result = timeratio<=1; % 1=catch, 0=escape

% miss distances are found for escape conditions
missdistance = zeros(1,N);
for i=1:N;
    if k(i)==0; %check imaginary
        missdistance(i) = 0;
        result(i) = 1;
    else if result(i)==0; % miss distance
        missdistance(i) = sqrt((x(i)-xpred(i)).^2+(y(i)-
ypred(i)).^2);
    end
end
end

% closest approach distances are found for escape conditions
closestpoint = zeros(1,N);
for i=1:N
    if k(i)==0; %check imaginary
        closestpoint(i) = 0;
    else if result(i)==0
        closestpoint(i) =
closestpoint1_beamcase_g(x(i),y(i),distance,r,R(i),v,V,timePrey(i));
    end
end
end
figure(1);
graph1 = plot(gforce,result); grid on; set(graph1,'Linewidth',3);
title('catch/escape vs g-force'); xlabel('g-force'); ylabel('1=catch.
0=escape');
figure(2)
graph2 = plot(gforce,missdistance); grid on;
set(graph2,'Linewidth',3);
title('miss-distance vs g-force'); xlabel('g-force'); ylabel('miss
distance in meters');
figure(3)
graph3 = plot(gforce,closestpoint); grid on;
set(graph3,'Linewidth',3);
title('closest-distance vs g-force'); xlabel('g-force');
ylabel('closest distance in meters');

```

```

%% NAZMI ASLAN MATLAB CODE
% MISSILE-VESSEL INTERACTIONS FOR CRITICAL g-force IN HEAD TO HEAD
% ATTACK SITUATION

clc; clear all; close all;

gforce = [0.01:0.0001:1];
g=9.81;

v=30;
V=300;
r=200;
R= (V.^2)./(gforce.*g);

distance = 500;
x0 = distance;
y0 = r;
X0 = 0;
Y0 = R;

p = -1*(Y0 - y0)./(X0-x0);
q = ((R.^2-r.^2)+(y0.^2-Y0.^2)+(x0.^2-X0.^2))./(-2.*(X0-x0));
a = 1+p.^2;
b = 2.*p.*(q-x0) - 2.*y0;
c = (q-x0).^2 + y0.^2 - r.^2;

% INTERSECTION POINT
y = (-b-sqrt(b.^2-4.*a.*c))./(2.*a);
x = (p.*y)+q;

k = abs(imag(y))<=0;

% PREDATOR CALCULATIONS
chordL = sqrt(y.^2 + x.^2);
centralAngle = 2.*(asin(chordL./(2*R)));
arcL = centralAngle.*R;
time = arcL./V;

% PREY1 CALCULATIONS;
chordLPrey = sqrt((y).^2 + (x-x0).^2);
centralAnglePrey = 2*(asin(chordLPrey./(2.*r)));
arcLPrey = centralAnglePrey.*r;
timePrey = arcLPrey./v;

% Predator position when the prey reaches to intersection point
arcL1 = timePrey*V;
circumferencel = 2*pi.*R;
centralAngle1 = 2*pi*arcL1./circumferencel;
xpred = X0 + R.*sin(centralAngle1);
ypred = Y0 - R.*cos(centralAngle1);

```

```

%comparing the time of Prey and Predator to find catch/escape
conditions
timeratio = time./timePrey;
result = timeratio<=1; % 1=catch, 0=escape

N = length(R);

% miss distances are found for escape conditions
missdistance = zeros(1,N);
for i=1:N;
    if k(i)==0; %check imaginary
        missdistance(i) = 0;
        result(i) = 1;
    else if result(i)==0; % miss distance
        missdistance(i) = sqrt((x(i)-xpred(i)).^2+(y(i)-
ypred(i)).^2);
    end
end
end

% closest approach distances are found for escape conditions
closestpoint = zeros(1,N);
for i=1:N
    if k(i)==0; %check imaginary
        closestpoint(i) = 0;
    else if result(i)==0
        closestpoint(i) =
closestpoint1_headtohead_g(Y0(i),x(i),y(i),r,R(i),v,V,timePrey(i));
    end
end
end

figure(1);
graph1 = plot(gforce,result); grid on; set(graph1,'Linewidth',3);
title('catch/escape vs g-force'); xlabel('g-force'); ylabel('1=catch.
0=escape');
figure(2);
graph2 = plot(gforce,missdistance);grid on; set(graph2,'Linewidth',3);
title('miss-distance vs g-force'); xlabel('g-force'); ylabel('miss
distance in meters');
figure(3)
graph3 = plot(gforce,closestpoint);grid on; set(graph3,'Linewidth',3);
title('closest-distance vs g-force'); xlabel('g-force');
ylabel('closest distance in meters');

```

APPENDIX E. CLOSEST APPROACH FUNCTIONS IN THE MATLAB CODES

```
%% NAZMI ASLAN MATLAB CODE
% CLOSEST APPROACH FUNCTIONS FOR OPTIMUM DISTANCE IN PURSUIT ATTACK
SITUATION
function closestpoint1 = closestpoint1(x0,x,y,r,R,v,V,timePrey)
y0 = r;
X0 = 0;
Y0 = R;
timePrey1=ceil(timePrey);
time = [0:0.01:2*timePrey1];%Time duration is between 0 and 2*timeprey
% PREDATOR POSITION CALCULATIONS
arcL1 = time.*V;
circumferencel = 2*pi*R;
centralAngle1 = 2*pi*arcL1./circumferencel;
xpred = X0 + R*sin(centralAngle1);
ypred = Y0 - R*cos(centralAngle1);
% PREY1 POSITION CALCULATIONS;
arcL2 = time.*v;
circumference2 = 2*pi*r;
centralAngle2 = 2*pi*arcL2./circumference2;
xprey = x0 + r*sin(centralAngle2);
yprey = r - r*cos(centralAngle2);
% FINDING CLOSEST POINT;
missdistance = sqrt((xprey-xpred).^2+(yprey-ypred).^2);
closestpoint1 = min(missdistance);
end
```

```
%% CLOSEST APPROACH FUNCTIONS FOR CRITICAL G-FORCE IN PURSUIT ATTACK
SITUATION
function closestpoint1 = closestpoint1(Y0,x,y,r,R,v,V,timePrey)
x0= 500;
y0 = r;
X0 = 0;
timePrey1=ceil(timePrey);
time = [0:0.001:2*timePrey1];
% PREDATOR POSITION CALCULATIONS
arcL1 = time.*V;
circumferencel = 2*pi.*R;
centralAngle1 = 2*pi*arcL1./circumferencel;
xpred = X0 + R.*sin(centralAngle1);
ypred = Y0 - R.*cos(centralAngle1);
% PREY1 POSITION CALCULATIONS;
arcL2 = time.*v;
circumference2 = 2*pi*r;
centralAngle2 = 2*pi*arcL2./circumference2;
xprey = x0 + r*sin(centralAngle2);
yprey = r - r*cos(centralAngle2);
% FINDING CLOSEST POINT;
missdistance = sqrt((xprey-xpred).^2+(yprey-ypred).^2);
closestpoint1 = min(missdistance);
end
```

```

%% NAZMI ASLAN MATLAB CODE
%CLOSEST POINT FUNCTIONS FOR OPTIMUM DISTANCE IN BEAM ATTACK SITUATION

```

```

function closestpoint1 = closestpoint1(x0,x,y,r,R,v,V,timePrey)
y0 = 0;
X0 = 0;
Y0 = R;

```

```

timePrey1=ceil(timePrey);
time = [0:0.1:2*timePrey1];
% PREDATOR POSITION CALCULATIONS
arcL1 = time.*V;
circumferencel = 2*pi*R;
centralAngle1 = 2*pi*arcL1./circumferencel;
xpred = X0 + R*sin(centralAngle1);
ypred = Y0 - R*cos(centralAngle1);
% PREY1 POSITION CALCULATIONS;
arcL2 = time.*v;
circumference2 = 2*pi*r;
centralAngle2 = 2*pi*arcL2./circumference2;
xprey = x0 + r.*cos(centralAngle2);
yprey = y0 + r.*sin(centralAngle2);
% FINDING CLOSEST POINT
missdistance = sqrt((xprey-xpred).^2+(yprey-ypred).^2);
closestpoint1 = min(missdistance);
end

```

```

%% CLOSEST POINT FUNCTIONS FOR CRITICAL G-FORCE IN BEAM ATTACK
SITUATION

```

```

function closestpoint1 = closestpoint1(x,y,distance,r,R,v,V,timePrey)
x0 = distance-r;
y0 = 0;
X0 = 0;
Y0 = R;

```

```

timePrey1=ceil(timePrey);
time = [0:0.01:2*timePrey1];
% PREDATOR POSITION CALCULATIONS
arcL1 = time.*V;
circumferencel = 2*pi.*R;
centralAngle1 = 2*pi*arcL1./circumferencel;
xpred = X0 + R.*sin(centralAngle1);
ypred = Y0 - R.*cos(centralAngle1);
% PREY1 POSITION CALCULATIONS;
arcL2 = time.*v;
circumference2 = 2*pi*r;
centralAngle2 = 2*pi*arcL2./circumference2;
xprey = x0 + r*cos(centralAngle2);
yprey = y0 + r*sin(centralAngle2);
% FINDING CLOSEST POINT
missdistance = sqrt((xprey-xpred).^2+(yprey-ypred).^2);
closestpoint1 = min(missdistance);
end

```

```

%% NAZMI ASLAN MATLAB CODE
% CLOSEST POINT FUNCTIONS FOR OPTIMUM DISTANCE IN HEAD TO HEAD ATTACK
SITUATION
function closestpoint1 = closestpoint1(x0,x,y,r,R,v,V,timePrey)
y0 = r;
X0 = 0;
Y0 = R;

timePrey1=ceil(timePrey);
time = [0:0.01:2*timePrey1];
% PREDATOR POSITION CALCULATIONS
arcL1 = time.*V;
circumferencel = 2*pi*R;
centralAngle1 = 2*pi*arcL1./circumferencel;
xpred = X0 + R*sin(centralAngle1);
ypred = Y0 - R*cos(centralAngle1);
% PREY1 POSITION CALCULATIONS;
arcL2 = time.*v;
circumference2 = 2*pi*r;
centralAngle2 = 2*pi*arcL2./circumference2;
xprey = x0 - r*sin(centralAngle2);
yprey = r - r*cos(centralAngle2);
% FINDING CLOSEST POINT
missdistance = sqrt((xprey-xpred).^2+(yprey-ypred).^2);
closestpoint1 = min(missdistance);
end

%% CLOSEST POINT FUNCTIONS FOR CRITICAL G-FORCE IN HEAD TO HEAD ATTACK
% SITUATION

function closestpoint1 = closestpoint1(Y0,x,y,r,R,v,V,timePrey)
y0 = r;
X0 = 0;
x0 = 500;

timePrey1=ceil(timePrey);
time = [0:0.01:2*timePrey1];
% PREDATOR POSITION CALCULATIONS
arcL1 = time.*V;
circumferencel = 2*pi.*R;
centralAngle1 = 2*pi*arcL1./circumferencel;
xpred = X0 + R.*sin(centralAngle1);
ypred = Y0 - R.*cos(centralAngle1);
% PREY1 POSITION CALCULATIONS;
arcL2 = time.*v;
circumference2 = 2*pi*r;
centralAngle2 = 2*pi*arcL2./circumference2;
xprey = x0 - r*sin(centralAngle2);
yprey = r - r*cos(centralAngle2);
% FINDING CLOSEST POINT
missdistance = sqrt((xprey-xpred).^2+(yprey-ypred).^2);
closestpoint1 = min(missdistance);
end

```

THIS PAGE INTENTIONALLY LEFT BLANK

LIST OF REFERENCES

- [1] Official: U.S. vessels harassed by high-speed Iranian boats. (2012, Jan. 13). CNN. [Online]. Available: <http://www.cnn.com/2012/01/13/us/iran-boats-tensions/>
- [2] A. H. Cordesman, "The Iranian sea-air-missile threat to Gulf shipping," Center for Strategic & Int. Stud., Feb. 2015.
- [3] Little boat, big danger: How a British-made speedboat has become a weapon in Iran's standoff with the U.S. (2012, Aug. 20). The Telegraph. [Online]. Available: <http://www.telegraph.co.uk/news/worldnews/middleeast/iran/9486815/Little-boat-big-danger-how-a-British-made-speedboat-has-become-a-weapon-in-Irans-standoff-with-the-US.html>
- [4] J. Bowles, "Turning characteristics and capabilities of high-speed monohulls," presented at the 3rd Chesapeake Power Boat Symp., Annapolis, MD, 2012.
- [5] Z. Zaoijan, "Prediction of ship manoeuvrability," class notes for Ship Maneuvering and Seakeeping, Shanghai Jiao Tong University, Shanghai, China, academic quarter 2006.
- [6] E. M. Lewandowski, *The Dynamics of Marine Craft*, Washington DC: World Scientific, 2004, pp. 361–396.
- [7] Ice Marine Homepage1. (2013, Feb. 19). Icemarine. [Online]. Available: <http://www.icemarine.com/homepage1/>
- [8] J. C. Hlavin, "Hydrostatic and hydrodynamic analysis of a lengthened DDG-51 destroyer modified repeat," M.S. thesis, Mech. and Aerospace Eng. Dept., NPS, Monterey, CA, 2010.
- [9] Ship motions. (n.d.). *Wikipedia*. Available: http://en.wikipedia.org/wiki/Ship_motions. Accessed Apr. 27, 2015.
- [10] O. M. Faltinsen, *Hydrodynamics of High-Speed Marine Vehicles*, New York: Cambridge Univ. Press, 2005.
- [11] U. Babaoglu, "Coupled directional stability of multiple ship formations," M.S. thesis, Mech. and Aerospace Eng. Dept., NPS, Monterey, CA, 2013.
- [12] M. G. Parsons, J. Li, and D. Singer, *Michigan Conceptual Ship Design Software Environment-User's Manuals*, Univ. of Mich., Ann Arbor, MI, 1998.

- [13] Waterline length. (n.d.). *Wikipedia*. Available: http://en.wikipedia.org/wiki/Waterline_length. Accessed Mar. 17, 2013.
- [14] R. B. Zubaly, *Applied Naval Architecture*. Society of Naval Architects and Marine Engineers, Cornell Maritime Press, 1996.
- [15] Bladerunner hull [image], Wordpress, n.d. Available: <https://geopolicraticus.files.wordpress.com/2010/04/bladerunner-51-hull.jpg>. Accessed Apr. 2015.
- [16] S. Denny and E. Hubble, “Prediction of craft turning characteristics,” *Marine Technol.*, vol. 28, pp. 1–13, 1991.
- [17] C. A. Lyster and H. L. Knights, “Prediction equations for ships’ turning circles,” *North East Coast Inst. of Eng. & Shipbuilders Trans.*, vol. 95, no. 4, pp. 217–222, 1979.
- [18] T. I. Fossen, *Handbook of Marine Craft Hydrodynamics and Motion Control*. United Kingdom: John Wiley & Sons, 2011.
- [19] T. Lauvdal and T. Fossen, “MATLAB simulation program for marine and flight vehicles,” Univ. of Trondheim, Norwegian Inst. of Technol., Dept. of Cybernetics, Trondheim, Norway, NTH Report, 1994.
- [20] Raju Datla, “Stability of high speed craft,” class notes for Stability and Control of Marine Craft, Stevens Institute of Technology, Hoboken, NJ, 2008.
- [21] F. A. Papoulias, “Dynamics of marine vehicles,” class notes for Mech. Eng., Naval Postgraduate School, Monterey, CA, 1993.
- [22] C. Tzeng and J. Chen, “Fundamental properties of linear ship steering dynamic models,” *J. Mar. Sci. Technol.*, vol. 7, pp. 79–88, 1999.
- [23] H. C. Howland, “Optimal strategies for predator avoidance: The relative importance of speed and manoeuvrability,” *J. of Theor. Biol.*, vol. 47, pp. 333–350, 1974.
- [24] D. Weihs and P. W. Webb, “Optimal avoidance and evasion tactics in predator-prey interactions,” *J. Theor. Biol.*, vol. 106, pp. 189–206, 1984.

INITIAL DISTRIBUTION LIST

1. Defense Technical Information Center
Ft. Belvoir, Virginia
2. Dudley Knox Library
Naval Postgraduate School
Monterey, California